Telemark University College
Faculty of technology
M.Sc. Programme

MASTER THESIS 2008

Candidate : Arild Sæther

Title : Control system for mass flow rate of solids in pneumatic conveying.

Faculty of Technology
Address: Kjolnes Ring 56, N-3914 Porsgrunn, Norway, tel: +47 35 57 50 00, fax: +47 35 55 75 47

Telemark University College
Faculty of Technology
M.Sc. Programme

WRITTEN REPORT MASTER THESIS, COURSE CODE FMH606

Student : Arild Sæther

Thesis Title : Control system for mass flow rate of solids in pneumatic conveying.

Signature : . . . . . .

Number of pages : 120

Keywords : Pneumatic conveying
System identification
Model predictive control

Supervisor : David Di Ruscio sign.: . . . . . .

2nd Supervisor : Chandana Ratnayake sign.: . . . . . .

Sensor : sign.: . . . . . .

External partner :

Availability : Open

Archive approval (supervisor signature): . . . . . **Date:** . . . . . .

Abstract:

The aim of the thesis is to make a model of the mass flow rate of solids in the pneumatic conveying systems situated at the POSTEC/Tel-Tek research facility to be used for the testing of model predictive control of these systems.

An approach to use system identification is explained in the thesis, relating to energy density. The system identification method used was the subspace method "combined Deterministic and Stochastic Realization method" (DSR). The measurement data available was of transporting the bulk material baryte in dense phase for plant A and dextrose in dilute phase for plant B. Tests for plant A and B gave a cumulative error ranging from ±1.2-7.5% of total conveyed mass. This implies that the DSR model using the energy density approach could be used for dense phase conveying as well as dilute phase. It also implies that it could be applied to the same type of conveying system of different size and dimension. For the DSR model to estimate properly, the condition of close to constant energy into the pneumatic conveying line has to be fulfilled.

The use of the DSR model based on the energy density approach, indicated relationships usable for later on making a rough mechanistic model. The disadvantage of the DSR model is that it has to have a measurement of the mass flow rate of solids for the calibration set.

The MPC was simulated based on the test set data sets from plant B, transporting dextrose in dilute phase. The MPC was used as a validation method, seeking out how realistic the MPC optimal controls would act on the real process. The MPC simulations gave an indication that the main air is not accurate enough as a control input using the DSR model. At the moment the MPC is usable as a mass flow rate of solids adjustor, controlling the bypass air.

Control system for mass flow rate of solids in pneumatic conveying

Arild Sæther

June 6, 2008

Contents

Acknowledgements

I would like to thank my supervisor David Di Ruscio at Telemark University-College for the use of his algorithm and helpful hints relating to system identification and model predictive control. I would like to thank the people at POSTEC for useful help and support. Especially Gisle Enstad, Chandana Ratnayake and Cecilia Arakaki for explaining me the basics of pneumatic conveying systems. I would also like to thank them for their moral support and the helpful and interesting discussions of the dynamics of transporting solids by air. I would like to thank my fellow student Apostolos Bartziokas for help on model predictive control issues in MatLab. An extra big hug to my girlfriend and colleague Cecilia for all the help and support. You are the best.

Chapter 1

Introduction

This is a master thesis performed at the Telemark University-College in cooperation with POSTEC/Tel-Tek. The work will be on model predictive control of mass flow rate of solids in pneumatic conveying. In order to do this a sufficiently accurate model of the mass flow rate of solids has to be attained. System identification has been chosen as the approach to get a model. The combined deterministic stochastic realization method (DSR) has been chosen as system identification method.

A particulate fluid in a pneumatic conveying is essentially a solids-gas two-phase mixture. However it is the mass flow rate of the solids phase that is of primary interest to operators of a pneumatic conveying system. From a flow measurement point of view, pneumatically conveyed solids can be regarded as single phase solids flow. Problems encountered in solids flow measurement are not normally associated with gas or liquid flows. Looking at the history of gas or liquid flow measurement, the most successful flow sensors have been restrictive/intrusive, with the exception of the electromagnetic flow meter which is non-restrictive/non-intrusive but measures only electrically conductive liquids. Since restrictive methods are unacceptable under pneumatic conveying conditions due to the highly abrasive nature of fast moving particles, reliable non-restrictive measurements techniques have to be sought out.

As with single-phase liquid or gas flow measurement, methodologies of metering the flow rate of solids in a pneumatic pipeline can be divided into two main categories, direct and inferential. A direct solids flow meter has a sensing element that responds directly to the mass flow rate of the solids through the instrument. An inferential solids flow meter is a soft sensor using direct measurements and then process them through a mathematical relationship to calculate the mass flow rate of solids. An inferential approach using system identification will be tried out in this thesis.

Many conveying systems do not have a measurement of the mass flow or an accurate measurement of the mass flow. A common way of measuring the mass flow is to use a load cell for weighing the mass in the blow tank or receiving tank. For large scale conveying systems using a load cell is not an accurate method for measuring the mass flow. This is because the accuracy of the load cells decreases as the weight of the mass in the blow tank or receiving tank is increasing. Load cells designed for 50 tons are considerably less accurate than a load cell designed for 1 ton.

The researchers at POSTEC/Tel-Tek are working on making inferential models for mass flow rate calculation of solids. The mass flow rate of solids is then measured by a virtual sensor/soft sensor using the direct pressure and air flow rate measurements and by then processing them through a mathematical relationship. The load cells in the pneumatic conveying rigs at POSTEC/Tel-Tek are used as an indicator of how accurate the inferential models prediction of the mass flow are.

Present data available is air flow measurements and pressure measurements collected during the transportation of solids. The aim will be to find the measurements that describe the system best and make a model on state space form using system identification.

To get a steady flow of particulate solids in pneumatic conveying, a control system is needed. Model predictive control is a control method using optimization over a prediction horizon. The model predictive controller is giving optimal control inputs for the process to be controlled. The problem is that such a controller needs a model to be implemented. To control "blind", that is using a soft sensor as measurement, the model has to estimate the real value with high accuracy. The goal will be to attain such a model that

is accurate enough for model predictive control. The model has to be simulated using the measured data using model predictive control, before being implemented on the real system. This thesis does not aim for implementation of the real system, but implementation of the model predictive control simulations.

There are two pneumatic conveying systems at the research facility at POSTEC/Tel-Tek. For simplicity they have been referred to as "plant A" and "plant B". Both systems are positive pneumatic conveying systems, using a blowtank without any form of feeding device. The conveying systems have an air inlet for controlling the blowtank pressure and fluidizing the particulate solids. They also have a support air inlet for regulation of the transport of solids. This support air is called the bypass air throughout the thesis. Both pneumatic systems are relatively small compared to industrial sized conveying systems. Plant A has a blowtank volume capacity of $3m^3$ and plant B $0.3m^3$. The pipeline of plant A is approximately $140m$ long and plant B $26m$. Both systems have pressure transducers placed along the pipeline. The measurement data available is of transporting the bulk material baryte in dense phase for plant A and dextrose in dilute phase for plant B. The description of the process and conditions of the tests will be given its own chapter called "Measurements setup".

The aim of the thesis is to make a model of the mass flow rate of solids in the pneumatic conveying systems situated at the POSTEC/Tel-Tek research facility to be used for the testing of model predictive control of the pneumatic conveying systems. Model predictive control is able to control unstable processes and handles cross couplings well. For limiting physical properties of the process, model predictive control can implement constraints with ease.

The second chapter in the thesis is dedicated to literature reviews of pneumatic conveying, system identification and model predictive control. Chapter three introduces the background behind selecting inputs for the system identification method. The fourth chapter is the measurement setup chapter, five discuss the results of the system identification model, chapter six discusses the model predictive control simulation on the tests and chapter seven is rounding of with the conclusion chapter.

Chapter 2

Literature reviews

2.1 Background of pneumatic conveying

Pneumatic comes from the word "*pneumatikos*", which means coming from the wind. Pneumatics means the use of pressurized air in science and technology [1]. Pneumatic conveying involves the transportation of a wide variety of dry powdered and granular solids in a gas stream. In most cases the gas is normally air. However, where special conditions prevail (e.g. risk of explosion, health, fire hazards, etc.), different gases are used [2]. One of the aims in this literature review chapter is to review essential pneumatic conveying concepts like the major parts of a conveying system, classification of conveying systems, modes of flow and classification of powders. Another aim is to shortly review some techniques for measuring the mass flow and the importance of such measurements. At the end of the chapter, a model for control and some proposed control strategies are mentioned [2].

2.1.1 History of pneumatic conveying

The concept of pipeline transportation of fluids is by no means modern. The history of its use dates back to antiquity. The Romans, for instance, used lead pipes for water supply and sewerage disposal, whilst the Chinese conveyed natural gas through bamboo tubes [2]. The record of pipeline transportation of solids in air is more recent. In the Peugot plant in France, the conveying principle was used for exhaust of dust from a number of grindstones using a exhaust fan in 1847. In 1864, an experimental pneumatic railway was built at Crystal palace with the intention of using the principle of vacuum applied to a railway tunnel to move a carriage, which had been fitted with a sealing diaphragm. Another application of vacuum pneumatic transport was reported in a ship unloading plant in London in 1890 [1]. The first large-scale application of pneumatic conveying was the vacuum conveying of grain in the late 19th century. By the mid 1920's, negative and positive pressure conveying of grain was common [2]. During the First World War, the development of pneumatic conveying was influenced by the high demand for foods, labour scarceness and risks of explosion. Since the pneumatic conveying systems were seen as the answer for those situations, a huge evolution of pneumatic transport was achieved during that time period. In the post-war period, pneumatic conveying systems were used for more industrial related materials like coal and cement. The development of theoretical approaches, invention of blowers, introduction of batch conveying blow tanks, etc., were among the highlighted milestones of the evolution of pneumatic transport systems during this era. Nowadays, pneumatic transport is a popular technique in the particulate material handling field. It has been reported that some plants have transport distances of more than 40 km, material flow rate of few hundreds tons per hour and solid loading ratio (the mass flow rate ratio between solid and air) of more than 500 [1].

2.1.2 Applications of pneumatic conveying

According to Ratnayake [1], the applications of pneumatic conveying systems can be seen in many industrial sectors. Some industrial fields where it has extensively been used are given below :

- Chemical process industry

- Pharmaceutical industry
- Mining industry
- Agricultural industry
- Mineral industry
- Food processing industry

Virtually, all powders and granular materials can be transported using this method. In Ref. [3], a list of more than 380 different products, which have been successfully conveyed pneumatically is presented. It consists of very fine powders, as well as big crystals such as quartz rock of size 80 mm. Even some strange products like prairie dogs, live chicken and finished manufactured parts of irregular shapes have been successfully conveyed through pipeline systems. Recently, some speculations have arisen about a transport method for human beings with the help of pneumatic conveying principles. This method is termed as capsule/tube transport, which has already been tested for lots of materials. Pneumatic capsule pipeline (PCP) uses wheeled capsules (vehicles) to carry cargoes through a pipeline filled with air. The air is used to push the capsules through the pipeline.

2.1.3 General description of pneumatic conveying

Pneumatic conveying is a material transportation process. Bulk particulate materials are moved within a piping system by a compressed air stream [1]. The transport of bulk particulate materials can be described according to different classifications of the pneumatic transport system, classifications of the transported particulate solid and modes of particulate solids flow. The transport systems can be classified into systems that use positive (blow), negative (vacuum) pressure or a combination of both to transport the particulate solids. Klinzing, Marcus, Rizk, and Leung [2] also introduce a closed loop system for transporting particulate solids, where the air is reused.

The particulate solids can be conveyed in different modes. The modes refer to the ratio between the particulate solids mass flow rate and the supplied gas mass flow rate, during transport. This ratio is referred to as solids loading ratio. The modes are often divided into dense phase and dilute phase. Conveying systems can also be classified into dilute and dense phase, this is often related to the feeding of the solids into the pipeline. Different particulate solids have different flow characteristics. A commonly used method of classification of particulate solids flow characteristics is the Geldart diagram. The Geldart diagram takes into account the particulate solids particle density and size, when characterizing the fluidization of the particulate solid.

2.1.4 Advantages and disadvantages of pneumatic conveying

Pneumatic conveying has a lot of advantages over other methods like mechanical conveyers. Some advantages can be listed as mentioned by Klinzing *et al* [2]:

1. Dust free transportation of a variety of products.
2. Flexibility in routing – can be transported vertically and horizontally by the addition of a bend in the pipeline.
3. Distribution to many different areas in a plant and pick-up from several areas.
4. Low maintance cost and low manpower costs.
5. Multiple use – one pipeline can be used for a variety of products.
6. Security – pipelines can be used to convey high-valued products.
7. Ease of automation and control.

When conveying health hazardous material a negative pressure system gives a dust free transportation of the particulate solids, since pneumatic systems are completely enclosed. Pneumatic conveying is specially used to deliver dry, granular or powdered materials via pipelines to remote areas that would be hard to reach economically with mechanical conveyors. This gives flexibility of installation by pneumatic conveying over other methods like mechanical conveyors. Pneumatic systems can be adopted to pick up the conveying bulk material from multiple sources and/or distribute them to several different destinations. In addition, reduced dimensions, progressive reduction of capital and installation costs, low maintenance costs (due to the small number of moving parts), repeated usage of conveying pipelines, easiness in control and automation are among the favorable advantages of pneumatic conveying over other methods of particulate material handling [1].

Although pneumatic conveying has been increasingly used in particulate material handling, it still has some disadvantages. These can be listed as mentioned by Klinzing *et al* [2] :

1. High power consumption.
2. Wear and abrasion of equipment.
3. Incorrect design can result in particle degradation.
4. Limited distance.
5. By virtue of the complex flow phenomena which take place, there is a requirement for high levels of skill to design, operate and maintain systems.

Specially, in dilute phase transport, high energy consumption, excessive product degradation and system erosion (pipelines, bends etc.) are some of the major problems. In dense phase conveying the occurrence of unstable plugging phenomena, severe pipe vibration and repeated blockages are experienced frequently [1]. Because of high power consumption, pneumatic systems are generally more suited to the conveyance of fine particles over shorter distances. The limitations are usually economic rather than technical. However, the economic factor is changing and recent developments have ensured the transportation of materials at lower energies [2]. Further, the lack of simple procedures for the selection of an optimal system is a major problem in pneumatic transport system design [1].

2.1.5 The major parts of pneumatic conveying systems

A pneumatic conveying system consists of several components. The pneumatic system is usually divided into four operative zones that carries out tasks that are important for the system to give the desired effect. Each zone has some specialized equipment. The four zones in a pneumatic system can be set up like mentioned by Klinzing *et al* [2] and Ratnayake [1] :

1. Conveying gas supply (prime mover):
   - To provide the necessary energy for the conveying gas, various types of compressors, fans, blowers and vacuum pumps are used as the prime mover. To get enough energy to move the solids in the system it is important when designing this zone, that it meets the requirements for reliable transportation.
2. Feeding mechanism :
   - In this zone the solids are introduced into the flowing gas stream. To feed the solid to the conveying line, a feeding mechanism such as a rotary valve, screw feeder, etc. is used.
3. Conveying line :
   - This consists of all straight pipe lines of horizontal and/or vertical sections, bends and other auxiliary components such as valves.
4. Separation equipment :

- At the end of the conveying line, solids have to be separated from the gas stream in which it has been transported. For this purpose, cyclones, bag filters, electrostatic precipitators are usually used in the separation zone.

2.1.6 Classification of pneumatic conveying systems

Pneumatic conveying systems can be classified according to two criteria. One criterion is related to pressure and the other criterion is related to the flow pattern (also called the mode). When classifying according to pressure, there are three different kinds of systems as mentioned by Ratnayake [1] :

1. Positive pressure systems :
   - In this type of conveying system the absolute pressure is always above atmospheric pressure. This kind of system pushes the particulate solids through the conveying pipeline. This type of conveying system is often used for multiple discharge systems, where the particulate solids are picked up at a single point and distributed to several receiving stations.
2. Negative pressure systems :
   - This type of conveying system is also termed vacuum/suction system, where the absolute pressure is below atmospheric pressure. This kind of conveying system is often used for systems with multiple feeding points that connect to a common collection station. The most simple application of this system is the domestic vacuum cleaner. The more advanced applications are when handling toxic and hazardous materials. Here, this system offers dust free feeding and leak free material handling.
3. Combined positive and negative pressure systems :
   - This type of conveying system combines the properties from the positive pressure and negative pressure systems. This implies that this type of conveying system is able to have multiple feeding points for particulate solids into the pneumatic pipeline and multiple collection stations. This type of system is also often referred to as a "suck-blow" system.

A fourth system is introduced by Klinzing *et al* [2]. It is a closed loop system where the conveying gas is recycled. This type of system is suitable for handling toxic and radioactive materials. Since the system is reusing the gas, this kind of system is also suited for systems using other gases than air.

2.1.7 Different modes in pneumatic conveying

The modes of flow is based on the ratio between the particulate solids mass flow rate and the gas mass flow rate, as mentioned earlier. A common classification of modes is dense phase and dilute phase, where the dilute phase has a low concentration of particulate solids in the suspension and dense phase has a high concentration of particulate solids in the suspension. There is different views amongst the researchers when it comes to defining the modes of pneumatic conveying transport. There is not an established clear definition of the modes yet. Klinzing *et al* [2] defines two modes for transport of particulate solids, dense phase and dilute phase. Where the dilute phase has a solids loading ratio ranging from 0-15 and the dense phase has a solids loading ratio greater than 15. Klinzing also mentions that some researchers has defined a third "medium" mode. Mills [4] defines the dilute phase as 0-10 and dense phase as greater than 10. In general dilute and dense phase can be described as mentioned by Ratnayake [1] :

1. Dilute phase conveying systems :
   - By employing large volumes of gas at high velocities, particulate solids transportation in suspension mode is usually termed dilute phase conveying.
2. Dense phase conveying systems :
   - By reducing the gas velocity, particulate solids can be transported through the pipeline as a plug or a moving bed.

2.1.8 Classification of powders, (the Geldart diagram)

There are many material characteristics that influence the flow behavior in pneumatic conveying. Some of them is mentioned by Ratnayake [1], like particle size and size distribution, particle shape, cohesiveness, Hardness and electrostatic charging. Geldart [5] worked out a classification of particulate solids and their behavior. The Geldart diagram is often referred to for classification of particulate solids in pneumatic conveying. The different groups are shown in figure (2.1).

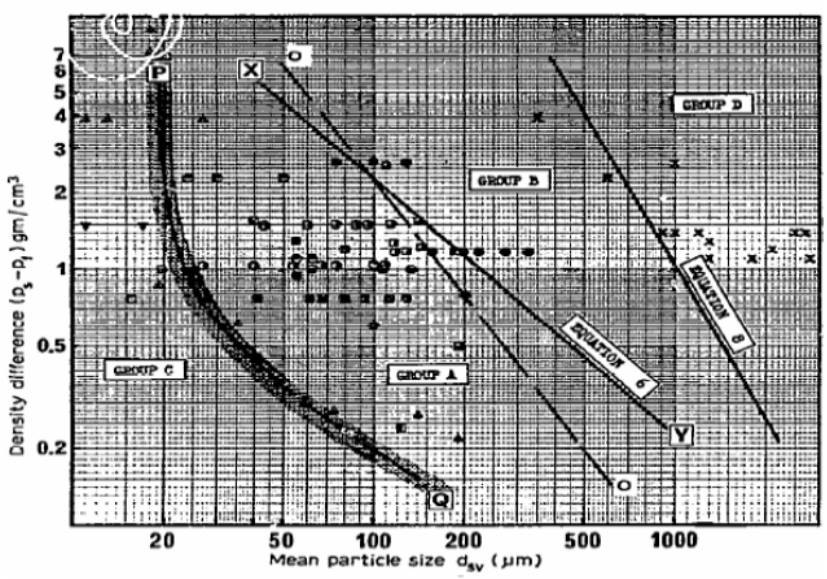

Figure 2.1: Powder classification diagram for fluidization by air (as in the original publication by Geldart [5]).

Geldart organized the different particulate solids behavior when subjected to fluidization by a gas. The diagram can briefly be explained like mentioned by Ratnayake [1] :

1. Group A
   - Materials having a small mean size and/or low particle density will generally exhibit considerable bed expansion before bubbling commences. When the gas supply is suddenly cut off, the bed collapses slowly.
2. Group B
   - Naturally occurring bubbles start to form in this type of material at, or slightly above, the minimum fluidizing velocity. Bed expansion is small and the bed collapses very rapidly when the gas supply is shut off.
3. Group C
   - This group contains powders, which are of small particle size and cohesive in nature. Consequently, normal fluidization is very difficult. The powder lifts as a plug in small diameter tubes or, preferentially channels.
4. Group D
   - This group contains large and/or high density particles. It is believed that the bubble sizes may be similar to those in group B and if gas is introduced only through a centrally located hole, this group can be made to spout.

The problem is related to conveying of particulate solids in dense phase. Group A and D products are suitable for dense phase conveying, while group B products can cause problems and group C products are the least suitable for dense phase conveying. Group C products will most probably plug the system in dense phase conveying.

2.1.9 Mass flow measurement in pneumatic conveying

According to Yan [6], a particulate fluid in a pneumatic conveying is essentially a solids-gas two-phase mixture. However it is the mass flow rate of the solids phase that is of primary interest to operators of a pneumatic conveyor. From a flow measurement point of view, pneumatically conveyed solids can be regarded as single phase solids flow. Problems encountered in solids flow measurement are not normally associated with gas or liquid flows. Looking at the history of gas or liquid flow measurement, the most successful flow sensors have been restrictive/intrusive, with the exception of the electromagnetic flow meter which is non-restrictive/non-intrusive but measures only electrically conductive liquids. Since restrictive methods are unacceptable under pneumatic conveying conditions due to the highly abrasive nature of fast moving particles, reliable non-restrictive measurements techniques have to be sought out. Although substantial research has demonstrated that restrictive flow sensors are applicable to mass flow measurements of gravity-fed solids in many cases, they are unsuitable for metering of bulk solids in pneumatic pipelines [6].

As with single-phase liquid or gas flow measurement, methodologies of metering the flow rate of solids in a pneumatic pipeline can be divided into two main categories, direct and inferential. A direct solids flow meter has a sensing element that responds directly to the mass flow rate of the solids through the instrument. An inferential solids flowmeter determines both the instantaneous volumetric concentration of solids and the instantaneous velocity of solids over the pipe cross section, from which the mass flow rate can be deduced according to equation (2.1).

The importance of inferential measurement of mass flow in pneumatic conveying

Many conveying systems do not have a measurement of the mass flow or an accurate measurement of the mass flow. A common way of measuring the mass flow is to use a load cell for weighing the mass in the blow tank or receiving tank. For large scale conveying systems using a load cell is not an accurate method for measuring the mass flow. This is because the accuracy of the load cells decreases as the weight of the mass in the blow tank or receiving tank is increasing. Load cells designed for 50 tons are considerably less accurate than a load cell designed for 1 ton. The researchers at POSTEC/Tel-Tek is working on making inferential models for mass flow measurement using pressure measurements. The mass flow is then measured by a virtual sensor/soft sensor using the direct pressure measurements and then process them through a mathematical relationship. The K-model of Ratnayake is one such model [1]. The load cells in the pneumatic conveying rigs at POSTEC/Tel-Tek are used as an indicator of how accurate the inferential models prediction of the mass flow are.

Yan [6] presents a practical example of a coal-fired power station. Where the coal is fed into a pulverizer mill and the coal is crushed to powder. This powder is then transported by pneumatic conveying to the furnace. He states the importance of having the right mass flow, solids velocity and particle distribution. These factors are important for energy efficiency while burning the coal in the furnace, reducing the wear on the pipeline and breakage of the bulk material. This is an example of the importance of measuring the mass flow, the solids velocity and particle distribution in pneumatic conveying.

Inferential measurement of mass flow using the velocity and concentration measurement

An example of direct measuring technique in pneumatic conveying is mentioned by Klinzing *et al* [2]. A soft sensor solution to measuring the mass flow is given by merging the measurements from a solids concentration sensor and a solids velocity sensor, through a relationship set up in an equation. The mass flow can be put up like in equation (2.1)

$$\dot{m}_s = \dot{V}_s \rho_s C_s \tag{2.1}$$

where

$$\begin{aligned} \dot{m}_s &= \text{Mass flow of solids} \\ \dot{V}_s &= \text{Volumetric flow of solids} \\ \rho_s &= \text{Solids density} \\ C_s &= \text{Volume concentration} \end{aligned}$$

Klinzing *et al* [2] gives an example of the use of two precision capacitors. The capacitance will change during transport of particulate solids. The measured capacitance in capacitor 1 x_1 is then cross correlated with the measured capacitance in capacitor 2 x_2. Using discrete cross correlation, it can be set up as in equation (2.2).

$$r_{12}(k) = \frac{1}{N} \sum_{n=0}^{N-1} x_1(n) \cdot x_2(n+k) \tag{2.2}$$

where

$$\begin{aligned} k &= \text{Discrete time step delay (multiply with sampling time } (dt) \text{ to get time delay)} \\ r_{12}(k) &= \text{Cross correlation factor} \\ N &= \text{Number of samples/discrete time steps} \end{aligned}$$

By normalizing the signals a cross correlation factor in percentage can be presented (2.3). This factor tells how similar the signals are in percentage.

$$\begin{aligned} \rho_{12}(k) &= \frac{r_{12}(k)}{\frac{1}{N}\sqrt{\sum_{n=0}^{N-1} x_1^2(n) \cdot \sum_{n=0}^{N-1} x_2^2(n)}} \cdot 100\% \qquad (2.3) \\ \rho_{12}(k) &= 100\% : 100\% \text{ correlation} \\ \rho_{12}(k) &= 0\% : 0\% \text{ correlation} \\ \rho_{12}(k) &= -100\% : 100\% \text{ correlation in opposite phase} \end{aligned}$$

Using the time delay and the distance between the two capacitors gives the velocity of the solids (2.4).

$$\begin{aligned} d &= \text{Distance between capacitors} \\ \tau &= k \cdot dt : \text{ Time delay} \\ v &= \frac{d}{\tau} \qquad (2.4) \end{aligned}$$

The distance between the two capacitors is crucial for getting a good correlation. If they are too far away from eachother the correlation will be too low, because of the stochastic behavior of the particulate solids flow. Klinzing *et al* [2] states that a cross correlation factor between 60-80% is obtained in actual practice, when capacitors are placed properly.

The concentration sensor proposed by Klinzing *et al* [2], was a capacitance sensor. This capacitance sensor measures the change in capacitance during transport. The ratio between the capacitance during transport and the capacitance when not conveying is proportional to the volume concentration C_s. A downside to this method of measuring concentration is that it needs calibration for the specific particulate solid to be conveyed during conveying. Another disadvantage is that this method is not suitable for measuring solid loading ratios below 5. This excludes measurement of the lower part of dilute phase conveying.

Merging the velocity measurement and the concentration measurement through the mass flow equation (2.1) gives a measurement of the mass flow rate.

Inferential measurement of mass flow using pressure drop flow meter

A differential pressure measuring device has been developed by Cabrejos and Klinzing [2] to measure the solids mass flow rate. The specific pressure drop defined as the ratio of differential pressure drop across a

straight section of pipe for dilute phase pneumatic conveying divided by the pressure drop due to the flowing gas alone is found to be linearly related to the solids loading ratio, $\left(\frac{\text{mass of solids}}{\text{mass of gas}}\right)$. Equation (2.5) shows this relationship.

$$\alpha = \frac{\Delta P_{total}}{\Delta P_{gas}} \tag{2.5}$$

Klinzing [2] further mentions the importance of measuring pressure fluctuations and analyze the information given in these fluctuations.

2.1.10 The pressure drop coefficient model for mass flow estimation

The pressure drop coefficient method also called the K-model was developed at TEL-TEK/POSTEC by Ratnayake [1]. Arakaki, Ratnayake, Datta and Lie [7] explained the K-model briefly like introduced below.

The K-model

If a small quantity of material is fed into a gas stream at a steady rate there is an increase in the conveying line pressure drop if the gas flow rate remains constant. The magnitude of this increase depends upon the concentration of the material in the gas. In a two-phase flow system, consisting of a gas and solid particles conveyed in suspension, part of the pressure drop is due to the gas alone and part is due to the conveying of the particles in the gas stream. In such a two-phase flow the particles are conveyed at a velocity below that of the conveying gas, a drag force being exerted on the particles by the gas for suspension modes of flow [4].

The model for the calculation of mass flow rate used in this paper has been derived from a model for the calculation of pressure drop [1]. The model for the pressure drop calculation was developed from the equation of Darcy which is in the simplest way as follows (2.6):

$$\Delta P = 4\frac{f\rho_a v^2 L}{2D} \tag{2.6}$$

where ΔP is the pressure drop, f is the friction factor which is a function of the Reynolds number for the flow and the pipe wall roughness, ρ_a is the density of air, v represents the mean velocity of flow, L is the length of the pipe section and is the diameter. This model relates to turbulent flow only. Laminar flow models have little or no application to flows encountered in pneumatic conveying pipelines. It can be seen from this mathematical model that pressure drop follows a square law relationship with respect to velocity i.e. if velocity is doubled, the pressure drop increases by a factor of four [4].

However, the equation of Darcy is a model for pressure drop in single-phase flow only. Some researchers have tried to modify Darcy's theory to suit multiphase flow situations. Ratnayake [1], modified the above mentioned equation for the two-phase flow experienced when pneumatic conveying. The principle applied in this modified equation is considering the two-phase flow, gas-solid system as a mixture having its own flow characteristics, instead of recognizing the two components separately. Therefore, a pressure drop coefficient; K, the solid suspension density; ρ_{sus}, and the entry velocity; v_{entry} were introduced to Equation (2.6) instead of $4f$, ρ_a, v respectively.

The pressure drop was addressed in a discrete way by considering horizontal and vertical straight pipe sections, bends and other pipe accessories separately. For a straight section the equation has the following form (2.7):

$$\Delta p_{st} = \frac{1}{2}K_{st}\rho_{sus}v_{entry}^2\frac{\Delta L}{D} \tag{2.7}$$

where v_{entry} is the gas velocity at the entry section of the concerned pipe section or pipe component, K_{st} is the pressure drop coefficient for straight pipe sections whether they are horizontal or vertical and ρ_{sus} can be defined as the density of the mixture when a short pipe element is considered. The equation to calculate ρ_{sus} is shown below (2.8):

$$\rho_{sus} = \frac{\dot{m}_s + \dot{m}_a}{\dot{V}_s + \dot{V}_a} \tag{2.8}$$

where is the $\dot{m}_s$ mass flow rate of solids, $\dot{m}_a$ is the mass flow rate of air, $\dot{V}_s$ is the volume flow rate of solids and $\dot{V}_a$ is the volume flow rate of air. Equation (2.8) could be re-arranged in order to get the mass flow rate of solids, as shown below (2.9):

$$\dot{m}_s = \frac{\rho_a \dot{Q} - \rho_{sus} \dot{V}_a}{\frac{\rho_{sus}}{\rho_s} - 1} \tag{2.9}$$

where $\dot{Q}$ is the volume flow rate of air obtained by adjusting the experimentally measured air volume flow rate according to the true pressure value at the concerned section of the pipeline. This is done in order to take into account the compressibility effect .

2.1.11 Control of pneumatic conveying systems

Klinzing *et al* [2] has written about pneumatic conveying and control systems. This chapter is a brief replication of his modelling of a positive pressure blowtank system for the use of PID-control.

Modelling a positive pressure blowtank system

A positive pressure conveying system with a blowtank, assuming the output of the particulate solids in the tank can be measured, can be modeled as a mass balance (2.10) as mentioned by Klinzing *et al* [2]

$$\frac{dm}{dt} = -\dot{m}_o \tag{2.10}$$

where

$$\begin{aligned} \frac{dm}{dt} &= \text{change in mass in storage tank} \\ \dot{m}_o &= \text{mass flow out of tank} \end{aligned}$$

By setting a reference point in the mass flow of particulate solids out of the tank , the error to control is then like in equation (2.11).

$$\varepsilon = \dot{m}_{oref} - \dot{m}_o \tag{2.11}$$

Where

$$\begin{aligned} \varepsilon &= \text{error in mass flow to control} \\ \dot{m}_{oref} &= \text{Reference point for mass flow} \\ \dot{m}_o &= \text{Measured mass flow} \end{aligned}$$

The output can be modeled as a function of blowtank pressure and the amount of mass of particulate solids in the tank. Assuming a linear relationship between the outflow of particulate solids and the pressure in the blowtank and the amount of mass of particulate solids in the blowtank gives the relationship in equation (2.12) as shown by Klinzing *et al* [2].

$$\dot{m}_o = \alpha m + \beta p_{\text{tank}} \tag{2.12}$$

where

$$\begin{aligned} p_{\text{tank}} &= \text{Pressure in blowtank} \\ \beta &= \text{Linear relationship factor for blowtank pressure relating to outflow} \\ \alpha &= \text{Linear relationship factor for mass in blowtank relating to outflow} \end{aligned}$$

Using a proportional relationship between the pressure in the blowtank and the error gives equation (2.13).

$$\begin{aligned} p_{\text{tank}} &= K \cdot \varepsilon \\ p_{\text{tank}} &= K \left(\dot{m}_{oref} - \dot{m}_o \right) \end{aligned} \tag{2.13}$$

Combining equation (2.12) and (2.13) gives equation (2.14).

$$\begin{aligned} \frac{dm}{dt} &= -\dot{m}_o \\ \frac{dm}{dt} &= -\left(\alpha m + \beta p_{\text{tank}}\right) \\ \frac{dm}{dt} &= -\left[\alpha m + \beta K\left(\dot{m}_{oref} - \dot{m}_o\right)\right] \end{aligned} \tag{2.14}$$

By applying the Laplace transform on equation (2.14) the transfer function is like in equation (2.15).

$$\begin{aligned} \frac{dm}{dt} + \alpha m &= -\beta K\left(\dot{m}_{oref} - \dot{m}_o\right) \\ sm(s) + \alpha m(s) + m(0) &= -\beta K\left(\dot{m}_{oref}(s) - \dot{m}_o(s)\right) \\ m(s) &= \frac{1}{s+\alpha}\left[m(0) - \beta K\left(\dot{m}_{oref}(s) - \dot{m}_o(s)\right)\right] \end{aligned} \tag{2.15}$$

where

$$m(0) = \text{The initial mass in the blowtank}$$

Applying a transport delay $e^{-\tau s}$ gives the transfer function (2.16).

$$m(s) = e^{-\tau s}\frac{1}{s+\alpha}\left[m(0) - \beta K\left(\dot{m}_{oref}(s) - \dot{m}_o(s)\right)\right] \tag{2.16}$$

This transfer function of the process can then be controlled by for instance a PID-controller. To avoid unnecessary oscillations in the control relating to noise, a PI-controller would be a good choice. Further on Klinzing *et al* [2] mentions that modelling by neural networks and control by fuzzy logic is also an alternative control option. He also mentions that the ultimate control system will use an adjustable Laval nozzle for supply of the conveying air flow rate and an ejector for line cleaning purposes.

2.2 Background of system identification

The process of going from observed data to a mathematical model is fundamental in science and engineering. In the control area this process has been termed "System Identification" and the objective is then to find dynamic models (difference or differential equations) from observed input and output signals. Its basic features are however common with general model building processes in statistics and other sciences. [8]. System identification is used when there is insufficient measurements or knowledge to model a process based on physical parameters and properties alone.

The area of system identification begins and ends up with real data. Data are required to build and to validate models. The result of the modelling process can be no better than what corresponds to the information contents in the data [8].

There is a wide variety of black box models in use today. A simple form of model for system identification is Finite Impulse Response (FIR) models. FIR models is made by introducing a change in the inputs , then the change in the outputs is recorded. A function of the changes is the made based on the observations. Other methods like Auto-regression with eXtra inputs (ARX) models and Auto-Regressive Moving Average with eXtra inputs (ARMAX) models, were early introduced to the field of system identification. Ordinary least square (OLS) gives an ARX model and recursive ordinary least square gives an ARMAX model.

The models above has the problem of structure identification, that is identifying the relationships within the observation data. This is because the methods above focuses on estimating the output and does not give information about how the inputs interact with eachother within the observation data. The methods above is multivariable methods.

Subspace identification focuses both on estimating the output of the model and identifying the structure within the observation data. The system identification method used in this thesis is a subspace identification method, the Deterministic Stochastic Realization method (DSR) [9]. This model use the state space form to describe the model. The main focus in this chapter will be related to the DSR-model.

Optimal estimation is the minimization of the prediction error (PE). This has resulted in, that in the field of control theory there has been an extensive research in Prediction Error Methods (PEM) for optimization of the predicted output. In this chapter some different methods of optimizing the predicted output will be discussed.

2.2.1 History of system identification

As told by Ljung [8], System identification has its roots in standard statistical techniques and many of the basic routines have direct interpretations as well known statistical methods such as Least Squares and Maximum Likelihood. The control community took an active part in the development and application of these basic techniques to dynamic systems right after the birth of "modern control theory" in the early 1960's. Maximum Likelihood estimation was applied to difference equations (ARMAX models) by Åstrøm and Bohlin in a paper 1965. Later a wide range of estimation techniques and model parameterization flourished. By now, the area is well matured with established and well understood techniques. Industrial use and application of the techniques has become standard. In the MatLab , The N4SID subspace identification algorithm is such an algorithm for modelling industrial processes. The N4SID algorithm is a part of the system identification toolbox in MatLab, based on an algorithm by Ljung [10]. Di Ruscio has developed a MatLab software package for DSR [9], which is a system identification toolkit for modelling industrial processes.

2.2.2 Applications of system identification

System identification has a wide range of usages in the industry. Many industry processes have not yet been modelled. Here system identification is a good tool for finding a model that gives an estimate of the real process. System identification is in the field of control theory and can be applied to numerous industry processes. In this thesis a subspace identification method is used to get a model of mass flow of particulate solids in pneumatic conveying. The observation input data are pressure measurements and airflow measurements and the observation output data is the measured mass flow. The goal is to estimate the mass flow without using a load cell. To put it in another way : To make a virtual measurement (soft sensor) of the mass flow instead of the physical measurement given by the load cell.

2.2.3 Advantages and disadvantages of system identification

Some advantages :

- Easy and fast to model complex processes
- Gives opportunity for advanced control systems where no physical model exists

Some disadvantages :

- model never better than real data, a representative data set needed
- Always an approximation, never as good as a representative physical model

2.2.4 Multivariate and univariate data

The system is called univariate when one input parameter is influencing one output parameter [11]. An example of univariate modelling is a simple ordinary least square using scalars, giving one input variable and one output variable. The system is called multivariable when a system has several input parameters that influence one or more output parameters. In statistics,methods handling multivariable systems are called multiple linear regression methods (MLR) [11]. Ordinary least squares and recursive least squares are examples of MLR. Problems arise when there is collinearity in the data. According Esbensen [11], collinearity means that the observation input variables (X-variables) are intercorrelated to a non-neglectable degree. That gives that the X-variables are linearly dependent to some degree. Multivariate methods handles these structural issues within the observation data set. Principal component regression (PCR) and partial

least square (PLS) are examples of multivariate methods. These methods handles the issue of collinearity by performing a principal component analysis (PCA). In system identification, a PCA can be performed by applying a singular value decomposition (SVD) to the observation data. The control theory field of system identification and the statistical field of chemometrics handles processes with multivariate data. An important note is that in the field of chemometrics versus the field system identification, there is often different definitions of what is multivariate and what is univariate. The most most important issue is that PCR,PLS and subspace identification handles identifying the structure within the observation data.

2.2.5 General description of system identification and optimal estimation

According to Di Ruscio [12], system identification can be defined as building mathematical models of systems based on observed data. Traditionally a set of model structures with some free parameters are specified and a prediction error (PE) measuring the difference between the observed outputs and the model outputs is optimized with respect to the free parameters. In general, this will result in a non-linear optimization problem in the free parameters even when a linear time invariant model is specified. A tremendous amount of research has been reported, resulting in the so called prediction error methods (PEM).

Ljung [8], sets up four points as the essence of system identification.

1. The observed data
    - This part includes removing trends and noise from observed data.
2. A set of candidate models
    - Selecting the proper method or model for the process to identify. Some models that can be chosen from is : Auto-regression with eXtra inputs (ARX), Auto-Regressive Moving Average with eXtra inputs (ARMAX), Output Error (OE), Box Jenkins (BJ). Subspace identification is another system identification method and two methods will be mentioned, N4SID and DSR. N4SID is a inbuilt MatLab system identification algorithm and DSR is a custom built system identification algorithm made by Di Ruscio[9].
3. A criterion of fit
    - Usually a prediction error criterion. Prediction error methods (PEM) are used for solving the problem of minimizing the prediction error criterion. An example of how to apply PEM to ordinary least square and recursive least square will be discussed. The Kalman filter algorithm will also be explained briefly.
4. Validation
    - There are several methods for validating the model, like leverage validation, cross validation and test set validation. There is also different methods for explaining the model accuracy, a common method used is the root mean square error of prediction (RMSEP). The validation methods and the RMSEP will be described briefly.

Subspace identification

Subspace identification resolves the problem of structure identification. This can be done by singular value decomposition (SVD) and projections of noise onto the matrices in a state space model. The DSR and N4SID methods are subspace identification methods.

Optimal estimation

Optimal estimation uses Prediction Error Methods (PEM) for optimizing the prediction error criterion. The ordinary least square (OLS) and recursive ordinary least square (ROLS) minimize a prediction error criterion to optimize the estimation of the resulting model. The DSR and N4SID methods gives Kalman filter estimates as a tool for optimizing the prediction error.

Parameter vector

A parameter vector θ is the unknown parameters in the process model. The parameter vector is used to set up an prediction error (PE) criterion. An example for a scalar deterministic system is shown in (2.17).

$$\begin{aligned} \bar{x}_{k+1} &= \overset{a}{\theta}_1 \bar{x}_k + \overset{b}{\theta}_2 u_k, \bar{x}_0 = \theta_5 \\ \bar{y}\left(\theta\right)_k &= \bar{x}_k + \overset{e}{\theta}_4 u_k \end{aligned} \tag{2.17}$$

where

$$\begin{aligned} \bar{x}_0 &= \text{Initial predicted state} \\ \bar{x}_k &= \text{Predicted state} \\ \bar{x}_{k+1} &= \text{Prediction of next state} \\ u_k &= \text{Input signal} \\ \theta &= \text{Parameter vector of unknown parameters} \\ \bar{y}\left(\theta\right)_k &= \text{Predicted output as a function of the unknown parameters } \theta \end{aligned}$$

and

$$\theta = \begin{bmatrix} \theta_1 \\ \theta_2 \\ \theta_3 \\ \theta_4 \end{bmatrix} = \begin{bmatrix} a \\ b \\ e \\ \bar{x}_0 \end{bmatrix}$$

See sub chapter in this chapter about state space model for more about state space models.

Prediction error (PE)

The prediction error is the error between the predicted output and the measured output. The prediction error can be put up as in equation (2.18).

$$\varepsilon_k = y_k - \bar{y}\left(\theta\right)_k \tag{2.18}$$

Prediction error criterion

Prediction error methods often uses a prediction error criterion $V_N\left(\theta\right)$ like shown in equation (2.19) for single output systems and (2.20) for multiple output systems.

$$V_N\left(\theta\right) = \frac{1}{N}\sum_{k=0}^{N-1} \varepsilon_k^2 \tag{2.19}$$

$$V_N\left(\theta\right) = \frac{1}{N}\sum_{k=0}^{N-1} \varepsilon_k^T \Lambda \varepsilon_k \tag{2.20}$$

where

$$\Lambda \text{ may be a weighting matrix, usually } \Lambda = I$$

Prediction error methods (PEM)

Prediction error methods is the term used for the methods that minimize the prediction error criterion. One such method is the recursive ordinary least squares (ROLS) method. Another method is using a Kalman filter. To minimize the prediction error, a prediction error criterion has to be sat up. The objective is to minimize the prediction error $V_N\left(\theta\right)$ with regards to the parameter vector estimate. This objective can be put up as in (2.21).

$$\hat{\theta}_N = \arg\min V_N\left(\theta\right) \tag{2.21}$$

where

$$\hat{\theta}_N \ = \text{The parameter vector that minimize the prediction error criterion}$$

Validation of the resulting model

Validation of the model attained from performing a system identification on process data is an important part for finding out and explain how good the model estimates the real process. Some methods for validation of the resulting model is mentioned below. Leverage and cross validation is mentioned briefly, but test set validation will be used as validation method in this thesis.

Leverage validation Leverage is a measure of the effect of an object on the model, which to a large extent is related to its distance from the model center. The leverage is scaled so that it always has a value between 0 and 1. An extreme object, far away from the model center, will have a high effect. A typical object, close to the model center will have a small effect. To be compared , the leverage validation apparently gives better results than cross validation. But Esbensen [11] states that the leverage corrected validation is a "quick and dirty" method. And he states that there are several situation in which grave distortions may arise, especially when dealing with special data structures where there is a strong colinearity. Leverage corrected validation is never to be used for the really important final validation. Leverage correction should only be used as a preliminary validation procedure and never for the final model assessment. Consequently it is often only used in the initial modeling stages to screen outliers, establish a homogenous data set for further calibration work. A usual choice is to use either test set or cross validation to validate the final model. For more details on leverage validation see Esbensen [11].

Cross validation When there is not enough data present to do test set validation, cross validation is a preferred method according to Esbensen [11]. Cross validation leaves out a part of the calibration data in a sequence to validate against the rest of the calibration data. Two methods of doing cross validation is full cross validation and segmented cross validation. Full cross validation is leaving out one object at the time in a sequence of running through all the objects. Segmented cross validation leaves at a segment of objects for each iterative step. For more details about cross validation see Esbensen [11].

Test set validation Test set validation is using a new data set for testing the model gotten from system identification. The data set used for making the model is called the calibration set. The data set used for testing or validating the model is called the test set. Esbensen [11] states that whenever possible, test set validation should be used for validating the model.

Measure of the prediction error There are many ways to describe the prediction error in the field of statistics and this is a large and advanced field. Going into detail in this subject is out of the scope of this thesis. A simple method for explaining the deviation between estimated output and the measured output will be used. A commonly used method for explaining the deviation of the model from the real data is the root mean square error of prediction (RMSEP). This method (2.22) is a way of defining how well a model corresponds to the real process.

$$RMSEP = \sqrt{residual\ variance} \tag{2.22}$$

where

$$residual\ variance = \frac{1}{n}\sum_{k=1}^{n}(\varepsilon_k)^2$$

and the prediction error (PE) is

$$\varepsilon_k = \hat{y}_k - y_k$$

and

$$n = \text{Number of samples (objects)}$$

2.2.6 The state space model

According Lie [13], a state space model is a set of first order ordinary differential state equations, describing the change in the states in the process. A state space model can be divided into a set of states (x), a set

of inputs (u), a set of known constants (θ) and a set of selected states as outputs (y). This can briefly be expressed as shown in (2.23) :

$$\frac{dx}{dt} = f(x, u; \theta) \tag{2.23}$$

Models on this form can be non-linear and needs an Ordinary Differential Equation (ODE) solver to compute a solution. The sets of ordinary differential state equations can be put up on matrix form for computational simplicity, when the problem can be considered linear. A state space model on matrix form can be made, assuming linear transition between the states.

Stochastic systems

Most real processes can be considered stochastic. Stochastic comes from the Greek word "*stochastikos*", which means : skillful in aiming [14]. A stochastic process is a process that has variables that can be considered random, like noise. The noise is often assumed to be fully stochastic, that means that the mean value of the noise is zero, giving that the noise is totally random. This sort of noise is called white noise. The noise can also be colored, that means that the noise can follow some pattern, but this is out of the scope of this thesis. A state space model on discrete matrix form, describing a stochastic process is shown in equation (2.24).

$$\begin{aligned} x_{k+1} &= Ax_k + Bu_k + Cv_k \\ y_k &= Dx_k + Eu_k + Fw_k \end{aligned} \tag{2.24}$$

where

$$\begin{aligned} x_k &= \text{Current states at discrete timestep } k \\ x_{k+1} &= \text{Next states at discrete timestep } k+1 \\ u_k &= \text{Control inputs} \\ v_k &= \text{Process noise} \\ w_k &= \text{Measurement noise} \end{aligned}$$

and

$$\begin{aligned} A &= \text{The state transition matrix} \\ B &= \text{The input matrix} \\ C &= \text{The external input matrix} \\ D &= \text{The output matrix} \\ E &= \text{The direct input to output matrix} \\ F &= \text{The direct external input to output matrix} \end{aligned}$$

The process noise is often assumed to be white noise, that is $E\left(v_k v_k^T\right) = 0$ and measurement noise $E\left(w_k w_k^T\right) = 0$. The transition matrix A, gives the linear transition/gradient for the states for each timestep k. The input matrix B, is a weighting matrix for the control inputs. The external input matrix C, is the weighting matrix for the process noise. The output matrix D, is used for determining/weighting the selected set of state/states as outputs. The direct input to output matrix E, is the feedforward matrix, describes the direct effect of the control input on the output. Not all systems has this direct effect from the input to the output, then this matrix is ignored. The direct external input to output matrix F, is the weighting matrix for the measurement noise.

Deterministic systems

A deterministic system, is a system where the outputs can be determined based on the initial states and the present control inputs. A deterministic system can be put up like in equation (2.25).

$$\begin{aligned} x_{k+1} &= Ax_k + Bu_k \\ y_k &= Dx_k + Eu_k \end{aligned} \tag{2.25}$$

Autonomous systems

Autonomous systems are systems that stabilize themselves. An autonomous system can be put up like in equation (2.26).

$$\begin{aligned} x_{k+1} &= Ax_k \\ y_k &= Dx_k \end{aligned} \tag{2.26}$$

Observable, controllable, detectable and stabilizable control systems

According to Di Ruscio [12], an observable system is a system where a change in the process states can be observed in the output states. The observability matrix can be put up like in (2.27), if this matrix is non-singular then the system is observable. This can be checked by checking that the rank of the observability matrix (2.28) equals n.

$$O_L = \begin{bmatrix} D \\ DA \\ DA^2 \\ \vdots \\ DA^{L-1} \end{bmatrix} \in \mathbb{R}^{Lm \times n} \tag{2.27}$$

where

$$\begin{gathered} L = \text{Number of block rows} \\ rank(O_L) = n \\ L \geq L_{\min} \end{gathered} \tag{2.28}$$

where the minimal number of block rows $L_{\min}$ is defined by (2.29)

$$L_{\min} \stackrel{def}{=} \begin{cases} n - rank(D) + 1 & \text{when } m < n \\ 1 & \text{when } m > n \end{cases} \tag{2.29}$$

If the system is not observable and the states that is not observable is stable, then the system is called detectable.

According to Di Ruscio [12], a system is called controllable when a change is the inputs, gives a change in the states. The controllability matrix (2.30) is a combination of the state transition matrix A and the input matrix B for deterministic systems. For stochastic systems, the external input matrix C (2.31) has to be added. The system is controllable when the rank of the controllability matrix (2.32) equals n.

$$C_L = \begin{bmatrix} B & AB & A^2B & \cdots & A^{L-1}B \end{bmatrix} \tag{2.30}$$

$$C_L = \begin{bmatrix} BC & ABC & A^2BC & \cdots & A^{L-1}BC \end{bmatrix} \tag{2.31}$$

where

$$\begin{gathered} L = \text{Number of block rows} \\ rank(C_L) = n \\ L \geq L_{\min} \end{gathered} \tag{2.32}$$

where the minimal number of block rows $L_{\min}$ is defined by (2.33) or (2.34).

$$L_{\min} \stackrel{def}{=} \begin{cases} n - rank(B) + 1 & \text{when } m < n \\ 1 & \text{when } m > n \end{cases} \tag{2.33}$$

$$L_{\min} \stackrel{def}{=} \begin{cases} n - rank(BC) + 1 & \text{when } m < n \\ 1 & \text{when } m > n \end{cases} \tag{2.34}$$

If the system is not controllable and the states that are not controllable is stable, then the system is stabilizable.

2.2.7 Prediction error methods

Prediction error methods is the term used for the methods that minimize the prediction error criterion. One such method is the recursive ordinary least squares (ROLS) method. Another method is using a Kalman filter. To minimize the prediction error, a prediction error criterion can to be put up.

PEM often uses a PE criterion $V_N(\theta)$ like shown in equation (2.35) for single output systems and (2.36) for multiple output systems.

$$V_N(\theta) = \frac{1}{N}\sum_{k=0}^{N-1}\varepsilon_k^2 \tag{2.35}$$

$$V_N(\theta) = \frac{1}{N}\sum_{k=0}^{N-1}\varepsilon_k^T \Lambda \varepsilon_k \tag{2.36}$$

where

Λ may be a weighting matrix, usually $\Lambda = I$

The objective is to minimize the prediction error $V_N(\theta)$ with regards to the parameter vector estimate. This objective can be put up as in (2.37).

$$\hat{\theta}_N = \arg\min V_N(\theta) \tag{2.37}$$

where

$\hat{\theta}_N$ = The parameter vector that minimize the prediction error criterion

The Least Squares method

The Ordinary Least square method The Ordinary Least Square (OLS) method is a common curve fitting method. The OLS method is a method for finding the curve that has the smallest squared error related to the measurement points. The data matrix X is a matrix that includes all influencing inputs relating to the output. The output matrix Y is the matrix or vector containing the measured outputs. In this manor the OLS method gives a function that explains the equipment/process that is being modeled, based on measured inputs and outputs. This equipment can be valves or any equipment/process with static properties. The OLS method can describe any curve given enough regression coefficients. The OLS method is shown in equation (2.38)

$$\begin{aligned} Y &= X \cdot B + e \\ X^T Y &= \left(X^T \cdot X\right) B + X^T e \\ E\left(X^T \cdot e^T\right) &= 0 \\ X^T Y &= \left(X^T \cdot X\right) B \\ B &= \left(X^T \cdot X\right)^{-1}\left(X^T Y\right) \end{aligned} \tag{2.38}$$

where

$$\begin{aligned} Y &= \text{Measured output data matrix} \\ X &= \text{Measured input data matrix} \\ e &= \text{Noise, here assumed to be white noise} \\ B &= \text{Vector containing regression coefficients} \end{aligned}$$

This kind of OLS gives a model on polynomial form, like (2.39) :

$$\bar{y}_k = b_1 \cdot x_1 + b_2 \cdot x_2 + ... + b_N \cdot x_n \tag{2.39}$$

where

$$\begin{aligned} \bar{y}_k &= \text{Predicted output} \\ N &= \text{Row number for regression coefficient} \\ n &= \text{Column number of the input matrix } X \end{aligned}$$

Another way of doing an OLS is to define a prediction error criterion and then try to minimize it. This is the same as above, trying to find the least square fit. The similarity can be explained through equation (2.40), where the objective is to minimize the square of the prediction error.

$$V_N(\theta) = ||y_k - \bar{y}_k(\theta)||^2 = (Y - X\theta)^T (Y - X\theta) \tag{2.40}$$

where

$$\begin{aligned} y_k &= Y \\ \varphi_k &= X \\ \theta &= B \\ \bar{y}_k(\theta) &= \varphi_k \theta \end{aligned}$$

If a real measurement parameter vector θ_0 is introduced, the regression coefficients are put into a parameter vector called θ and a matrix containing both inputs and outputs are put into a matrix φ_k, then it is possible to put up a OLS for the state space form. The OLS for the real measurement can then be put up like in equation (2.41).

$$y_k = \varphi_k \theta_0 + e_k \tag{2.41}$$

where

$$\begin{aligned} y_k &= \text{Measured output} \\ \varphi_k &= \text{Matrix of measured inputs and outputs} \\ \theta_0 &= \text{Real process parameters} \\ e_k &= \text{Noise, assumed to be white noise} \end{aligned}$$

The prediction error can now be introduced (2.42) as the squared error between measured and predicted output.

$$\begin{aligned} \varepsilon_k &= y_k - \bar{y}_k(\theta) \\ \varepsilon_k &= y_k - \varphi_k \theta \end{aligned} \tag{2.42}$$

by using the prediction error criterion (2.36), an OLS estimate can be found by setting the partial derivative of the prediction error with regards to parameter vector θ to be zero.

$$\begin{aligned} V_N(\theta) &= \frac{1}{N} \sum_{k=0}^{N-1} \varepsilon_k^T \Lambda \varepsilon_k \\ \frac{\partial (V_N(\theta))}{\partial \theta} &= 0 \end{aligned}$$

Solving this gives, start with setting up the expression :

$$\frac{\partial (V_N(\theta))}{\partial \theta} = \frac{1}{N} \sum_{k=0}^{N-1} \frac{\partial \varepsilon_k}{\partial \theta} \cdot \frac{\partial \left(\varepsilon_k^T \Lambda \varepsilon_k\right)}{\partial \varepsilon_k}$$

Solving each partial derivative term :

$$\begin{aligned} \frac{\partial \left(\varepsilon_k^T \Lambda \varepsilon_k\right)}{\partial \varepsilon_k} &= 2\Lambda \varepsilon_k \\ \varepsilon_k &= y_k - \varphi_k \theta \\ \frac{\partial \varepsilon_k}{\partial \theta} &= \frac{\partial (y_k - \varphi_k \theta)}{\partial \theta} = -\varphi_k^T \end{aligned}$$

Setting the solution of the partial derivatives into the equation again :

$$\begin{aligned}\frac{\partial\left(V_N\left(\theta\right)\right)}{\partial\theta} &= \frac{1}{N}\sum_{k=0}^{N-1}-\varphi_k^T\left(2\Lambda\varepsilon_k\right)\\ \frac{\partial\left(V_N\left(\theta\right)\right)}{\partial\theta} &= -2\cdot\frac{1}{N}\sum_{k=0}^{N-1}\varphi_k^T\Lambda\left(y_k-\varphi_k\theta\right)\end{aligned}$$

Solving the prediction error criterion for when it is put to zero :

$$\begin{aligned}-2\cdot\frac{1}{N}\sum_{k=0}^{N-1}\varphi_k^T\Lambda\left(y_k-\varphi_k\theta\right) &= 0\\ -2\cdot\frac{1}{N}\sum_{k=0}^{N-1}\varphi_k^T\Lambda y_k-\varphi_k^T\Lambda\varphi_k\theta &= 0\\ -\frac{2}{N}\sum_{k=0}^{N-1}\varphi_k^T\Lambda y_k+\frac{2}{N}\sum_{k=0}^{N-1}\varphi_k^T\Lambda\varphi_k\theta &= 0\end{aligned}$$

Solving for the OLS estimate of the parameter vector θ

$$\begin{aligned}\frac{2}{N}\sum_{k=0}^{N-1}\varphi_k^T\Lambda\varphi_k\theta &= \frac{2}{N}\sum_{k=0}^{N-1}\varphi_k^T\Lambda y_k\\ \sum_{k=0}^{N-1}\varphi_k^T\Lambda\varphi_k\theta &= \sum_{k=0}^{N-1}\varphi_k^T\Lambda y_k\\ \theta &= \left(\sum_{k=0}^{N-1}\varphi_k^T\Lambda\varphi_k\right)^{-1}\left(\sum_{k=0}^{N-1}\varphi_k^T\Lambda y_k\right)\end{aligned}$$

The OLS estimate of the parameter vector $\hat{\theta}_N$ using a prediction error method then gives (2.43).

$$\hat{\theta}_N=\left(\sum_{k=0}^{N-1}\varphi_k^T\Lambda\varphi_k\right)^{-1}\left(\sum_{k=0}^{N-1}\varphi_k^T\Lambda y_k\right) \tag{2.43}$$

Recursive Ordinary Least Squares (ROLS) method The recursive ordinary least square (ROLS) method is a method for optimizing the ordinary least square (OLS) result. The OLS method gives an ARX model, while the ROLS gives an ARMAX model. The ROLS and the Kalman filter has similarities, they will only be discussed briefly. The ROLS method starts with the result of the OLS (2.43). To stress the dependence for $\hat{\theta}$ with regards to time t, the N is replaced with t like in equation (2.44) below. For convenience the discrete timestep k is shifted to start at $k=1$ instead of $k=0$.

$$\hat{\theta}_t=\left(\sum_{k=1}^{t}\varphi_k^T\Lambda\varphi_k\right)^{-1}\left(\sum_{k=1}^{t}\varphi_k^T\Lambda y_k\right) \tag{2.44}$$

A covariance matrix P_t can be defined like in (2.45). The covariance matrix P_t can be divided into a series of the past input observation data from P_{t-1} ranging from $k=1$ to $k=(t-1)$ (2.46) and a part containing the present input observation data. Combining them gives equation (2.47).

$$P_t=\left(\sum_{k=1}^{t}\varphi_k^T\Lambda\varphi_k\right)^{-1} \tag{2.45}$$

$$P_{t-1} = \left(\sum_{k=1}^{t-1} \varphi_k^T \Lambda \varphi_k \right)^{-1} \tag{2.46}$$

$$P_t = \left(\sum_{k=1}^{t-1} \varphi_k^T \Lambda \varphi_k + \varphi_t^T \Lambda \varphi_t \right)^{-1} \tag{2.47}$$

The covariance matrix P_t can be computed recursively through the equation for the inverse of P_t (2.48) at each discrete timestep.

$$P_t^{-1} = \sum_{k=1}^{t-1} \varphi_k^T \Lambda \varphi_k + \varphi_t^T \Lambda \varphi_t \tag{2.48}$$

The equation for P_t^{-1} can be written as (2.50) through the relationship of (2.48) and (2.49).

$$P_{t-1}^{-1} = \sum_{k=1}^{t-1} \varphi_k^T \Lambda \varphi_k \tag{2.49}$$

$$P_t^{-1} = P_{t-1}^{-1} + \varphi_t^T \Lambda \varphi_t \tag{2.50}$$

The basic idea is to compute the optimal parameter estimate $\hat{\theta}_t$ with the help of an optimized covariance matrix P_t (2.51).

$$\hat{\theta}_t = P_t \sum_{k=1}^{t} \varphi_k^T \Lambda y_k \tag{2.51}$$

By dividing the parameter estimate $\hat{\theta}_t$ into a series of the past observation data from $\hat{\theta}_{t-1}$ ranging from $k = 1$ to $k = (t-1)$ (2.52) and a part containing the present observation data. Combining them gives equation (2.54).

$$\hat{\theta}_{t-1} = P_{t-1} \sum_{k=1}^{t-1} \varphi_k^T \Lambda y_k \tag{2.52}$$

$$P_{t-1}^{-1} \hat{\theta}_{t-1} = \sum_{k=1}^{t-1} \varphi_k^T \Lambda y_k \tag{2.53}$$

$$\hat{\theta}_t = \left(P_t \sum_{k=1}^{t-1} \varphi_k^T \Lambda y_k + \varphi_t^T \Lambda y_t \right) \tag{2.54}$$

The parameter estimate $\hat{\theta}_t$ can be put up as (2.55) through the relationships (2.53) and (2.54).

$$\hat{\theta}_t = P_t \left(P_{t-1}^{-1} \hat{\theta}_{t-1} + \varphi_t^T \Lambda y_t \right) \tag{2.55}$$

The relationship given in (2.50) can be rewritten to (2.53) for simplicity.

$$P_{t-1}^{-1} = P_t^{-1} - \varphi_t^T \Lambda \varphi_t \tag{2.56}$$

Substituting (2.56) into (2.55) gives (2.57).

$$\hat{\theta}_t = P_t \left(\left(P_t^{-1} - \varphi_t^T \Lambda \varphi_t \right) \hat{\theta}_{t-1} + \varphi_t^T \Lambda y_t \right) \tag{2.57}$$

Rearranging (2.57) gives (2.58).

$$\begin{aligned}
\hat{\theta}_t &= P_t P_t^{-1} \hat{\theta}_{t-1} - \varphi_t^T \Lambda \varphi_t \hat{\theta}_{t-1} + P_t \varphi_t^T \Lambda y_t \\
\hat{\theta}_t &= I \hat{\theta}_{t-1} - P_t \varphi_t^T \Lambda \varphi_t \hat{\theta}_{t-1} + P_t \varphi_t^T \Lambda y_t \\
\hat{\theta}_t &= \hat{\theta}_{t-1} + P_t \varphi_t^T \Lambda y_t - P_t \varphi_t^T \Lambda \varphi_t \hat{\theta}_{t-1} \\
\hat{\theta}_t &= \hat{\theta}_{t-1} + P_t \varphi_t^T \Lambda \left(y_t - \varphi_t \hat{\theta}_{t-1} \right)
\end{aligned} \tag{2.58}$$

This can rewritten as (2.59).

$$\hat{\theta}_t = \hat{\theta}_{t-1} + K_t \left(y_t - \varphi_t \hat{\theta}_{t-1} \right) \tag{2.59}$$

where

$$K_t = P_t \varphi_t^T \Lambda$$

The ROLS algorithm is an two step iterative process. Step 1 involves setting the initial values of covariance matrix P_t and the parameter estimate θ_t. Step 2 involves updating the values of covariance matrix P_t and the parameter estimate θ_t.Step 2 is repeated until finished. At each timestep the inverse of the covariance matrix P_t (2.60) is computed.

$$P_t = \left(P_{t-1}^{-1} + \varphi_t^T \Lambda \varphi_t \right)^{-1} \tag{2.60}$$

The computation of the inverse of the covariance matrix P_t (2.60) can be done by using the matrix inversion lemma (2.61).

$$(A + BCD)^{-1} = A^{-1} A^{-1} B \left(C^{-1} + D A^{-1} B \right)^{-1} D A^{-1} \tag{2.61}$$

This gives (2.62).

$$\begin{aligned} P_t &= \left(P_{t-1}^{-1} \right)^{-1} \left(P_{t-1}^{-1} \right)^{-1} \varphi_t^T \left(\Lambda^{-1} + \varphi_t \left(P_{t-1}^{-1} \right)^{-1} \varphi_t^T \right)^{-1} \varphi_t \left(P_{t-1}^{-1} \right)^{-1} \\ P_t &= P_{t-1} P_{t-1} \varphi_t^T \left(\Lambda^{-1} + \varphi_t P_{t-1} \varphi_t^T \right)^{-1} \varphi_t P_{t-1} \end{aligned} \tag{2.62}$$

The parameter estimate $\hat{\theta}_t$ (2.59) can then be updated. It can be proved that the optimal weighting matrix Λ is the inverse of the measurements noise covariance matrix W. This can be proved through a comparison with the Kalman filter. See Di Ruscio [15] chapter 12.7.1 *"Comparing ROLS and the Kalman filter"* for proof.

Kalman filter The Kalman filter is a prediction error method. The aim is to minimize the prediction error given by the innovation process ε_k (2.63). The innovation form can be put up like (2.64).

$$\varepsilon_k = (y_k - \bar{y}_k) \tag{2.63}$$

The innovation form

$$\left.\begin{aligned} \bar{y}_k &= D \bar{x}_k \\ \bar{x}_{k+1} &= A \bar{x}_k + B u_k + \tilde{K} \varepsilon_k \end{aligned}\right\} \tag{2.64}$$

where

$$\begin{aligned} \bar{x}_{k+1} &= A \left(\bar{x}_k + K \left(y_k - \bar{y}_k \right) \right) + B u_k \\ \bar{x}_{k+1} &= A \bar{x}_k + A K \left(y_k - \bar{y}_k \right) + B u_k \\ \bar{x}_{k+1} &= A \bar{x}_k + \tilde{K} \left(y_k - \bar{y}_k \right) + B u_k \end{aligned}$$

The apriori-aposteriori method The apriori-aposteriori form is a kalman filter method that estimates the states using the present output and input parameters. First we need an estimated initial state $\bar{x}_0$. A usual choice of the initial estimated states is $\bar{x}_0 = 0$ or the estimated states value for steady state of the process $\bar{x}_0 = x_s$, if the steady states are known.

The algorithm for calculating the estimates is like the following :

- Step 1 : Calculating the estimated output based on the estimated states $\bar{x}_k$. The estimated states $\bar{x}_k$ is called the apriori estimates.

$$\bar{y}_k = D \bar{x}_k$$

- Step 2 : Get an updated optimal estimate of the states $\hat{x}_k$ by adjusting the present estimate of the states $\bar{x}_k$. This is done by adding an adjusting factor $\tilde{K} \left(y_k - \bar{y}_k \right)$. Where $\tilde{K}$ is the innovation kalman gain for the innovation process $\left(y_k - \bar{y}_k \right)$. The innovation process is the prediction error $\varepsilon_k = (y_k - \bar{y}_k)$ between the real measured output y_k and the estimated output $\bar{y}_k$. $\hat{x}_k$ is called the aposteriori estimate and is the optimal estimate.

$$\hat{x}_k = \bar{x}_k + \tilde{K} \left(y_k - \bar{y}_k \right)$$

- Step 3 : Get a prediction of the next apriori estimated state $\bar{x}_{k+1}$. This is done by using the present optimal aposteriori estimate $\hat{x}_k$. This prediction of the next apriori estimated state $\bar{x}_{k+1}$, will then be used as $\bar{x}_k$ in the next iteration of this iterative process starting at step 1 again.

$$\bar{x}_{k+1} = A\hat{x}_k + Bu_k$$

The apriori-aposteriori kalman filter method gives the present optimal aposteriori estimate $\hat{x}_k$.

2.2.8 Principle Component Regression (PCR)

This small sub chapter on principal Component regression (PCR) is based on lecture notes in system identification, given by professor David Di Ruscio in the spring semester 2007 at the university college of Telemark. Before doing PCR a principle component analysis (PCA) of the data matrix x needs to be performed. PCA is done by doing a singular value decomposition and choosing appropriate realization of the scores and loadings of the data matrix x. PCA and PCR are least squares methods which can be used when $x^T x$ is singular and when OLS estimate does nor exists. ($B_{OLS} = \left(x^T x\right)^{-1} x^T x$).

Singular value decomposition (SVD)

Singular value decomposition is a method for breaking down a data matrix X. The eigenvalue decomposition (2.65) uses the same basis E_v for row and column space, but the SVD uses two different bases V, U. The eigenvalue decomposition generally does not use an orthonormal basis, but the SVD does. The eigenvalue decomposition is only defined for square matrices, but the SVD exists for all matrices.

$$X = E_v \Lambda E_v^{-1} \tag{2.65}$$

For symmetric positive definite matrices A, the eigenvalue decomposition and the SVD are equal [16]. Doing a SVD on a data matrix X will give an orthogonal matrix U, a diagonal singular value matrix S and an orthogonal matrix V^T. The relationship between the eigenvalue decomposition and the SVD can be explained as in (2.66), (2.67), (2.68) and (2.69), when matrix X is symmetric positive definite.

$$X = USV^T \tag{2.66}$$

where

$$\text{The columns of } U \text{ is the eigenvectors } (E_v) \text{ of } X \cdot X^T \tag{2.67}$$

and

$$\text{The columns of } V \text{ is the eigenvectors } \left(E_v^{-1}\right) \text{ of } X^T \cdot X \tag{2.68}$$

and

$$\text{The diagonal of } S \text{ consists of the squareroot of the eigenvalues } (\Lambda) \text{ of } X \cdot X^T \text{ or } X^T \cdot X \tag{2.69}$$

The matrices U and V^T are orthogonal, this gives that one can use the relationship (2.70) and (2.71).

$$U \cdot U^T = I \tag{2.70}$$
$$V^T \cdot V = I \tag{2.71}$$

Otherwise if X is a $m \times n$ matrix the SVD can be explained as decomposing X, into a $m \times m$ orthogonal U matrix, a $m \times n$ diagonal S matrix and a $n \times n$ orthogonal V matrix. An example is shown in (2.72)

$$\overbrace{\begin{bmatrix} x_{11} & x_{12} \\ x_{21} & x_{22} \\ x_{31} & x_{32} \end{bmatrix}}^{X} = \overbrace{\begin{bmatrix} u_{11} & u_{12} & u_{13} \\ u_{21} & u_{22} & u_{23} \\ u_{31} & u_{32} & u_{33} \end{bmatrix}}^{U} \cdot \overbrace{\begin{bmatrix} s_1 & 0 \\ 0 & s_2 \\ 0 & 0 \end{bmatrix}}^{S} \cdot \overbrace{\begin{bmatrix} v_{11} & v_{21} \\ v_{12} & v_{22} \end{bmatrix}}^{V^T} \tag{2.72}$$

The diagonal singular value matrix S, gives the singular values for the model. The rank of this matrix gives the number of singular values. This can be related to number of principal components in chemometrics.

Chemometrics focus more on the covariance related to the principal components than the actual decomposing of the data and also use other techniques for decomposition of the data like for instance total least square. Usually the diagonal singular value matrix S contains small singular values, which is consider noise. This noise is often called residuals. The SVD is therefore often dived in two parts, one relating to the model (2.74) and one relating to noise (2.75). This splitting can be shown as in equation (2.73).

$$X = USV^T = \begin{bmatrix} U_1 & U_2 \end{bmatrix} \begin{bmatrix} S_1 & 0 \\ 0 & S_2 \end{bmatrix} \begin{bmatrix} V_1 & V_2 \end{bmatrix}^T \tag{2.73}$$

this can be rewritten as :

$$\begin{aligned} X &= U_1 S_1 V_1^T + U_2 S_2 V_2^T \\ X &\approx U_1 S_1 V_1^T \end{aligned}$$

where

$$U_1 S_1 V_1^T \text{ is considered the data used for building the model} \tag{2.74}$$

and

$$U_2 S_2 V_2^T \text{ is considered the residual data, and discarded for usage in the model} \tag{2.75}$$

Principal component analysis (PCA)

Principal component analysis (PCA) can be done by performing SVD, like mentioned above. PCA is simply an data analysis of the data matrix X. PCA is, when used for the purpose of using principal component regression (PCR), used to analyze the rank of the diagonal singular matrix S. In chemometrics PCA is used more extensively for interpreting relationships in the data. As a curiosity the relationship with chemometrics can be shown as in (2.76) and (2.77).

Relationship between SVD and PCA in chemometrics :

$$X = U_1 S_1 V_1^T + U_2 S_2 V_2^T \tag{2.76}$$
$$X = T \cdot P^T + G \tag{2.77}$$

where

$$\begin{aligned} T &= U_1 S_1 -> \text{score vector} \\ P &= V_1^T -> \text{loading vector} \\ G &= U_2 S_2 V_2^T, \text{ considered as residuals} \end{aligned}$$

2.2.9 PCR

Principal component regression (PCR) is the building of a system identification model after performing a PCA. The problem can now be put up (2.78) as with the ARX-model (OLS).

$$y = XB_{PCR} + E \tag{2.78}$$

use the PCA approximation of x, i.e., $x \approx U_1 S_1 V_1^T$

$$y = U_1 S_1 V_1^T \cdot B_{PCR} + E$$

Then solve the equation with regards to the regression coefficient vector B_{PCR} :

$$\begin{aligned} U_1^T \cdot |y &= U_1 S_1 V_1^T \cdot B_{PCR} + E \\ U_1^T y &= U_1^T U_1 S_1 V_1^T \cdot B_{PCR} + U_1^T E \\ U_1^T U_1 &= I \\ U_1^T y &= S_1 V_1^T \cdot B_{PCR} + U_1^T E \\ S_1^{-1} \cdot |U_1^T y &= S_1 V_1^T \cdot B_{PCR} + U_1^T E \\ S_1^{-1} U_1^T y &= S_1^{-1} S_1 V_1^T \cdot B_{PCR} + S_1^{-1} U_1^T E \\ S_1^{-1} S_1 &= I \\ V_1 \cdot |S_1^{-1} U_1^T y &= V_1^T \cdot B_{PCR} + S_1^{-1} U_1^T E \\ V_1 S_1^{-1} U_1^T y &= V_1 V_1^T B_{PCR} + S_1^{-1} U_1^T E \\ V_1 V_1^T &= I \text{ and } S_1^{-1} U_1^T E \approx 0 \end{aligned}$$

Finally the PCR regressors can be found in the regression vector B_{PCR}

$$B_{PCR} = V_1 S_1^{-1} U_1^T y$$

2.2.10 Partial Least Squares Regression (PLS)

According to Esbensen [11], PLS claims to do the same job as PCR, only with fewer bilinear components. Further Di ruscio [15] states that the PLS method for univariate data (usually denoted PLS1) is optimal in a prediction sense. Unfortunately (or not), the PLS algorithm for multivariate data (usually denoted PLS2 in the literature) is not optimal in the same way as PLS1. It is often judged that PLS has good predictive properties. This statement is based on experience and numerous applications. This may well be true. Di Ruscio further states that he believes the predictive performance of PLS1 and PLS2 is different. The reason for this is that PLS1 is designed to be optimal on the identification data, while PLS2 is not. If the model structure is correct and time invariant, then PLS1 would also be good for prediction. Di Ruscio [15] propose a new method that combines the predictive properties of PLS1 and PLS2. This method combines the conjugate gradient method and PLS. This new method, called CPLS has better prediction properties than both PLS1 and PLS2.

Di Ruscio [15] propose this CPLS method :

$$B_{CPLS} = K_a \left(K_a^T X^T X \right)^{-1} K_a X^T Y$$

where

$$\begin{aligned} K_a &= \begin{bmatrix} A & AB & A^2B & ... & A^{a-1}B \end{bmatrix} \\ A &= X^T X \\ B &= X^T Y \end{aligned}$$

2.2.11 MatLaB N4SID system identification algorithm

The N4SID algorithm is a part of the MatLab system identification toolbox [17]. The N4SID is a subspace identification method. It estimate state space models on innovations form (2.79). Both time-domain and frequency-domain input signals are supported.

$$\left.\begin{aligned} x_{k+1} &= Ax_k + Bu_k + K\varepsilon_k \\ y_k &= Dx_k + Eu_k + \varepsilon_k \end{aligned}\right\} \tag{2.79}$$

where

$$\begin{aligned} K &= \text{Kalman innovations gain} \\ \varepsilon_k &= \text{The innovation process } (y_k - \bar{y}_k) \end{aligned}$$

The N4SID has the opportunity to set the direct input to output matrix $E = 0$, when there is no direct coupling in the process from the inputs to the outputs. The order of the model can be set, with the option to choose the "best" model order by giving a range of orders as input. Time delays can be set, when using time-domain data. An indication of the uncertainty can be stored in a hidden state space model containing covariance information. The algorithm has the option to make the model focus on prediction, simulation or stability. It is possible to choose from two methods of weighting the matrices in the SVD. The construction of the algorithm is based on a paper by Ljung[10].

2.2.12 The combined Deterministic and Stochastic system identification and Realization (DSR) method

The DSR method is a subspace identification method like N4SID. The DSR divides the data into a horizon J to the past and a prediction horizon L into the future. The DSR uses the state space form on innovation form like in equation (2.80). The reason for this is that the DSR can estimate the C and F matrices, while the N4SID cannot. Equation (2.80) can easily be rewritten to (2.81), where the Kalman innovation gain can be attained through the relationship shown in(2.82).

$$\left.\begin{array}{c} x_{k+1} = Ax_k + Bu_k + Ce_k \\ y_k = Dx_k + Eu_k + Fe_k \end{array}\right\} \tag{2.80}$$

$$\left.\begin{array}{c} x_{k+1} = Ax_k + Bu_k + \tilde{K}\varepsilon_k \\ y_k = Dx_k + Eu_k + \varepsilon_k \end{array}\right\} \tag{2.81}$$

where

$$\tilde{K} = CF \cdot F^{-1} \tag{2.82}$$

where

$$\begin{array}{rcl} CF & = & \text{Covariance matrix for } F \\ F & = & \text{External direct input to output} \\ \varepsilon_k & = & y_k - \bar{y}_k, \text{ innovation process} \\ \tilde{K} & = & AK, \text{ Kalman innovation gain} \\ K & = & \text{Kalman gain} \\ A & = & \text{State transition matrix} \end{array}$$

From the state space on innovation form (2.80) it is possible to set up a matrix equation (2.83).

$$Y_{J|L} = O_L X_J + H_L^d U_{J|L} + H_L^s E_{J|L} \tag{2.83}$$

Setting up the extended output matrix equation

$$\begin{array}{rcl} x_{k+1} & = & Ax_k + Bu_k + Ce_k, x_0 = known \\ y_k & = & Dx + Eu_k + Fe_k \end{array}$$

With a prediction horizon of $L = 4$ this stochastic state space model can be put up like an iterative process :

$$\begin{array}{rcl} x_0 & = & known \\ y_0 & = & Dx_0 + Eu_0 + Fe_0 \\ x_{0+1} & = & Ax_0 + Bu_0 + Ce_0 \\ y_1 & = & Dx_1 + Eu_1 + Fe_1 = D\left(Ax_0 + Bu_0 + Ce_0\right) + Eu_1 + Fe_1 \\ x_{1+1} & = & Ax_1 + Bu_1 + Ce_1 = A\left(Ax_0 + Bu_0 + Ce_0\right) + Bu_1 + Ce_1 \\ y_2 & = & Dx_2 + Eu_2 + Fe_2 = D\left(A\left(Ax_0 + Bu_0 + Ce_0\right) + Bu_1 + Ce_1\right) + Eu_2 + Fe_2 \\ x_{2+1} & = & Ax_2 + Bu_2 + Ce_2 = A\left(A\left(Ax_0 + Bu_0 + Ce_0\right) + Bu_1 + Ce_1\right) + Bu_2 + Ce_2 \\ y_3 & = & Dx_3 + Eu_3 + Fe_3 = D\left(A\left(A\left(Ax_0 + Bu_0 + Ce_0\right) + Bu_1 + Ce_1\right) + Bu_2 + Ce_2\right) + Eu_3 + Fe_3 \end{array}$$

Summarize this :

$$\begin{aligned}
x_0 &= known \\
y_0 &= Dx_0 + Eu_0 + Fe_0 \\
x_1 &= Ax_0 + Bu_0 + Ce_0 \\
y_1 &= DAx_0 + DBu_0 + DCe_0 + Eu_1 + Fe_1 \\
x_2 &= A^2x_0 + ABu_0 + ACe_0 + Bu_1 + Ce_1 \\
y_2 &= DA^2x_0 + DABu_0 + DACe_0 + DBu_1 + DCe_1 + Eu_2 + Fe_2 \\
x_3 &= A^3x_0 + A^2Bu_0 + A^2Ce_0 + ABu_1 + ACe_1 + Bu_2 + Ce_2 \\
y_3 &= DA^3x_0 + DA^2Bu_0 + DA^2Ce_0 + DABu_1 + DACe_1 + DBu_2 + DCe_2 + Eu_3 + Fe_3
\end{aligned}$$

Can see that the model can be set up as an iterative function of the initial state x_0 and the past and present inputs and the past and present noise. Putting this up on matrix form gives (2.84).

$$\overbrace{\begin{bmatrix} y_0 \\ y_1 \\ y_2 \\ y_3 \end{bmatrix}}^{y_{0|4}} = \overbrace{\begin{bmatrix} D \\ DA \\ DA^2 \\ DA^3 \end{bmatrix}}^{O_4} x_0 + \overbrace{\begin{bmatrix} E & 0 & 0 & 0 \\ DB & E & 0 & 0 \\ DAB & DB & E & 0 \\ DA^2B & DAB & DB & E \end{bmatrix}}^{H_4^d} \cdot \overbrace{\begin{bmatrix} u_0 \\ u_1 \\ u_2 \\ u_3 \end{bmatrix}}^{u_{0|4}} + \overbrace{\begin{bmatrix} F & 0 & 0 & 0 \\ DC & F & 0 & 0 \\ DAC & DC & F & 0 \\ DA^2C & DAC & DC & F \end{bmatrix}}^{H_4^s} \cdot \overbrace{\begin{bmatrix} e_0 \\ e_1 \\ e_2 \\ e_3 \end{bmatrix}}^{e_{0|4}} \tag{2.84}$$

where

$$\begin{aligned}
u_{0|4} &= \text{The input vector} \\
e_{0|4} &= \text{The noise vector} \\
x_0 &= \text{Initial state} \\
O_4 &= \text{The observability matrix} \\
H_4^d &= \text{Lower triangular Toeplitz matrix for (A,B,D,E)} \\
H_4^s &= \text{Lower triangular Toeplitz matrix for (A,C,D,F)} \\
y_{0|4} &= \text{The outputs}
\end{aligned}$$

By extending the output vector $y_{J|L}$,the input vector $u_{J|L}$ and the noise vector $e_{J|L}$ to the hankel matrices $Y_{J|L}, U_{J|L}$ and $E_{J|L}$ respectively, we will end up with the extended output matrix equation (2.83).

$$Y_{J|L} = O_L X_J + H_L^d U_{J|L} + H_L^s E_{J|L}$$

where $Y_{J|L}$ is a hankel matrix containing the past outputs and future outputs. The matrix has the form (2.85).

$$Y_{J|L} = \begin{bmatrix} y_J & y_{J+1} & \cdots & y_{J+K-1} \\ y_{J+1} & y_{J+2} & \cdots & y_{J+K} \\ \vdots & \vdots & \ddots & \vdots \\ y_{J+L-1} & y_{J+L} & \cdots & y_{J+K+L-2} \end{bmatrix} \tag{2.85}$$

O_L is the extended observability matrix (2.86)

$$O_L = \begin{bmatrix} D \\ DA \\ \vdots \\ DA^{L-1} \end{bmatrix} \tag{2.86}$$

X_J is the past states to the future states(2.87)

$$X_J = \begin{bmatrix} x_J & x_{J+1} & \cdots & x_{J+K-1} \end{bmatrix} \tag{2.87}$$

H_L^d is a toeplitz matrix for the output matrix D, the transition matrix A, the input matrix B and the direct input to output matrix E (2.88).

$$H_L^d = \begin{bmatrix} E & 0 & 0 & \cdots & 0 \\ DB & E & 0 & \cdots & 0 \\ DAB & DB & E & \cdots & 0 \\ \vdots & \vdots & \vdots & \ddots & \vdots \\ DA^{L-2}B & DA^{L-3}B & DA^{L-4}B & \cdots & E \end{bmatrix} \tag{2.88}$$

$U_{J|L}$ is a hankel matrix containing the inputs from the past to the future(2.89)

$$U_{J|L+g} = \begin{bmatrix} u_J & u_{J+1} & ... & u_{J+K-1} \\ u_{J+1} & u_{J+2} & ... & u_{J+K} \\ ... & ... & ... & ... \\ u_{J+L+g-1} & u_{J+L+g} & ... & u_{J+K+L+g-2} \end{bmatrix} \tag{2.89}$$

H_L^s is a toeplitz matrix for the output matrix D, the transition matrix A, the external input matrix C and the direct external input to output matrix F (2.90).

$$H_L^s = \begin{bmatrix} F & 0 & 0 & ... & 0 \\ DC & F & 0 & ... & 0 \\ DAC & DC & F & ... & 0 \\ ... & ... & ... & ... & ... \\ DA^{L-2}C & DA^{L-3}C & DA^{L-4}C & ... & F \end{bmatrix} \tag{2.90}$$

$E_{J|L}$ is a hankel matrix containing the is the noise from the past to the future(2.91)

$$E_{J|L} = \begin{bmatrix} e_J & e_{J+1} & ... & e_{J+K-1} \\ e_{J+1} & e_{J+2} & ... & e_{J+K} \\ ... & ... & ... & ... \\ e_{J+L-1} & e_{J+L} & ... & e_{J+K+L-2} \end{bmatrix} \tag{2.91}$$

Estimating the state space matrices using DSR

A stochastic system has both a deterministic part and a stochastic part. First start with identifying and removing the noise based on past and future data. A stochastic system can be written as shown below (2.92).

$$\left.\begin{aligned} x_{k+1} &= Ax_k + Bu_k + Ce_k \\ y_k &= Dx_k + Eu_k + Fe_k \end{aligned}\right\} \tag{2.92}$$

The output data matrix has now deterministic and stochastic terms ()

$$Y_{J|L} = O_L X_J + H_L^d U_{J|L+g-1} + H_L^s E_{J|L} \tag{2.93}$$

The system has a direct input to output matrix E, hence $g = 1$. This gives the extended output matrix equation (2.94)

$$Y_{J|L} = O_L X_J + H_L^d U_{J|L} + H_L^s E_{J|L} \tag{2.94}$$

The stochastic term can be removed by a projection of the future outputs onto the future inputs, past inputs and past outputs. This is done by (2.95).

$$Y_{J|L} / \begin{bmatrix} U_{J|L} \\ U_{0|J} \\ Y_{0|J} \end{bmatrix} = O_L X_J / \begin{bmatrix} U_{J|L} \\ U_{0|J} \\ Y_{0|J} \end{bmatrix} + H_L^d U_{J|L} / \begin{bmatrix} U_{J|L} \\ U_{0|J} \\ Y_{0|J} \end{bmatrix} + H_L^s E_{J|L} / \begin{bmatrix} U_{J|L} \\ U_{0|J} \\ Y_{0|J} \end{bmatrix} \tag{2.95}$$

The projection of future noise onto future inputs, past inputs and past outputs removes the noise term (2.96), while the projection does not effect the future inputs (2.97).

$$\overbrace{E_{J|L} / \begin{bmatrix} U_{J|L} \\ U_{0|J} \\ Y_{0|J} \end{bmatrix}}^{E(e_k u_k)=0} = 0 \tag{2.96}$$

$$U_{J|L}/\begin{bmatrix} U_{J|L} \\ U_{0|J} \\ Y_{0|J} \end{bmatrix} = U_{J|L} \tag{2.97}$$

This then gives a deterministic system (2.98) (removed the noise).

$$\overbrace{Y_{J|L}/\begin{bmatrix} U_{J|L} \\ U_{0|J} \\ Y_{0|J} \end{bmatrix}}^{Z^d_{J|L}} = O_L \overbrace{X_J/\begin{bmatrix} U_{J|L} \\ U_{0|J} \\ Y_{0|J} \end{bmatrix}}^{X^d_J} + H^d_L U_{J|L} \tag{2.98}$$

This can be rewritten on a more convenient form (2.99).

$$Z^d_{J|L} = O_L X^d_J + H^d_L U_{J|L} \tag{2.99}$$

The the C and F matrix can be computed from this equation (2.100) by QR decomposition. For more details about this see Di Ruscio [9].

$$Y_{J|L} - Z^d_{J|L} = H^s_L E_{J|L} \tag{2.100}$$

Can now perform an orthogonal projection of the deterministic system (2.99). $Z_{J|L}$ is found by finding a projection matrix P so $Z_{J|L}$ is on the form $Z_{J|L} = O_L \tilde{X}_J$. This is done as in (2.101).

$$\overbrace{Z^d_{J|L}P}^{Z_{J|L}} = O_L \overbrace{X^d_J P}^{\tilde{X}_J} \tag{2.101}$$

It is desirable to remove the deterministic part $H^d_L U_{J|L}$, this is done by finding a projection matrix P that gives $U_{J|L}P = 0$. this means that the P matrix must be 90° on the $U_{J|L}$ matrix for the result to be 0. This can be done by setting P to be orthogonal to $U_{J|L}$. This is shown in equation (2.102).

$$P = U^\perp_{J|L} = I - U^T_{J|L} \overbrace{\left(U_{J|L}U^T_{J|L}\right)^+}^{pseudo\ invers} U_{J|L} \tag{2.102}$$

One can also use inverse instead of pseudo inverse as long as $\left(U_{J|L}U^T_{J|L}\right)$ is invertible. That is the $\left(U_{J|L}U^T_{J|L}\right)$ is non-singular, which means that $det\left(U_{J|L}U^T_{J|L}\right) \neq 0$ and that none of the eigenvalues are zero.

Can prove this :

$$\begin{aligned} U_{J|L}P &= U_{J|L}\left(I - U^T_{J|L}\left(U_{J|L}U^T_{J|L}\right)^+ U_{J|L}\right) \\ U_{J|L}P &= U_{J|L} - U_{J|L}U^T_{J|L}\left(U_{J|L}U^T_{J|L}\right)^+ U_{J|L} \\ U_{J|L}U^T_{J|L}\left(U_{J|L}U^T_{J|L}\right)^+ &= I \\ U_{J|L}P &= U_{J|L} - I \cdot U_{J|L} \\ U_{J|L}P &= U_{J|L} - U_{J|L} = 0 \end{aligned}$$

Now use the projection matrix to project the deterministic part into the output data matrix $Z^d_{J|L}$ and the state matrix X^d_J, which gives (2.103).

$$\begin{aligned} \overbrace{Z^d_{J|L}P}^{Z_{J|L}} &= O_L \overbrace{X^d_J P}^{\tilde{X}_J} + \overbrace{H^d_L U_{J|L}P}^{=0} \\ &\Downarrow \\ Z_{J|L} &= O_L \tilde{X}_J \end{aligned} \tag{2.103}$$

All the projections can now be put up for $\tilde{X}_J$(2.104) and $Z_{J|L}$(2.105).

$$\tilde{X}_J = X_J^d U_{J|L}^{\perp} \tag{2.104}$$

$$Z_{J|L} = Z_{J|L}^d U_{J|L}^{\perp} \tag{2.105}$$

where

$$X_J^d = X_J / \begin{bmatrix} U_{J|L} \\ U_{0|J} \\ Y_{0|J} \end{bmatrix}$$

$$Z_{J|L}^d = Y_{J|L} / \begin{bmatrix} U_{J|L} \\ U_{0|J} \\ Y_{0|J} \end{bmatrix}$$

$$U_{J|L}^{\perp} = I - U_{J|L}^T \left(U_{J|L} U_{J|l}^T \right)^+ U_{J|L}$$

The aim is now to find the states transition matrix A and the input matrix B. By shifting the $Z_{J|L}$ one step forward to $Z_{J+1|L}$(2.106), it is possible to find the $\tilde{A}_L$ and $\tilde{B}_L$ matrices.

$$Z_{J+1|L} = \tilde{A}_L Z_{J|L} + \tilde{B}_L U_{J|L+1} \tag{2.106}$$

where the A and B matrices could be found through the relationship of (2.107) and (2.108), respectively. For more details see Di Ruscio[9].

$$\tilde{A}_L = O_L A \left(O_L^T O_L \right)^{-1} O_L^T \tag{2.107}$$

$$\tilde{B}_L = \begin{bmatrix} O_L B & H_L^d \end{bmatrix} - \tilde{A}_L \begin{bmatrix} H_L^d & 0_{Lm \times r} \end{bmatrix} \in \mathbb{R}^{Lm \times (L+g)r} \tag{2.108}$$

Finding the system order and the extended observability matrix

The systems order n can be estimated by use of singular value decomposition (SVD) on the $Z_{J|L}$ matrix to cut it up into an orthogonal matrix U, a diagonal matrix S of singular values and a orthogonal V^T matrix. The diagonal matrix S decides the system order. The size of S depends on the noise level. The SVD is divided into a data part and a noise part. The rank of the S matrix of data part of the SVD decides the system order.

$$Z_{J|L} = \begin{bmatrix} U_1 & U_2 \end{bmatrix} \begin{bmatrix} S_1 & 0 \\ 0 & S_2 \end{bmatrix} \begin{bmatrix} V_1 & V_2 \end{bmatrix}^T$$

$$Z_{J|L} = U_1 S_1 V_1^T + U_2 S_2 V_2^T \approx U_1 S_1 V_1^T$$

$$U_2 S_2 V_2^T \approx 0$$

where $U_1 S_1 V_1^T$ is the data part and $U_2 S_2 V_2^T$ is the noise part. The system order can be found by

$$n = rank(S_1)$$

It is needed to find the extended observability matrix in order to find the A and B matrices in the relationship (2.107) and (2.108) mentioned above. The extended observability matrix O_L can be estimated by dividing the SVD matrices U_1,S_1 and V_1^T into a extended observability O_L part and a state matrix $\tilde{X}_J$ part. There are three ways of dividing the SVD. The output normal realization (2.109), the input normal realization (2.110) and the balanced realization (2.110).

$$\left.\begin{matrix} O_L = U_1 \\ \tilde{X}_J = S_1 V_1^T \end{matrix}\right\} \tag{2.109}$$

$$\left.\begin{matrix} O_L = S_1 V_1^T \\ \tilde{X}_J = U_1 \end{matrix}\right\} \tag{2.110}$$

$$\left.\begin{matrix} O_L = U_1 \sqrt{S_1} \\ \tilde{X}_J = \sqrt{S_1} V_1^T \end{matrix}\right\} \tag{2.111}$$

For more details about the DSR method, see Di Ruscio [9].

2.3 Background of Model Predictive Control

2.3.1 Introduction

"*The process industry is characterized by ever tighter product quality specifications, increasing productivity demands, new environmental regulations and fast changes in the economical market. Over the last two decades predictive control has proven to be a very successful controller design strategy, both in theory and practice. The main reason for this acceptance is that it provides high performance controllers that can easily be applied to difficult high-order and multivariable processes. Process constraints are handled in a simple and systematic way. However a general stability and robustness theory is lacking. Predictive control is a class of control strategies based on the explicit use of a process model to generate the predicted values of the output at future time instants, which are then used to compute a sequence of control moves that optimize the future behavior of a plant. Predictive control is rather a methodology than a single technique. The difference in the various methods is mainly the way the problem is translated into a mathematical formulation. The explicit use of a model is the main difference between predictive control and the classical PID controller. Its advantage is that the behavior of the controller can be studied in detail, simulations can be done and performance can be evaluated. One of the drawbacks is the need of an appropriate model of the process. The benefits obtained are affected by the discrepancies existing between the real process and the model. According to some researchers 80% of the work done is in modeling and identification of the plant. The results almost always show that the effort is paid back in short time. Another drawback is that although the resulting control law is easy to implement and requires little computation, its derivation is more complex than that of the PID. If the process dynamics do not change, the derivation can be done beforehand, but in the adaptive control case all the computation has to be carried out at each sampling time. When constraints are considered, the amount of computation is even higher.*" [18]

In this thesis MPC has been applied to a system identification model of the mass flow rate of particulate solids. The MPC is using a state space model as the basis for the prediction model in the object function. A general description of the building of the MPC matrices is given in this literature review. The results and calculations is done in the "MPC results & discussion" chapter.

2.3.2 History of Model Predictive Control

"*The development of modern control concepts can be traced back to the work of Kalman in the early 1960s with the linear quadratic regulator (LQR) designed to minimize an unconstrained quadratic objective function of states and inputs. The infinite horizon endowed the LQR algorithm with powerful stabilizing properties. However it had little impact on the control technology development in the process industries. The reason for this lies in the absence of constraints in its formulation, the nonlinearities of the real systems, and above all the culture of the industrial process control community at the time, in which instrument technicians and control engineers either had no exposure to optimal control concepts or regarded them as impractical. Thus the early proponents of MPC for process control proceeded independently, addressing the needs of the industry.*

In the late 1970s various articles reported successful applications of model predictive control in the industry, principally the ones by Richalet et al. (1978) presenting Model Predictive Heuristic Control (later known as Model Algorithmic Control (MAC)) and those of Cutler and Ramaker (1980) with Dynamic Matrix Control (DMC). The common theme of these strategies was the idea of using a dynamic model of the process (impulse response in the former and step response in the later) to predict the effect of the future control actions, which were determined by minimizing the predicted error subject to operational restrictions. The optimization is repeated at each sampling period with updated information from the process. These formulations were algorithmic and also

heuristic and took advantage of the increasing potential of digital computers at the time. Stability was not addressed theoretically and the initial versions of MPC were not automatically stabilizing. However, by focusing on stable plants and choosing a horizon large enough compared to the settling time of the plant, stability is achieved after playing with the weights of the cost function.

Later on a second generation of MPC such as quadratic dynamic matrix control (QDMC; Garcia, Morshedi, 1986) used quadratic programming to solve the constrained open-loop optimal control problem where the system is linear, the cost quadratic, the control and state constraints are defined by linear inequalities. Another line of work arose independently around adaptive control ideas developing strategies essentially for

mono-variable processes formulated with transfer function models (for which less parameters are required in the identification of the model) and Diophantine equation was used to calculate future input. The first initiative came from Astron et al. (1970) with the Minimum Variance Control where the performance index to be minimized is a quadratic function of the error between the most recent output and the reference (i.e. the prediction horizon $Ny = 1$). In order to deal with non-minimum phase plants a penalized input was placed in the objective function and this became the Generalized Minimum Variance (GVM) control. To overcome the limitation on the horizon, Peterka (1984) developed the Predictor-Based Self-Tuning Control. Extended Prediction Self–Adaptive Control (EPSAC) by De Keyser et al. (1985) proposes a constant control signal starting from the present moment while using a sub-optimal predictor instead of solving a Diophantine equation. Later on the input was replaced by the increment in the control signal to guarantee a zero steady-state error. Based on the ideas of GVM Clarke et al. (1987) developed the Generalized Predictive Control (GPC) and is today one of the most popular methods. A closed form for the GPC is given by Soeterboek. State-space versions of unconstrained GPC were also developed.

Stability has always been an important issue for those working with predictive control. Due to the finite horizon stability is not guaranteed and is achieved by tuning the weights and horizons. Mohtadi proved specific stability theorems of GPC using statespace relationships and studied the influence of filter polynomials on robustness improvement. However a general stability property for predictive controllers, in general, with finite horizons was still lacking. This lead researchers to pursue new predictive control methods with guaranteed stability in the 1990s. With that purpose a number of design modifications have been proposed since then including the use of terminal constraints (Kwon et al., 1983; Meadows et al. 1995), the introduction of dual-mode designs (Mayne and Michalska, 1993) and the use of infinite prediction horizons (Rawlings and Muske, 1993), among others. Clarke and Scattolini (1991) and Mosca et al. (1990) independently developed stable predictive controllers by imposing end-point equality constraints on the output after a finite horizon. Kouvaritakis et al. (1992) presented a stable formulation for GPC by stabilizing the process prior to the minimization of the objective function. Many of these techniques are specialized for state-space representations of the controlled plant, and achieve stability at the expense of introducing additional constraints and modifying the structure of the design. Practitioners, however, avoid changing the structure of the problem and prefer to achieve stability by tuning the controller. For that a good doses of heuristics is used.

Recently a theoretical basis for MPC has started to emerge. Researchers have revisited the LQR problem arguing that model predictive control essentially solves standard optimal control problems with receding horizon, ideas that can be traced back to the 1960s (Garcia et al., 1989). MPC is characterized as a mathematical programming problem since the slow dynamics of process industry plants allow on-line solution to open-loop problems in which case the initial state is the current state of the system being controlled. Determining the feedback solution, on the other hand, requires the solution of the Hamilton-Jacobi-Bellman (a dynamic programming problem) differential or difference equation which turns out to be more difficult. Riccati equation appears as a particular case to some optimal control problems. It is shown (Mayne et al., 2000) that the difference between MPCs approach and the use of dynamic programming is purely one of implementation. This line of research has an early representative in the work of Kwon and Pearson (1983) and Keerthi and Gilbert (1988) and has recently gained popularity through multiple advocates, such as the work of Muske and Rawlings (1993). More recently two major approaches to the control problem are very popular. The first one employs the optimal cost function, for a fixed horizon, as a Lyapunov function and the second approach takes advantage of the monotonicity property of a sequence of the optimal cost function for various horizons. Note that for linear systems the presence of hard constraints makes the design of the controller a nonlinear problem so that the natural tool for establishing stability is Lyapunov theory. Obtaining a formulation which can relate the tuning parameters of MPC to properties such as stability and performance is the major goal of this line of work and recent advances show promising results. Solving the dynamic programming problem, however, is not practical and this can be accounted for the resistance of the industry to adopt these new methods."[18]

2.3.3 Applications of Model Predictive Control

Model Predictive Control, or MPC, is an advanced method of process control that has been in use in the process industries such as chemical plants and oil refineries since the 1980s. Model predictive controllers rely on dynamic models of the process, most often linear empirical models obtained by system identification [19].

Model predictive control (MPC) has had an enormous impact in the process industry over the last 20 years. It is an effective means of dealing with multivariable constrained control problems and the many reports of industrial applications confirm its popularity [18].

2.3.4 General description of Model Predictive Control

"*The methodology of all predictive controllers consists in predicting, at each time t, the future outputs for a determined horizon Ny , called the prediction horizon. This prediction of the outputs, $\hat{y}(t+i|t)$ for $i = 1$ to Ny , is based on the model of the process and depends on the known values of past inputs and outputs up to instant t. The set of future control signals is calculated by optimizing a given criterion (called objective function or performance index) in order to keep the process as close as possible to the reference trajectory $r(t+i)$, which can be the set point or an approximation of it. Different algorithms present different forms of objective functions, which usually take the form of a quadratic function of the errors between the predicted output signal and the predicted reference trajectory. Some algorithms use the states of the process as opposed to the outputs. The control effort is included in the objective function in most cases. Weights are used to adjust the influence of each term in the equation. The solution to the problem is the future control sequence that minimizes the objective function equation. For that, a model is used to predict future outputs or states. A typical objective function equation of a single-output single-input process is (2.112)*

$$J = \sum_{i=Ny1}^{Ny2} q(i) \left(r\left(t+i\right) - \hat{y}(t+i|t)\right)^2 + \sum_{i=2}^{Nu} r(i)\Delta u\left(t+i-1\right)^2 \tag{2.112}$$

It is a quadratic function of future inputs, u(t +i), and the error between future values of reference $r(t+i)$ and predicted outputs, $\hat{y}(t+i|t)$. Weights q and r are used to adjust the influence of the error and inputs respectively. The sequences of predicted outputs and future inputs are limited to horizons $Ny2$ and Nu respectively. The limitation on the sequence of inputs, $u(t+i)$ from $i = 1$ to Nu , comes from the assumption that the control action is constant after Nu steps ahead. The prediction horizon, on the other hand, limits the sequence of predicted output considered in the objective function equation. The control horizon has to be smaller than the prediction horizon. Weights and horizons are tuning parameters of the controller. The optimization of the objective function requires a prediction of the future outputs. The predicted output is the addition of two signals (2.113)

$$\hat{y}(t+i|t) = y0(t+i|t) + G\Delta u(t+i) \tag{2.113}$$

the constant forcing response and forced response. The constant forcing response, $y0(t+i|t)$, corresponds to the prediction of the evolution of the process under the consideration that future input values will be constant. The forced response, $G\Delta u(t+i)$ where G is the dynamic matrix of the process, corresponds to the prediction of the output when the control sequence is made equal to the solution of the minimization of the objective function. The expression for the predicted outputs can be substituted in the objective function and the solution to the minimization problem leads to the desired control sequence. Once the control sequence has been obtained only the first control move is implemented. Subsequently the horizon is shifted and the values of all sequences are updated and the optimization problem is solved once again. This is known as the Receding Horizon Principle and is adopted by all predictive control strategies. It is not advisable to implement the entire sequence over the next Nu intervals because it is impossible to perfectly estimate the unavoidable disturbances that cause the actual output to differ from the predictions made. Furthermore the operation might decide to change the set point over the next Nu intervals. The various predictive control algorithms only differ themselves in the model used to represent the process, the model for the noise and the objective function to be minimized. The models used can be Impulse/Step response models, transfer function models or state space models." [18]

2.3.5 Advantages and disadvantages of Model Predictive Control

There is numerous advantages with the MPC controllers. Advanced controllers like linear quadratic (LQ) and linear quadratic-gaussian controllers are similar with the unconstrained MPC. LQ and LQG controllers are better than unconstrained MPC for an infinite horizon.

Some advantages for MPC can be listed [15]:

- The main advantage and motivation of using an MPC controller is the ability to cope with constraints on the process variables in a simple and efficient way. Linear models, linear constraints and a linear quadratic objective results in a quadratic programming (QP) problem, which can be efficiently solved.
- An algorithm which is based on a state space model can be used to control unstable systems. The extended model predictive control (EMPC) algorithm is based on the extended state space model (ESSM) given by the DSR method. The EMPC algorithm works similarly on stable as well as on unstable systems. However it may be important to tune the prediction horizon and the weighting matrices properly.
- MPC controllers are perfect to control multivariable systems with cross-couplings.
- Another application of the MPC algorithm is to use it for operator support. The MPC algorithms can be used to only compute and to propose the future process controls. The operators can then use the control u_k^*, which is proposed by the MPC algorithm, as valuable information for operating the process. This is not possible by conventional controllers like the PID-controller.
- The DSR algorithm can build both the prediction model and the state observer to be used in MPC algorithms. The DSR algorithm is in use with some commercial MPC controllers. The use of the DSR method for MPC will improve effectiveness considerably. First of all due to the considerable amount of time reduced spent on model building.

Some disadvantages for MPC can be listed [15] :

- A dynamic model for the process is needed to implement a MPC controller. This dynamic model is used for the prediction model used in the objective criterion to minimize.
- Most MPC algorithms are using quadratic control objective functions J_k. However, different methods may be different because they are using different quadratic functions with different weights. MPC control theory is advanced and needs personnel with knowledge of MPC to implement the controller and tune the weighting matrices.

Nunes further mentions :"*Most industrial plants have many outputs and manipulated variables. In certain cases a manipulated variable mainly affects the corresponding controlled variable and each of the input-output pairs can be considered as a single-input single-output (SISO) plant and controlled by independent loops. In cases where the interaction between the different variables is not negligible the plant must be considered as a multiple-inputs and multiple-outputs (MIMO) process. These interactions may result in poor performance and even instability if the process is treated as multiple SISO loops. In practice all processes are subject to restrictions and these can be considered in the objective function equation as constraints on the inputs and outputs. In many industrial plants the control system will operate close to the boundaries due to operational conditions. This has lead to the widespread belief that the solution to the optimization problem lies at the boundaries. On the other hand the design of multivariable predictive controllers requires the specification of horizons and weights for all inputs and outputs. Therefore a big number of parameters must be selected, a task that may prove challenging even for systems of modest size. Badly tuned predictive controllers tend to take the plant to extreme and sometimes unstable conditions, frequently unnoticed because of physical constraints such as valve opening, maximum flow rate, etc., masking the instability problem and fooling operational groups into concluding that the plant has been optimized.*" [18].

2.4 MPC control in pneumatic conveying

Plant B was selected as the conveying rig for using model predictive control. The reason for this is that this rig has measurements of the controllable inputs to the pneumatic conveying rig. In plant B at POSTEC/Tel-Tek, there are only two controllable variables. These are the main air and the bypass air inlet. Both variables are controlled by controlling an airflow. There is only one state in the system identification model and that is the mass flow rate of solids. The inputs are 5 pressure measurements and two air flow measurements. The pressure measurements are passive inputs and consists of :

- the pressure at the main air inlet (P_m)
- the pressure at the bypass air inlet (P_{by})
- the blowtank pressure (P_0)
- the pressure at the lowest elevation of the conveying line (P_8)
- the pressure transducer that explains the elevation of the pneumatic conveying line the best (P_{11}).

See figure (....) under the "measurement setups" chapter for details about the rig setup. The development of the state space model used for the MPC control is explained in the chapter "Modelling pneumatic systems by the energy density approach using system identification".

Model Predictive Control (MPC) have to have a model to make a prediction model. A prediction model is a model that is looking one step and the length of a prediction horizon into the future for the output states. A prediction model can be written on the form shown in equation (2.114).

$$y_{k+1|L} = F_L u_{k|L} + P_L \tag{2.114}$$

where

$$\begin{aligned} y_{k+1|L} &= \text{Future outputs with prediction horizon } L \\ F_L &= \begin{bmatrix} O_L B & H_L^d \end{bmatrix} \\ O_L &= \text{Observability matrix} \\ H_L^d &= \text{Lower triangular toeplitz matrix} \\ u_{k|L} &= \text{Present input} \\ P_L &= O_L A x_k \\ x_k &= \text{Present state} \end{aligned}$$

and

$$y_{k+1|L} = \begin{bmatrix} y_{k+1} \\ y_{k+2} \\ y_{k+3} \\ \vdots \\ y_{k+L+1} \end{bmatrix} \text{ and } u_{k|L} = \begin{bmatrix} u_k \\ u_{k+1} \\ u_{k+2} \\ \vdots \\ u_{k+L} \end{bmatrix}$$

$$O_L = \begin{bmatrix} d \\ da \\ da^2 \\ \vdots \\ da^{L-1} \end{bmatrix} \text{ and } H_L^d = \begin{bmatrix} 0 & 0 & 0 & ... & 0 \\ dB & 0 & 0 & ... & 0 \\ daB & dB & 0 & ... & 0 \\ ... & ... & ... & ... & ... \\ da^{L-2}B & da^{L-3}B & da^{L-4}B & ... & 0 \end{bmatrix}$$

This prediction model is related to system identification theory, where a model can be extracted from a data set with known inputs and outputs to get a state space model. The model gotten from the Deterministic Stochastic Realization method (DSR) made by professor David Di Ruscio at the University-College of Telemark was a deterministic model. A deterministic model means that the outputs can be determined by knowing the present inputs. Different types of models like autonomous and stochastic models are described in the literature review for system identification. The deterministic model given by DSR was (2.114).

$$\left.\begin{array}{c} x_{k+1} = Ax_k + Bu_k, x_0 = known \\ y_k = Dx_k \end{array}\right\} \tag{2.115}$$

where

$$\begin{aligned} x_{k+1} &= \text{The next state (here: state=mass flow)} \\ A &= \text{The transition matrix (here: scalar } a) \\ B &= \text{The input matrix} \\ D &= \text{Output matrix (here: } D = d = 1) \\ x_k &= \text{The present state (here:state=mass flow)} \\ x_0 &= \text{Initial state (Here: start value for mass flow)} \\ u_k &= \text{Present inputs (here: } P_m, P_{by}, P_0, P_8, P_{11}, \dot{V}_m, \dot{V}_{by}) \end{aligned}$$

and

$$\begin{aligned} x_0 &= -0.1291 \\ a &= 0.0341 \\ B &= \begin{bmatrix} 0.0033 & 0.1245 & -0.0295 & 0.3358 & -0.3999 & -0.0951 & -0.2011 \end{bmatrix} \cdot 10^{-3} \end{aligned}$$

The pressures can not be manipulated directly, but the air inlets can be controlled. The pressures can be put into a disturbance vector v_k and the air inlets can remain in the control vector u_k. The model can now be rewritten as (2.116).

$$\left.\begin{array}{c} x_{k+1} = Ax_k + Bu_k + v_k, x_0 = known \\ y_k = dx_k \end{array}\right\} \tag{2.116}$$

where

$$\begin{aligned} x_0 &= -0.1291 \\ a &= 0.0341 \\ B &= \begin{bmatrix} -0.0951 & -0.2011 \end{bmatrix} \cdot 10^{-3} \\ v &= \begin{bmatrix} 0.0033 & 0.1245 & -0.0295 & 0.3358 & -0.3999 \end{bmatrix} \cdot 10^{-3} \end{aligned}$$

2.4.1 MPC as a PI-controller

A pure proportional controller (P-controller) gives a steady state error. To get rid of this steady state error an integration effect can be added (PI-controller), giving zero steady state error. This can be done by augmenting the model with the previous output as a state in the state vector x_k. To remove known disturbances, the model can be put up on deviation form (2.117). Already have the model (2.116), on deviation form this model is (2.117) :

$$\begin{aligned} x_{k+1} - x_k &= (ax_k + Bu_k + v_k) - (ax_{k-1} + Bu_{k-1} - v_k) \\ y_k - y_{k-1} &= dx_k - dx_{k-1} \\ &\Downarrow \\ &\left.\begin{array}{c} \Delta x_{k+1} = a\Delta x_k + B\Delta u_k \\ y_k = y_{k-1} + d\Delta x_k \end{array}\right\} \end{aligned} \tag{2.117}$$

Augmenting the model gives (2.118) :

$$\begin{aligned} \overbrace{\begin{bmatrix} \Delta x_{k+1} \\ y_k \end{bmatrix}}^{\tilde{x}_{k+1}} &= \overbrace{\begin{bmatrix} a & 0 \\ d & I \end{bmatrix}}^{\tilde{A}} \cdot \overbrace{\begin{bmatrix} \Delta x_k \\ y_{k-1} \end{bmatrix}}^{\tilde{x}_k} + \overbrace{\begin{bmatrix} B \\ 0 \end{bmatrix}}^{\tilde{B}} \Delta u_k \\ y_k &= \overbrace{\begin{bmatrix} d & I \end{bmatrix}}^{\tilde{D}} \cdot \overbrace{\begin{bmatrix} \Delta x_k \\ y_{k-1} \end{bmatrix}}^{\tilde{x}_k} \\ &\Downarrow \\ &\left.\begin{array}{c} \tilde{x}_{k+1} = \tilde{A}\tilde{x}_k + \tilde{B}\Delta u_k \\ y_k = \tilde{D}\tilde{x}_k \end{array}\right\} \end{aligned} \tag{2.118}$$

This now gives a new prediction model (2.119):

$$y_{k+1|L} = F_L \Delta u_{k|L} + P_L \tag{2.119}$$

where

$$\begin{aligned} F_L &= \begin{bmatrix} O_L \tilde{B} & H_L^d \end{bmatrix} \\ p_L &= O_L \tilde{A} \tilde{x}_k \end{aligned}$$

and

$$\Delta u_{k|L} = S^{-1} u_{k|L} - S^{-1} c u_{k-1}$$

2.4.2 The MPC control objective criterion

The control criterion gives the control objective. It is an optimization problem. The objective is to control the state to a desired set point. This gives that the difference between a measured or estimated output and the set point should be as close as possible to zero. In MPC the control objective criterion relates the difference between set point value and measured/estimated value and a cost function. The difference between known future set points and measured/estimated output can be put up in a control deviation term in the objective criterion. The cost function is used to minimize the control signal with regards to the control signal. The prediction horizon gives a interval into the future where the control inputs are optimized with regards to the objective criterion.

This cost function can be a minimizing of:

- the input amplitude
- change in input amplitude

The cost function tells that the control signal has a cost and gives it a weighting. The cost functions purpose is to minimize the control signal and reduce the energy cost of a control signal. In pneumatic conveying the cost function can be chosen to be a rate of change of the inputs. This then gives a minimization of the control signal with regards to rapid changes in the control signal. This slows down the control, but conserves the energy cost related to the control of the pneumatic conveying. The control objective criterion can then be set up as a linear quadratic (LQ) problem (2.120) :

$$J_k = \overbrace{\left(r_{k+1|L} - y_{k+1|L}\right)^T Q \left(r_{k+1|L} - y_{k+1|L}\right)}^{\text{deviation term}} + \overbrace{\Delta u_{k|L}^T R \Delta u_{k|L}}^{\text{cost function}} \tag{2.120}$$

where

$$\begin{aligned} r_{k+1|L} &= \text{Known future set points over the prediction horizon } L \\ y_{k+1|L} &= \text{Prediction model (PM)} \\ \Delta u_{k|L} &= \text{Change in control signal} \\ Q &= \text{Diagonal weighting matrix for the deviation in output from set point} \\ R &= \text{Diagonal weighting matrix for the rate of change of the inputs} \\ L &= \text{Prediction horizon} \end{aligned}$$

$$Q = \begin{bmatrix} q_1 & 0 & 0 & 0 \\ 0 & q_2 & 0 & 0 \\ 0 & 0 & \ddots & \vdots \\ 0 & 0 & \cdots & q_L \end{bmatrix}, R = \begin{bmatrix} r_1 & 0 & 0 & 0 \\ 0 & r_2 & 0 & 0 \\ 0 & 0 & \ddots & \vdots \\ 0 & 0 & \cdots & r_L \end{bmatrix}$$

$$\text{usually} \quad : \quad q_1 = q_2 = q_L \text{ and } r_1 = r_2 = r_L$$

2.4.3 Computing the optimal unconstrained control signal

First it is convenient to set up the objective criterion as a more general linear quadratic relationship. Start with setting in the prediction model into the objective criterion (2.121) :

$$\begin{aligned} J_k &= \left(r_{k+1|L} - y_{k+1|L}\right)^T Q \left(r_{k+1|L} - y_{k+1|L}\right) + \Delta u_{k|L}^T R \Delta u_{k|L} \\ &\Downarrow \\ J_k &= \left(r_{k+1|L} - F_L \Delta u_{k|L} + p_L\right)^T Q \left(r_{k+1|L} - F_L \Delta u_{k|L} + p_L\right) + \Delta u_{k|L}^T R \Delta u_{k|L} \end{aligned} \tag{2.121}$$

Can now expand:

$$\begin{aligned} J_k &= \left(\left(-\Delta u_{k|L}\right)^T F_L^T + \left(r_{k+1|L}\right)^T - p_L^T\right) Q \left(-F_L \Delta u_{k|L} + r_{k+1|L} - p_L\right) + \Delta u_{k|L}^T R \Delta u_{k|L} \\ &\Downarrow \\ J_k &= \left(-\Delta u_{k|L} F_L\right)^T Q \left(-F_L \Delta u_{k|L}\right) \text{ can be written } \Delta u_{k|L}^T \left(F_L^T Q F_L\right) \Delta u_{k|L} \\ &\quad + \left(-\Delta u_{k|L} F_L\right)^T Q \left(r_{k+1|L} - p_L\right) \text{ can be written } \left(F_L^T Q \left(p_L - r_{k+1|L}\right)\right) \Delta u_{k|L} \\ &\quad + \left(r_{k+1|L} - p_L\right)^T Q \left(-F_L \Delta u_{k|L}\right) \text{ can be written } \left(F_L^T Q \left(p_L - r_{k+1|L}\right)\right) \Delta u_{k|L} \\ &\quad + \left(r_{k+1|L} - p_L\right)^T Q \left(r_{k+1|L} - p_L\right) \\ &\quad + \Delta u_{k|L}^T R \Delta u_{k|L} \end{aligned}$$

The expression can now be set up like (2.122) :

$$\begin{aligned} J_k &= \Delta u_{k|L}^T \overbrace{\left(F_L^T Q F_L + R\right)}^{H} \Delta u_{k|L} \\ &\quad + 2 \overbrace{\left(F_L^T Q \left(p_L - r_{k+1|L}\right)\right)}^{f} \cdot \Delta u_{k|L} \\ &\quad + \overbrace{\left(r_{k+1|L} - p_L\right)^T Q \left(r_{k+1|L} - p_L\right)}^{J_0} \end{aligned}$$

this gives:

$$J_k = \Delta u_{k|L}^T H \Delta u_{k|L} + 2 f \Delta u_{k|L} + J_0 \tag{2.122}$$

where

$$\begin{aligned} H &= \text{The quadratic term} \\ f &= \text{The linear term} \\ J_0 &= \text{The constant term} \end{aligned}$$

The control objective criterion needs to be minimized. This can be done by taking the partial derivative of the objective criterion with regards to the control signal (2.123).

$$\frac{\partial J_k}{\partial \Delta u_{k|L}} = 0 \tag{2.123}$$

This is then set to zero since the desired state of the process is the set point. When at set point, the change in the process should be close to zero. This is called the first order necessary condition for minimum.

Now compute the first order necessary condition for minimum:

$$\frac{\partial J_k}{\partial \Delta u_{k|L}} = 2H \Delta u_{k|L} + 2f = 0$$

Can now compute the unconstrained optimal control $\Delta u_{k|L}^*$ (2.124) :

$$\begin{aligned} 2H \Delta u_{k|L} + 2f &= 0 \\ \Delta u_{k|L}^* &= -H^{-1} f \end{aligned} \tag{2.124}$$

Can rewrite this to (2.125).

$$\begin{aligned} \Delta u^*_{k|L} &= \overbrace{-\left(F_L^T Q F_L + R\right)^{-1} F_L^T Q}^{G} \left(p_L - r_{k+1|L}\right) \\ \Delta u^*_{k|L} &= G\left(p_L - r_{k+1|L}\right) \end{aligned} \tag{2.125}$$

where

$$G = \text{The unconstrained optimal gain}$$

2.4.4 Adding constraints to the control objective criterion J_k

The inputs are volumetric flow of air in pneumatic plant B. The constraints should be within the maximum volumetric flow the air compressor can give. Plugging is a problem in pneumatic conveying and this is related to the mass flow of solids. Instead of adding an output constraint on the mass flow it is better to implement a plug detector and change the volumetric flow of air accordingly. A rate of change constraint can be applied since there is restrictions in how fast a valve can open or close. Then the characteristics of the valve needs to be known. Constraints can be equality constraints or inequality constraints. Three different types of inequality constraints that are commonly used are:

1. input amplitude constraints
$$u_{\min} \leq u_{k|L} \leq u_{\max} \tag{2.126}$$
2. rate of change constraints
$$\Delta u_{\min} \leq \Delta u_{k|L} \leq \Delta u_{\max} \tag{2.127}$$
3. output amplitude constraints
$$y_{\min} \leq y_{k+1|L} \leq y_{\max} \tag{2.128}$$

The input amplitude and rate of change constraints are chosen as constraints for the pneumatic conveying MPC. The output amplitude is not chosen as a constraint. The inequality constraints can be put up on the form (2.129).

$$\Lambda u_{k|L} \leq b \tag{2.129}$$

The the rate of change constraints can be written as in (2.130) and (2.131).

$$\Delta u_{k|L} \leq \Delta u_{\max} \tag{2.130}$$
$$-\Delta u_{k|L} \leq -\Delta u_{\min} \tag{2.131}$$

Have the relationship between the input amplitude $u_{k|L}$ and change $\Delta u_{k|L}$ (2.132).

$$u_{k|L} = S\Delta u_{k|L} + cu_{k-1} \tag{2.132}$$

where

$$S = \begin{bmatrix} I & 0 & 0 & 0 & 0 \\ I & I & 0 & 0 & 0 \\ I & I & I & 0 & 0 \\ \vdots & \vdots & \vdots & \ddots & 0 \\ I & I & I & \cdots & I \end{bmatrix} \text{ and } c = \begin{bmatrix} I \\ I \\ I \\ \vdots \\ I \end{bmatrix}$$

Set up the rate of change constraints $u_{\max}$ (2.133) and $-u_{\min}$ (2.134).

$$\begin{aligned} u_{k|L} &\leq u_{\max} \\ S\Delta u_{k|L} + cu_{k-1} &\leq \Delta u_{\max} \\ S\Delta u_{k|L} &\leq u_{\max} - cu_{k-1} \end{aligned} \tag{2.133}$$

$$\begin{aligned} -u_{k|L} &\leq -u_{\min} \\ -\left(S\Delta u_{k|L} + cu_{k-1}\right) &\leq -u_{\min} \\ -S\Delta u_{k|L} &\leq -u_{\min} + cu_{k-1} \end{aligned} \tag{2.134}$$

Now we can set the constraints up on the form (2.129) again

$$\Lambda u_{k|L} \leq b$$

and get all the inequality constraints in a Λ matrix and b vector (2.135).

$$\overbrace{\begin{bmatrix} I \\ -I \\ S \\ -S \end{bmatrix}}^{\Lambda} u_{k|L} \leq \overbrace{\begin{bmatrix} \Delta u_{\max} \\ -\Delta u_{\min} \\ u_{\max} + cu_{k-1} \\ -u_{\min} - cu_{k-1} \end{bmatrix}}^{b} \tag{2.135}$$

In this thesis only the input amplitude constraints was implemented. See "MPC results & discussion" for more details about the results of the MPC constraints.

2.4.5 The Lagrangian method for adding constraints to the objective criterion

Already have the optimal unconstrained objective criterion

$$J_k = \Delta u_{k|L}^T H \Delta u_{k|L} + 2f^T \Delta u_{k|L} + J_0$$

this gives that the minimized optimal objective criterion has no constraints attached to it. To include constraints like input amplitude constraints and rate of change constraints, they have to be included in the optimal objective criterion. This can be done by the use of a Lagrange multiplier λ.Adding the constraints into the objective criterion gives the Lagrange function (2.136).

$$L_k = \Delta u_{k|L}^T H \Delta u_{k|L} + 2f^T \Delta u_{k|L} + J_0 + \lambda_k^T \left(\Lambda \Delta u_{k|L} - b\right) \tag{2.136}$$

Then minimize the Lagrange function with regards to the control vector $\Delta u_{k|L}$ (2.137) and the Lagrange multiplier λ_k (2.138).

$$\frac{\delta L_k}{\delta \Delta u_{k|L}} = 2H\Delta u_{k|L} + 2f + \Lambda^T \lambda_k = 0 \tag{2.137}$$

$$\frac{\delta L_k}{\delta \lambda_k} = \Lambda \Delta u_{k|L} - b = 0 \tag{2.138}$$

Start first with finding the optimal control vector $\Delta u_{k|L}^*$ (2.139).

$$\begin{aligned} 2H\Delta u_{k|L} + 2f + \Lambda^T \lambda_k &= 0 \\ H\Delta u_{k|L} &= -f - \frac{1}{2}\Lambda^T \lambda_k \\ \Delta u_{k|L}^* &= -H^{-1}\left(f + \frac{1}{2}\Lambda^T \lambda_k\right) \end{aligned} \tag{2.139}$$

Using this calculation (2.139) for the optimal control vector $\Delta u_{k|L}^*$ and put it into the minimized function (2.138) for the Lagrange multiplier λ_k will give the optimal Lagrange multiplier λ_k^* (2.140).

$$\begin{aligned} \Lambda \Delta u_{k|L}^* - b &= 0 \\ \Lambda\left(-H^{-1}\left(f + \frac{1}{2}\Lambda^T \lambda_k\right)\right) - b &= 0 \\ -\Lambda H^{-1} f - \frac{1}{2}\Lambda H^{-1} \Lambda T \lambda_k &= b \\ \lambda_k^* &= -\frac{1}{2}\left(\Lambda H^{-1\Lambda T}\right)^{-1}\left(\Lambda H^{-1} f + b\right) \end{aligned} \tag{2.140}$$

Can now compute the optimal control vector $\Delta u_{k|L}^*$ (2.141) based on the optimal Lagrange vector λ_k^* (2.140).

$$\Delta u_{k|L}^* = -H^{-1}\left(f + \frac{1}{2}\Lambda^T \lambda_k^*\right) \tag{2.141}$$

This optimal control vector $\Delta u_{k|L}^*$ takes into account the constraints. To solve the constraints, the active set method can be used or MatLabs 'quadprog' command, which is a QP solver that also handles constraints.

2.4.6 Active set method

The active set method is used for inequality constraints. Use a Lagrange multiplier λ_i to solve the inequalities. if $\lambda_i < 0$ then the constraint is considered inactive and $\lambda_i = 0$. If $\lambda_i > 0$ then the constraint is considered active and $\lambda_i = the\ solution$.

Chapter 3

The Energy Density approach to modelling pneumatic systems

Pneumatic conveying can be viewed as a multiphase flow problem, consisting of air and particulate solids. The energy density concept is based on calculating the energy transfer between the energy stored in the air to move the particulate solids. Conveying solid particles by air, gives that the energy stored in the air is transferred to kinetic energy to move the solids. In the research facility at POSTEC/Tel-Tek this is done by filling a tank with solids and pressurize the tank by filling it with air. This tank is called the blowtank. At the research facility at POSTEC/Tel-Tek there are two different rigs with blowtanks of two different sizes. The energy density concept is based on the energy per unit volume stored in the air. Pressure can be viewed as energy density. The conventional approach to describe pressure, is to set it up as a force per unit area. By expanding it like in equation (3.1) pressure can be viewed as energy density.

$$P = \frac{F \cdot l}{A \cdot l} = \frac{E}{V} \tag{3.1}$$

That is energy per unit volume. Compressed air can be viewed as a stored energy in a volume, like stored energy in a spring. A pressure transducer can measure this stored energy density by a pressure measurement. As the air expands through a pipe, the stored energy density in the air converts to kinetic energy density. In other words the compressed air expands and set the air into motion, the pressure drops and the velocity of the air increases. Elevation of the pipe gives that the velocity of the air drops due to gravity, this gives that some of the kinetic energy density is converted into potential energy density. The total pressure can be put up like in the Bernoulli equation (3.2).

$$P_t = \overbrace{\underbrace{P_1}_{\text{static pressure}}}^{\text{static energy density}} + \overbrace{\underbrace{\frac{1}{2}\rho_1 v_1^2}_{\text{dynamic pressure}}}^{\text{kinetic energy density}} + \overbrace{\rho_1 g h_1}^{\text{potential energy density}} \tag{3.2}$$

If pressure is viewed as a force, the total pressure gives the force produced by the air in the pipe. If pressure is viewed as energy density, the total energy density gives the amount of energy per unit volume produced by the air in the pipe. This may look like the same way of thinking, but it is not. The reason is that when the pressure is viewed as a force that push the particulate solids, other forces needs to be calculated as well. Forces like drag, pipewall friction and particle collisions. In pneumatic conveying these forces can be quite difficult to measure or calculate.

By viewing the pressure as energy density, it will describe how the energy density of the air is transferred into energy to move the particulate solids. The energy density in the air is changing accordingly to the mass flow. This is due to the fact that the air is compressible and the solids is treated as incompressible. The mass of particulate solids in the pipe prevents the air from flowing freely and the air compresses, increasing the static pressure and decreasing the air velocity. If then the mass of particulate solids are reduced in the pipe, this leads to less compression of the air and the static pressure decreases and the air velocity increases.

This gives that the pressure fluctuations is due to expansion and compression of the air. The fluctuations is caused by the amount of solids in the pipe and characteristics of the solids. The change in pressure and the air flow rate gives an indication of change in energy density of the air. By measuring the pressure at places in the pipeline that describes the elevation of the pipeline, the potential energy density is also accounted for.

3.1 Modelling the pneumatic conveying pipeline by the energy density approach

A simple example can be given, calculating the total energy density at the start of the pipe and at the end of the pipe. See figure (3.1) for a sketch of the pressure transducers position in the conveying line. Figure (3.1) is a sketch of "Plant A" at POSTEC/Tel-Tek.

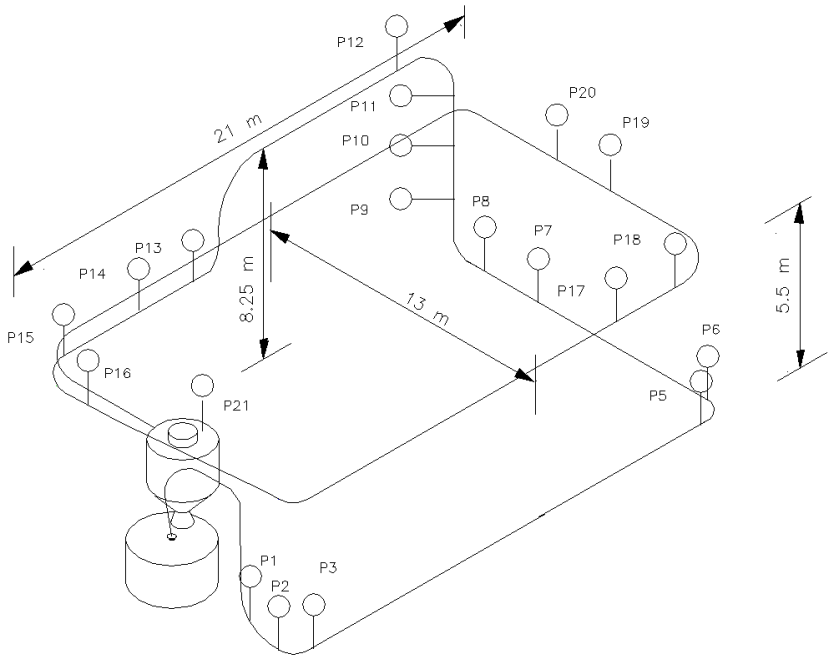

Figure 3.1: Layout og the pressure transducers along the pipeline.

The total energy density at the start of the pipe can be put up as in (3.3).

$$P_{1tot} = P_1 + \frac{1}{2}\rho_1 v_1^2 + \rho_1 g h_1 \tag{3.3}$$

Where

$$\begin{aligned} P_{1tot} &= \text{Total energy density at position of } P_1 \\ P_1 &= \text{Measured static pressure at position of } P_1 \\ \rho_1 &= \text{Density of air at position of } P_1 \\ v_1 &= \text{Velocity of air at position of } P_1 \\ g &= \text{Gravitational force} \\ h_1 &= \text{Elevation of pipeline at position of } P_1 \end{aligned}$$

The total energy density at the end of the pipe can be put up as in (3.4).

$$P_{21tot} = P_{21} + \frac{1}{2}\rho_{21} v_{21}^2 + \rho_{21} g h_{21} \tag{3.4}$$

Where

$$\begin{aligned} P_{21tot} &= \text{Total energy density at position of } P_{21} \\ P_{21} &= \text{Measured static pressure at position of } P_{21} \\ \rho_{21} &= \text{Density of air at position of } P_{21} \\ v_{21} &= \text{Velocity of air at position of } P_{21} \\ g &= \text{Gravitational force} \\ h_{21} &= \text{Elevation of pipeline at position of } P_{21} \end{aligned}$$

The energy density loss can be found by subtracting the total energy density at the end of the pipe from the total energy density at the start of the pipe (3.5).

$$E_{loss} = P_{1tot} - P_{21tot} \tag{3.5}$$

This energy density loss can be divided into a loss E_m relating to setting the particulate solids into motion and a loss E_f due to pipe wall friction and particle collisions plus other particle forces (3.6).

$$E_{loss} = E_m + E_f \tag{3.6}$$

The energy density loss E_m due to setting the particulate solids into motion, can be used for calculating the mass flow rate of the particulate solids.

$$E_m = \frac{1}{2} m_s v_s^2 + m_s g h_{21}$$

Where

$$\begin{aligned} E_m &= \text{Is the energy used to set the particulate solids into motion} \\ m_s &= \text{Is the mass of the solids} \\ v_s &= \text{Average velocity of the solids at the end of the pipeline} \\ g &= \text{Gravitational force} \\ h_{21} &= \text{Total Elevation of the pipeline, given at position of } P_{21} \end{aligned}$$

The problem here is that the velocity needs to be measured or calculated. Somehow the velocity of the solids has to be found, or else the mass flow rate cannot be estimated. One way is to measure the mass flow rate of the particulate solids by a load cell, the velocity has to be calculated since there is no direct measurement of the velocity of the particulate solids. This gives that this model is dependent on measurement of mass flow rate and is not able to estimate the mass flow rate without this measurement. The average velocity at the end can be calculated (3.8) through the relationship of the measured mass flow rate (3.7).

$$\dot{m}_s = \frac{dm}{dt} = \frac{kg}{s} \tag{3.7}$$

$$\begin{aligned} \frac{\dot{m}_s}{\rho_s} &= \frac{\rho_s \cdot dV}{dt \cdot \rho_s} = \frac{dV}{dt} = \frac{\frac{kg}{m^3} \cdot m^3}{s \cdot \frac{kg}{m^3}} = \frac{m^3}{s} \\ v_s &= \frac{\dot{V}_s}{A} = \frac{dV}{dt \cdot A} = \frac{dx}{dt} = \frac{m^3}{s \cdot m^2} = \frac{m}{s} \end{aligned} \tag{3.8}$$

Using this approach gives a prediction of the mass flow, but a measurement by a load cell is needed. In many cases a load cell in pneumatic conveying systems is not possible or for large systems not accurate enough. The example above gives a rough estimate of the flow using the energy density approach for the pipeline based on load cell measurement of the mass flow rate. A black box model approach can be used to find the energy transfer from air to particulate solids using system identification. The black box model is then identifying the relationships relating to the Bernoulli equation within the measured data. A black

box model can be attained using the energy density approach for the pipeline by using $P0, P1, P2, P13$ and $\dot{V}_{air}$ as input variables and the measured mass flow rate as the output variable. These variables can then be used for making a calibration model. A sketch showing how the variables is related is shown in figure (3.2). After the calibration model is attained, the mass flow rate can be estimated without the use of a load cell. A disadvantage is that to attain the calibration model, a direct measurement of the mass flow rate is needed.

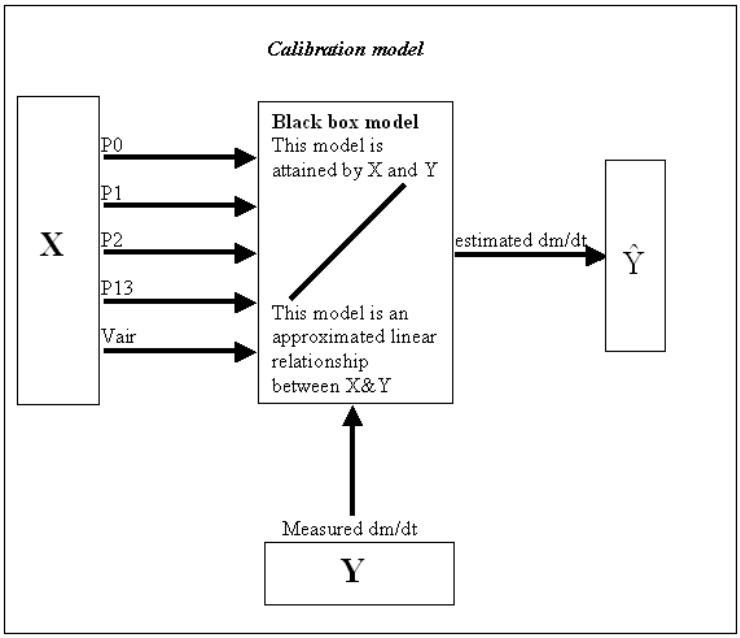

Figure 3.2: Simple sketch of system identification model for estimating the mass flow rate.

Since the model is based on how the particulate solids travel in the pipeline, none of the input variables is directly controllable. This gives that the model gotten from this approach is not usable for control purposes. The inlet main air and inlet bypass air is not taken into account. This gives that this kind of modelling predicts the mass flow rate based on measurements, but it does not help for control purposes. The problem is to find the initial velocity of the solids related to have much main air and bypass air that is given. The acceleration of the solids through the pipeline can then be found by selecting proper pressure measurements. The final velocity of solids at the end of the conveying line can then be calculated.

To do this, the energy density approach must take into account the blowtank. The velocity of particulate solids out of the blowtank can be considered as the initial velocity of the particulate solids. To model the blowtank a mass balance is needed to find the mass of air into the blowtank and the mass of air out of the blowtank. The initial mass of solids in the blowtank and the volume of the blowtank is also needed. Further an energy balance of the energy density into the blowtank and out of the blowtank is also needed.

3.2 Modelling the blowtank by the energy density approach

Figure (3.3) shows a simple sketch of a blowtank. The blowtank has a stored static energy density, that can be measured by a pressure transducer. This energy density is the driving energy for conveying of solids. This energy density in the blowtank is mainly controlled by a air inlet called main air inlet.

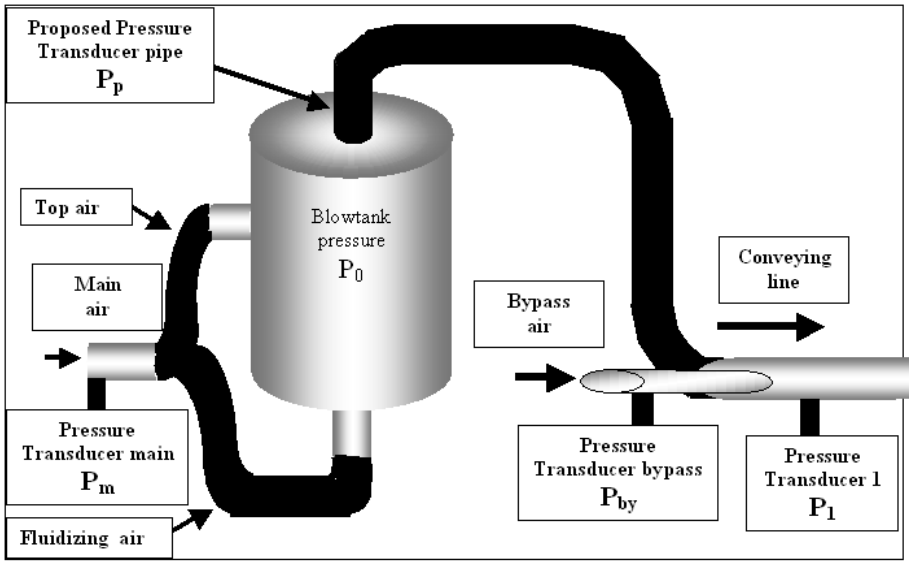

Figure 3.3: Simplified sketch of the blowtanks at the POSTEC/Tel-Tek research facility.

The main air inlet has a pressure transducer P_m, this pressure transducer gives the static energy density outside the blowtank, where the main air flow comes into the blowtank. The main airflow gives the kinetic energy density added to the blowtank. Both rigs at POSTEC/Tel-Tek have an bypass air inlet, the purpose of this air inlet is to prevent plugging by diluting the suspension and to give a support back pressure to the blowtank preventing to much solids to come out and create a plug. The bypass air inlet also have a pressure measurement P_{by} which gives an indication of the compression of air, which gives the static energy density given by the bypass air. The bypass airflow gives the added kinetic energy density given by the bypass air. Pressure transducer P_1 is the first transducer after the blowtank and bypass air inlet. This measurement point is describing the total energy density in the pipeline at the start of the pipeline. This pressure transducer should be as close as possible to the juncture where the bypass air is coupled to the pipeline. This is because, then the total amount of energy density transferred into the pipeline can be measured as accurately as possible. Both rigs should have an extra pressure transducer P_P as close as possible to the blowtank outlet, since this point describes the total energy density out of the blowtank. This energy density is useful for describing the initial velocity of the particulate solids.

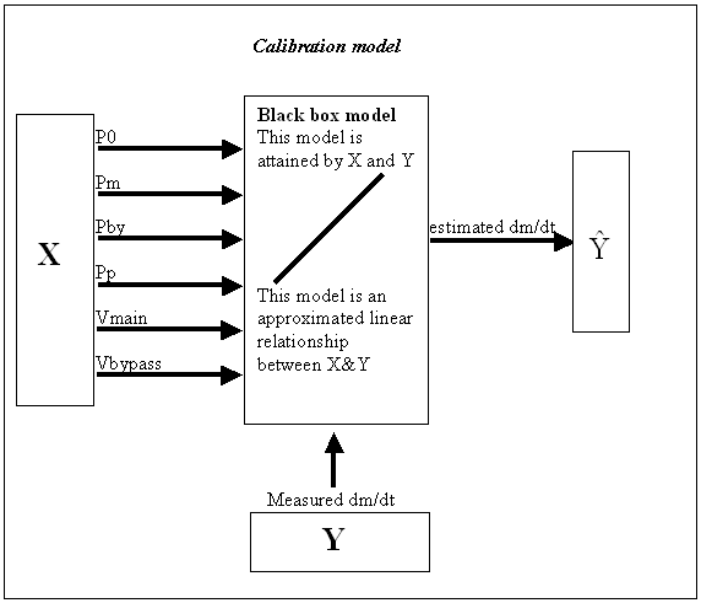

Figure 3.4: Simple sketch of system identification model for estimating the mass flow rate.

A system identification model can be attained as shown in figure (3.4). This model will give an approximated output value of the mass flow rate of particulate solids at the end of the pipe. This model also needs a measurement of the mass flow rate of solids for the calibration model. To get the initial velocity of the particulate solids, a mechanistic model has to be put up. That is a model based on mass balances and an energy balance. This is out of the scope of this thesis and is an ongoing doctoral thesis at POSTEC/Tel-Tek. Instead a system identification model for the whole system is made. This model includes both measurements in the pipeline and the measurements around the blowtank.

3.3 Modelling the whole pneumatic conveying system by the energy density approach (hybrid of conveying line and blowtank model)

This approach treats the whole system as one unit, using the approach of modelling the pipeline and the blowtank into one model. By measuring all the air into and out of the pneumatic conveying rig, pressure measurements around the blowtank as described earlier and pressure measurements describing the total elevation of the conveying pipeline, a system identification model can be attained. The information in the measured inputs for the pneumatic conveying system, of the change in energy density, is then correlated with the measured mass flow rate of solids. This gives that the calibration model needs a measurement of the mass flow rate. This model have controllable inputs and is usable in MPC. Figure (3.5) shows a sketch of such a system identification calibration model with input and output variables.

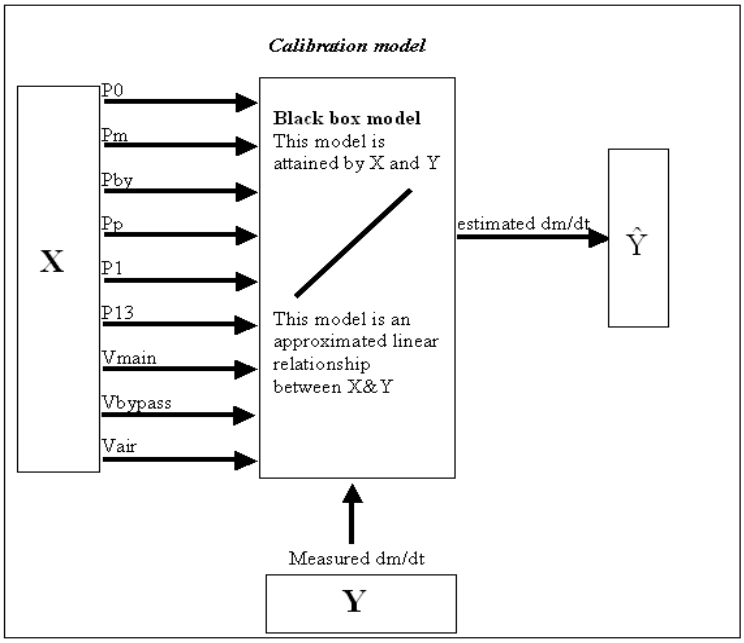

Figure 3.5: Simple sketch of system identification model for estimating the mass flow rate.

Chapter 4

Measurement setup

There are two rigs at POSTEC/Tel-Tek . Both are positive pressure pneumatic systems. This means that both rigs use air to blow the particulate solids from the blowtank through a pipeline to a receiving tank. Both rigs uses fluidization air to fluidize the particulate solids in the blowtank. One rig is bigger than the other, for simplicity the biggest rig will be called "plant A" from now on and the smaller rig "plant B". The air flowing into the blowtank is called the main air. The main air for plant A is divided into two parts. One part of the main air is flowing in at the bottom, fluidizing the particulate solids. The other part of the main air is flowing in at the top part of the blowtank, accelerating the particulate solids set into motion by the fluidization air. The ratio between these two airflows is currently used for controlling the mass flow rate of the particulate solids. The control system for the ratio control is a Fuzzy logic controller. Plant B does not have fluidization air in the same sense as plant A. Plant B has a main air inlet from one pipe that is split into a juncture. The juncture splits the main air into a air inlet at the top and the bottom of the blowtank, with no valves making it impossible to control the ratio. The rigs have different pipeline construction, pipeline diameter and elevation. None of the rigs have any form of feeding device into the pipeline, the particulate solids are just blown through the pipeline by the air in the blowtank and an adjustor flow called bypass air. The bypass air is a support airflow to prevent plugs during conveying. The bypass air gives back pressure to the blowtank, preventing too much particulate solids flowing into the pipeline. The bypass air also dilutes the suspension of particulate solids and air, this also prevents plugs. The two rigs were tested for two different powders. Baryte was conveyed in dense phase in plant A and dextrose was conveyed in dilute phase for plant B.

4.1 The measurement setup for plant A

Plant A is a positive pressure pneumatic conveying system. The exhaust air is measured for calculation of air velocity. The exhaust air is measured at the end of the conveying line and is a measurement of all the air travelling through the pipeline. The pressure transducers are placed all around the pipeline, like shown in figure (4.2). Figure(4.1) shows a picture of the blowtank and receiving tank for plant A. The air supply was an air compressor able to deliver an air flow up to $1000Nm^3/h$. This is a limitation for control purposes of the pneumatic conveying, since this is the maximum limit for air flow in the pneumatic conveying system. The blowtank has a $3m^3$ capacity and can withstand a maximum pressure of $10bar$.

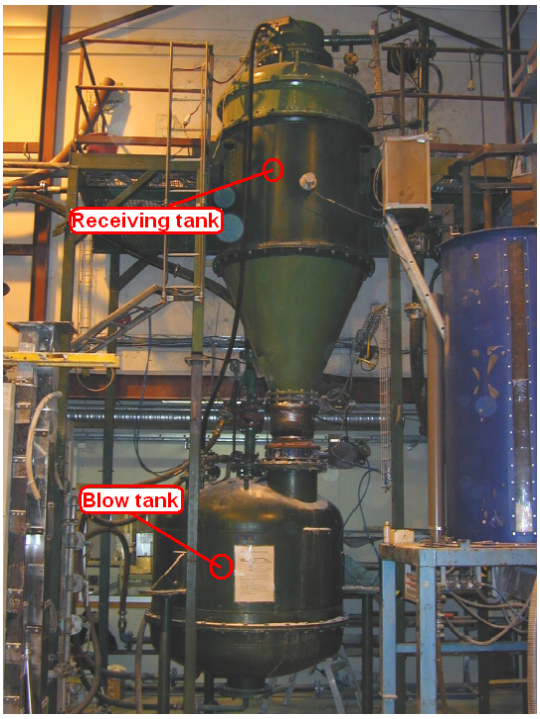

Figure 4.1: Picture of the blow tank and the receiving tank for plant A.

The conveying line was a constant diameter pipeline which was approximately $140m$ long and of $75mm$ diameter. The pipeline made a closed loop conveying system by mounting the receiving tank just on top of the blow tank, so that the conveying material could be re-circulated after each test run. Pressure transducers, as shown in figure (4.2), were placed on the conveying line in positions, so that the pressure drop values could be determined across different features, like straight pipe sections, bends, etc. All bends used in the conveying line were 90° standard bends, while there was a fully open butterfly valve between pressure transducers P19 and P20. A load cell in the receiving tank was used for measuring the transported mass of solids.

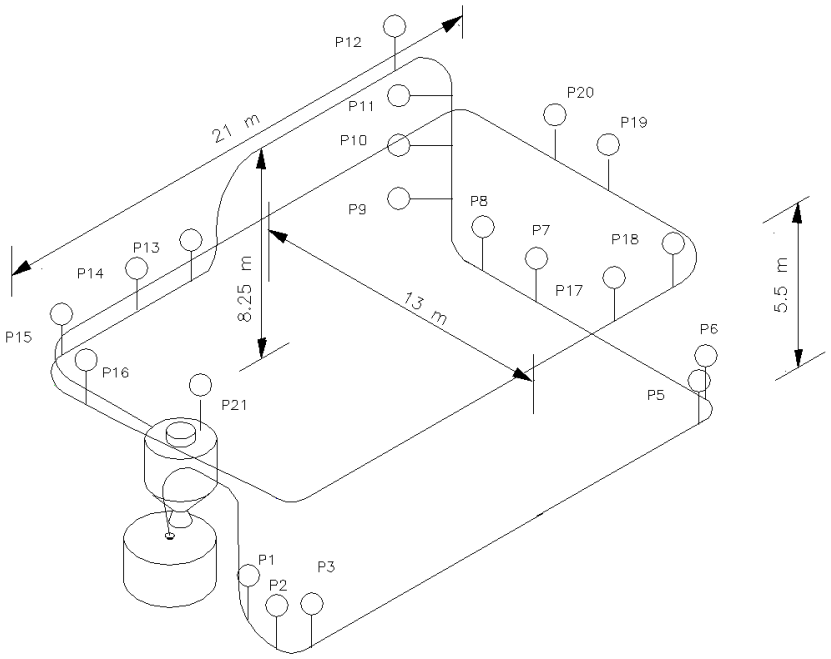

Figure 4.2: Layout og the pressure transducers along the pipeline for plant A.

The main air and bypass air was not recorded in the data set. This resulted in a model of the pipeline, with the blowtank as a starting point. The blowtank pressure is kept as stable as possible at a constant pressure. Later it was installed a PID-controller for controlling the blowtank pressure. The data used in this thesis does not have a controller for the blowtank pressure, this control was done manually by valves. This resulted in variations in the blowtank pressure data. The blowtank pressure data given in table (1) is an rough average of the blowtank pressure data as an indication of the blowtank pressure during conveying.

4.1.1 Test procedure for plant A

The average blowtank pressure is ranging from 3 to 4.5 bar for the different test runs. The inlet air velocity was calculated as an average during conveying at the location of P1. This is because P1 is right after the juncture where the bypass air is attached to the pipeline, giving the first measurement where all the air is pumped into the pipeline. The suspension density is a term used at POSTEC/Tel-Tek in relationship with the K-model. The average suspension density at the inlet at position P1 was calculated as an indication of the conveying mode at the start of the pipeline. For more details on calculation of the suspension density, see Ratnayake [1]. Solids loading ratio was calculated as an indication of the overall conveying mode for the conveying. The solids loading ratio for the baryte was ranging from 28.1 to 79.2 and this is conveying in dense phase. According to Mills[3] dense phase is when the solids loading ratio is larger than 10 and according to Klinzing[2] et al, dense phase conveying is when the solids loading ratio is larger than 15. Six data sets from six different test runs were used. One was used as a calibration set and the other five as test sets. Table (1) shows the conditions for each test run.

Table 1 **Test conditions for pneumatic conveying test runs of baryte**

Test number	Blowtank pressure (bar)	Inlet air velocity (m/s)	Solids loading ratio	Suspension density (kg/m^3)
30110505 –Calibration set	3.5	5.5	79.3	289
01120501 –Test set	4.0	6.3	50.3	275
01120502 –Test set	3.5	6.1	60.8	312
01120504 –Test set	3.0	8.4	28.1	216
30110502 –Test set	4.5	8.3	48.9	218
30110507 –Test set	3.0	5.9	68.2	256

During the test runs, all the data including the pressure values have been recorded using a data logging system. The signals from all the pressure transmitters were recorded every 0.5 second. After the test runs, the variation of air mass flow rate and the different pressure readings were studied, using the data logging and retrieving software program. During test runs, samples were collected online and tested for particle size distribution in order to check any size degradation. As soon as size degradation could be noticed, the bulk powder was always replaced with a fresh powder. For those interested, the details of the test procedure is reported elsewhere [1].

4.1.2 Test material for plant A

The material used for the tests was baryte, which is used in oil industry as a weighting material. The tested quality of baryte has a mean particle size of $12\mu m$ and a particle density of $4200kg/m^3$. For each test, approximately $0.5 - 1.0m^3$ of bulk material was used. Baryte is classified as a group C material according to the Geldart classification of materials. This gives that baryte is not suitable for dense phase conveying, but during conveying it was conveyed in dense phase. This implicates that baryte behaves more like a class A material.

4.2 The measurement setup for plant B

Plant B is also a positive pressure pneumatic conveying system. The main air and bypass air is measured for calculation of air velocity. The main air and bypass air is measured at the start of the conveying line and together they are measurements of all the air travelling through the pipeline. The pressure transducers are placed all around the pipeline, like shown in figure (4.4). Figure(4.3) shows a picture of the blowtank and the receiving tank for plant A. The air supply was an air compressor able to deliver an air flow up to $1000Nm^3/h$. This is a limitation for control purposes of the pneumatic conveying, since this is the maximum limit for air flow in the pneumatic conveying system. The blowtank has a $0.34m^3$ capacity and can withstand a maximum pressure of $8bar$.

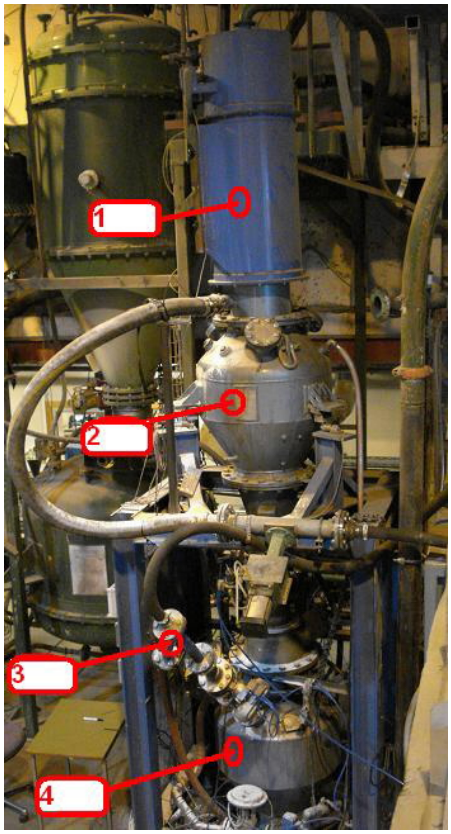

Figure 4.3: 1. Air filter, 2. Receiving tank, 3. Bypass air juncture, 4. Blow tank

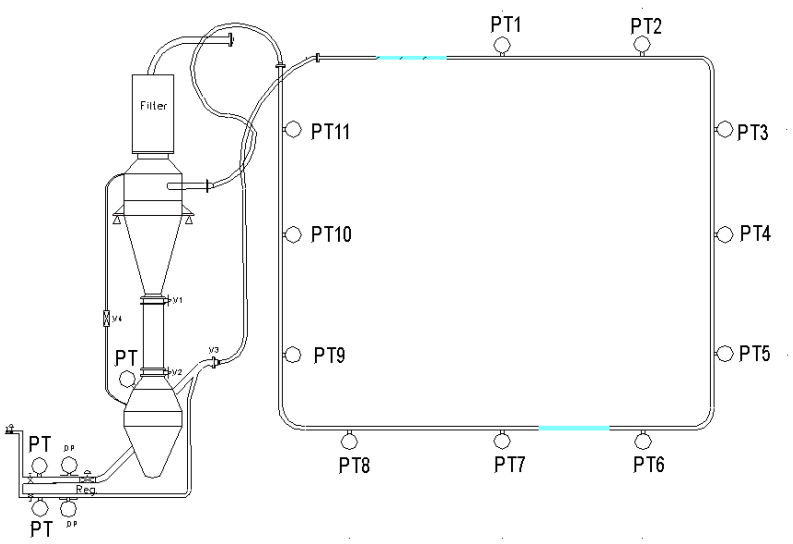

Figure 4.4: Layout of the pressure transducers placement in the small pneumatic conveying rig.

The conveying line was a constant diameter pipeline which was approximately $26m$ long and of $58mm$ diameter. The pipeline made a closed loop conveying system by mounting the receiving tank just on top of the blow tank, so that the conveying material could be re-circulated after each test run. Pressure transducers, as shown in figure (4.4), were placed on the conveying line in positions so that the pressure drop values could be determined across different features, like straight pipe sections, bends, etc. All bends used in the conveying line were 90° standard bends. An arrangement of load cells in the receiving tank was used for measuring the transported mass of solids.

The main air and bypass air was measured. This resulted in a model for the whole pneumatic conveying system, which has controllable inputs making model predictive control possible. The model attained from plant B data was used for the MPC which is described later in its own chapter. The blowtank pressure is kept as stable as possible at a constant pressure. This was done by an on-off controller. The on-off controller gives a more stable pressure than the manual control for plant A. Still the on-off controller is not an ideal controller and has pressure variations during conveying of approximately $200mbar$. The blowtank pressure data given in table (2) is an average of the blowtank pressure data as an indication of the blowtank pressure during conveying.

4.2.1 Test procedure for plant B

The average blowtank pressure is ranging from 1.6 to 2.1 bar for the different test runs. Pressure transducer 1 (PT1) is used as the starting point for calculating the inlet air velocity. The inlet air velocity was calculated as an average during conveying at the location of PT1. The suspension density is a term used at POSTEC/Tel-Tek in relationship with the K-model. The average suspension density at the inlet at position P1 was calculated as an indication of the conveying mode at the start of the pipeline. For more details on calculation of the suspension density, see Ratnayake [1]. Solids loading ratio was calculated as an indication of the overall conveying mode for the conveying. The solids loading ratio for the dextrose was ranging from 3.22 to 9.15 and this is conveying in dilute phase. Four data sets from four different test runs were used. One was used

as a calibration set and the other three as test sets. Table (2) shows the conditions for each test run.

Table 2 **Test conditions for pneumatic conveying test runs of dextrose**

Test number	Blowtank pressure (bar)	Inlet air velocity (m/s)	Solids loading ratio	Suspension density (kg/m^3)
16110704 –Calibration set	1.7	33.6	3.23	4.5
20110707 –Test set	2.1	30.3	4.41	4.8
19100701 –Test set	1.6	35.2	3.22	4.4
19100708 –Test set	2.1	21.1	9.15	7.1

During the test runs, all the data including the pressure values have been recorded using a data logging system. The signals from all the pressure transmitters were recorded every 0.1 second. After the test runs, the variation of air mass flow rate and the different pressure readings were studied, using the data logging and retrieving software program. During test runs, samples were collected online and tested for particle size distribution in order to check any size degradation. As soon as size degradation could be noticed, the bulk powder was always replaced with a fresh powder.

4.2.2 Test material for plant B

The powder used for the experiments was dextrose monohydrate provided by Tate & Lyle, Belgium. Crystalline dextrose monohydrate contains 91% dry substance, 99% dextrose content and 0.5% other sugars in the dry substance. It can be used as a sweetening agent or fermentable sugars source in a wide range of food and fermentation applications. In addition it can be used as an excipient in pharmaceutical applications particularly for powdered and tabletted dosage forms. It provides sweetness in confectionery and a cooling effect in tablets and panned products and it can also be used to produce fondants. In spices and seasoning mixes it provides sweetness, bulk, fermentable sugars and a source of reducing sugars which can promote Maillard browning reactions and flavor development in cooked meat products. In bakery mixes it is a source of fermentable sugars to promote yeast activity and it may be used to substitute sucrose economically. In addition it can contribute to a finer crumb structure in cakes and biscuits. Crystalline dextrose monohydrate may be used as a sucrose substitute or a readily available energy source in sports drinks, isotonic drinks and baby foods. It may be used in industrial applications as a chemical building block (chemically pure dextrose or glucose) and it is widely used for the production of ecologically sound surfactants [19].

The tested quality of dextrose monohydrate had a mean particle size of $138\mu m$ and a particle density of $1522kg/m^3$. For each test, approximately $0.1 - 0.15m^3$ of bulk material was used. Dextrose is classified as a group A material according to the Geldart classification of materials. This gives that dextrose is suitable for dense phase conveying, but during conveying it could only be conveyed in dilute phase. This implicates that dextrose behaves more like a class C material.

Chapter 5

Results & discussion of model results

5.1 Modelling pneumatic systems by the energy density approach using system identification

The modelling of the positive pressure pneumatic systems at TEL-TEK/POSTEC resulted in two approaches. One approach focusing on the pipeline and one approach focusing on the blowtank. A third hybrid approach, combining them was then introduced. In this chapter the pipeline and hybrid approaches with results will be discussed. The model predictive control results of the hybrid model will be discussed in the next chapter.

5.2 System identification model of the mass flow rate with emphasis on the pipeline (mass flow rate model for plant A)

For modelling plant A with the energy density approach, it is needed to have measurement of the total air flow rate and pressure measurements describing the energy density change at key points in the conveying system. The key points that was measured in the plant A data for baryte, was the pressure in the blowtank, the pressure at the bypass air intersection, the pressure at the earliest lowest elevation of the pipeline and the pressure at the point in the pipeline that describes the total elevation best. Together these measurements describes the energy density changes at these key points during transport of particulate solids. By comparing the changes in energy density at the key points with the measured mass flow rate at the end of the conveying line, a model describing the mass flow rate can be found by using system identification.

5.2.1 Selecting the proper inputs and outputs for use in the mass flow rate model for plant A

The selection of measurement input variables for the DSR method is based on conservation of energy related to the air and the Bernoulli effect. System identification was used to find the relationship between the change in energy density (i.e., Energy per unit volume) of air and the mass flow of solids.

Input measurement, air flow rate

For plant A the exhaust air (air) was measured at the end of the pipeline. This measurement gives information of the total mass flow rate of air used for transporting the particulate solids. This measurement carries information about the kinetic energy density at the end of the conveying line.

Input measurement, blow tank pressure (P0)

The blowtank pressure (P0) was measured and this pressure gives the energy density stored in the blowtank. This static pressure consists of compressed air. When the compressed air expands through the pipeline this

pressure is gradually converted into kinetic energy density. The pressure measurements along the pipeline gives information of how the energy density is changing through the pipeline.

Input measurement, bypass air intersection pressure (P1)

The bypass air is support air pumped into the pipeline. This air gives back pressure to the blowtank, reducing the mass flow rate of the particulate solids. The bypass air also increase the amount of air in the pipeline, increasing the energy density of the air. In other words, the bypass air reduce the mass flow rate of particulate solids and increase the mass flow rate of air. This gives that the bypass air increase the energy density in the air for transporting the particulate solids and reduce the amount of particulate solids to be transported. The intersection where the bypass air is introduced to the conveying pipeline is a key point to measure pressure in the conveying pipeline. This intersection has a pressure transducer (P1).

Input measurement of vertical conveying, pressure transducers P2 and P13

To take into account the vertical conveying, a pressure measurement of the earliest lowest elevated point in the pipeline and the point describing the total elevation is needed. These measurement points gives an indication of the conversion from kinetic energy density to potential energy density of the air during conveying. The pressure transducer measuring the earliest lowest elevated point in the pipeline was pressure transducer P2. The pressure transducer measuring the total elevation of the pipeline was pressure transducer P13.

Output measurement, measurement of mass flow rate of solids

The mass of solids was measured by a load cell in the receiving tank. By calculating the change in measured load cell data (dm/dt), a measured mass flow was obtained. This measured mass flow was chosen as output variable for the calibration set, using DSR.

Model errors related to measurements

The transference from energy density of air into kinetic energy of solids generates a loss in energy density of the air. Due to forces like drag, pipe wall friction and particle collisions there is an additional loss in kinetic energy of the transported solids. This loss of kinetic energy for the solids also causes a loss in the energy density of the air. These losses are hard to distinguish from eachother and approximate correctly and leads to an error in the model. Turbulence is hard to model by system identification and also leads to an error in the model.

5.2.2 Results and discussion for the model for plant A

The model was made from a calibration set (30110505) and the rest of the data sets were used as test sets. Test sets are data sets used for validation of the calibration model. The model gotten from system identification was a state space model (5.1).

$$\begin{aligned} x_{k+1} &= ax_k + Bu_k, x_0 - given \\ y_k &= x_k \end{aligned} \tag{5.1}$$

where

$$
\begin{aligned}
x_0 &= 19.9815 \text{ The initial state at discrete time step } k = 0 \\
x_k &= \text{The present state, which is the mass flow of solids at present discrete time step } k \\
x_{k+1} &= \text{The next state, which is the mass flow of solids at the next discrete time step } k + 1 \\
a &= 0.2548 \text{ The transition matrix, which is a scalar here since there is only one state} \\
u_k &= \begin{bmatrix} p_0 - \text{Blowtank pressure} \\ p_1 - \text{Juncture pressure} \\ p_2 - \text{Lowest elevation pressure} \\ p_{13} - \text{Total elevation pressure} \\ air - \text{Conveying air} \end{bmatrix} \begin{pmatrix} \text{The control vector, which consists of} \\ \text{all the inputs to the process} \\ \text{at present time step } k \end{pmatrix} \\
B &= \begin{bmatrix} 0.0013 & 0.0031 & -0.0049 & 0.0033 & -0.0041 \end{bmatrix} \\
&\quad \text{The input control matrix, which is a row vector since there is only one state} \\
&\quad \text{The input control row vector consists of a weighting of the inputs to the process} \\
y_k &= \text{The predicted output state at present time step } k, \\
&\quad \text{which is the mass flow of solids at present time step } k
\end{aligned}
$$

In figure (5.1) and figure (5.2) the measured cumulative mass flows are plotted against the predicted cumulative mass flows, using the DSR-model for 5 different experiments on transport of baryte with a mean particle size of $12\mu m$. For comparison, the estimation of the cumulative mass flow by the K-method for the same experiments are also plotted in figure (5.1) and figure (5.2). The whole line in figure (5.1) and (5.2) shows the measured mass in the receiving tank. The dotted line shows the predicted cumulative mass for the K-method and the thick line shows the prediction for the DSR-method.

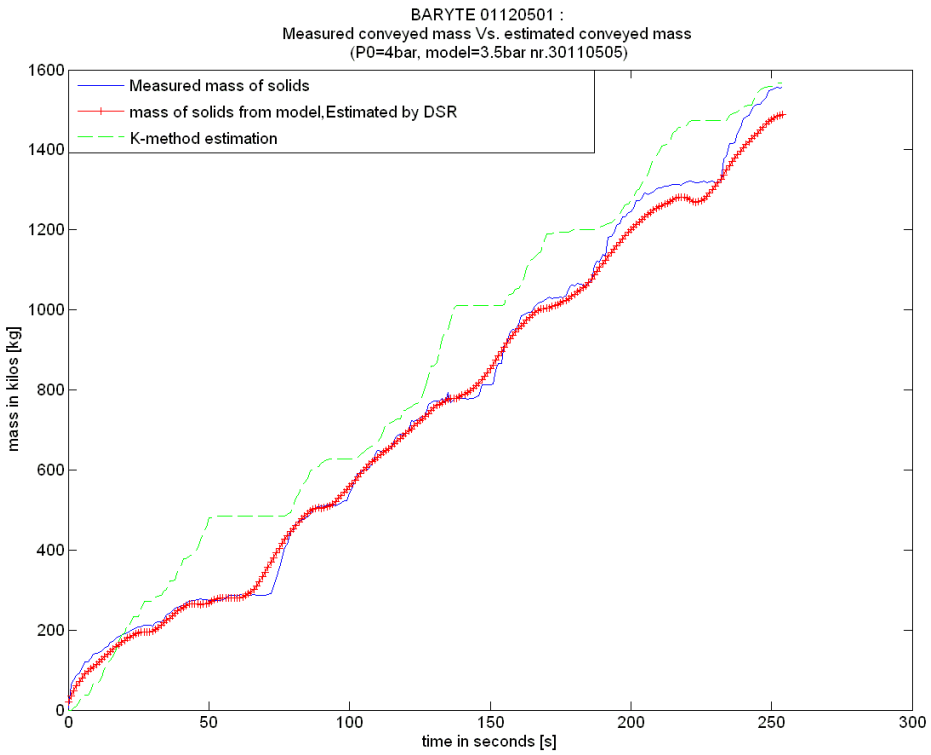

Figure 5.1: Comparison of the mass flow estimations for the DSR- and K-method models.

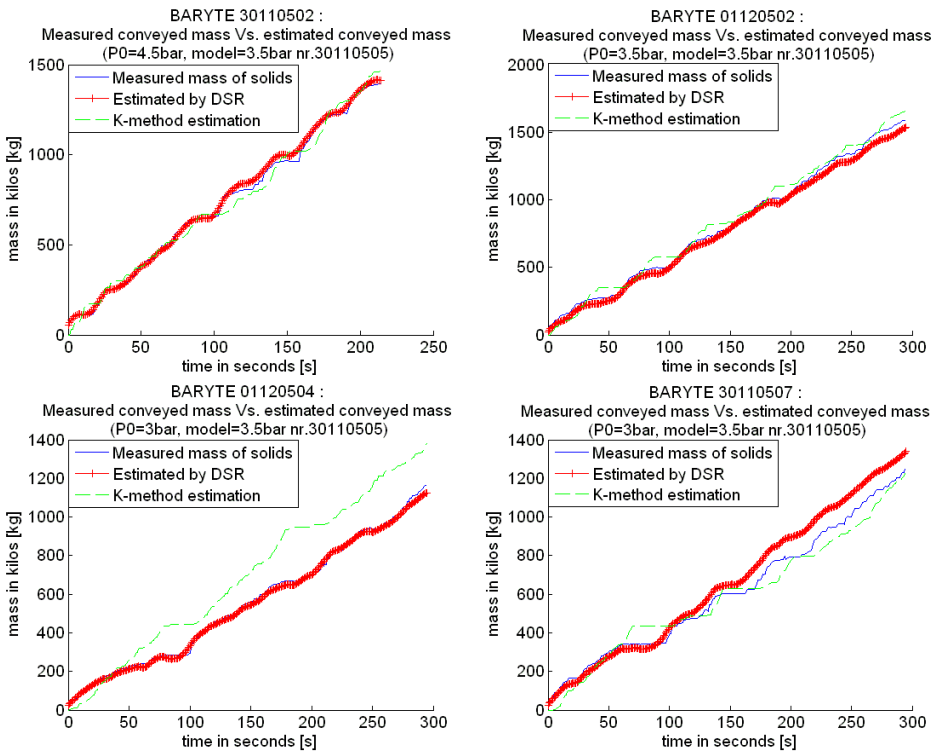

Figure 5.2: Comparison of the mass flow estimations for the DSR- and K-method models.

Figure (5.3a) shows the root mean square error of prediction (RMSEP) for the predicted cumulative mass of solids conveyed for the K-method and the DSR-model in percentage of the total measured cumulative mass conveyed. This plot shows how good the prediction of the cumulative mass follows the measured mass, i.e. how good the model follows the real process. The RMSEP of the predicted cumulative mass in percentage of total mass of solids conveyed was calculated by equation (5.2). The cumulative prediction error is shown in figure (5.3b), this plot shows how well the prediction ends up compared to the measured cumulative mass.

$$RMSEP\ of\ cum\ in\ \% = \left(\frac{\sqrt{\frac{1}{N}\sum_{i=1}^{N}(\hat{y}_i - y_i)^2}}{mass\ conveyed} \right) \cdot 100\% \tag{5.2}$$

$RMSEP\ of\ cum\ in\ \%$	=	RMSEP of predicted cumulative mass in percentage of total conveyed mass
$\hat{y}$	=	predicted cumulative mass of solids
y	=	measured cumulative mass of solids
N	=	number of samples
$mass\ conveyed$	=	Total mass of solids conveyed under test run

Table (2) shows the root mean square error of prediction (RMSEP) for the K-method and the DSR-model against the measured mass flow. The RMSEP was calculated by equation (5.2). Table (3) shows the cumulative error in conveyed mass of solids in percentage for the K-method and DSR model predictions.

Table 3 : RMSEP			*Table 4 :* Cumulative error [%]		
Experiment nr.	K-method	DSR model	Experiment nr.	K-method	DSR model
01.12.05.01	13.0098	9.0136	01.12.05.01	0.61	−4.40
30.11.05.02	12.9826	8.3481	30.11.05.02	5.55	1.21
01.12.05.02	10.3070	7.4739	01.12.05.02	4.16	−3.48
01.12.05.04	8.1714	5.9370	01.12.05.04	18.28	−3.70
30.11.05.07	9.0002	6.5170	30.11.05.07	−1.25	7.48

Figure (5.3) shows a graphical presentation of the RMSEP and cumulative error in conveyed mass of solids in percentage.

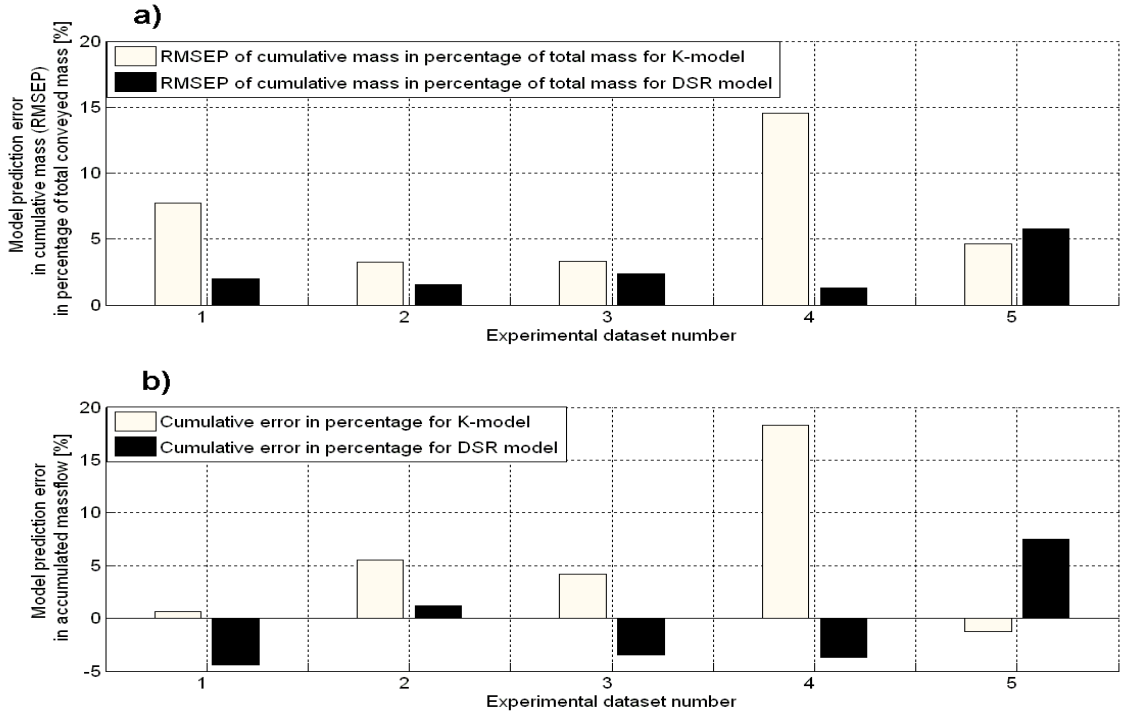

Figure 5.3: a) RMSEP of predicted cumulative mass in percentage of measured total mass conveyed. b) Total cumulative error in transport in percentage.

Figure (5.3a) gives that the cumulative RMSEP expressed in percentage of total conveyed mass for the DSR model ranges from $1.3 - 5.8\%$ error in mass estimation, while the error for the K-method ranges from $3.2 - 14.5\%$ error in mass estimation. It is evident from the experimental data that the DSR model follows the measured cumulative mass better than the K-method for these experiments. From figure (5.3b) the cumulative error for the DSR model is ranging from $\pm 1.2 - 7.5\%$, while the K-method ranges from $\pm 1.3 - 18.3\%$. It is evident from the experimental data that the DSR model has a smaller range of cumulative error than the K-method for these experiments.

The model based on system identification by DSR is robust considering different blowtank pressures compared to the K-method which has a different model for different blowtank pressures. The reason for this is that the DSR model takes into account the blowtank pressure fluctuations in the model. This makes the DSR model more robust regarding variations in the blowtank pressure than the K-method. The DSR model data is unfiltered while the K-method needs filtering of the raw data to give a good estimation. This is due to the sensitivity of the pressure gradient Δp_{st}, using the K-method. This sensitivity to noise in the pressure measurements is a weakness in the K-method, since a small deviation in pressure gradient affects

the calculation of the suspension density. The DSR model is more robust to such noise variations in the pressure measurements. This can explain the reason why the DSR method has a smaller range of cumulative error than the K-method. The DSR model is based purely on the relationships within the measurement data and is sensitive to boundary conditions for the process, like saturation of inlet airflow and large variations in blowtank pressure, unless a model is made from a data set that takes this into account. Such a model may suffer from less accuracy under normal conditions. The K-method uses an estimation of the mass flow at an earlier stage in the pneumatic conveying process rather than at the end, this results in a time delay in the estimation of the mass flow. This time delay can be seen in figure (5.1) and figure (5.2). The DSR model makes a model that takes this into account by making an estimation based on when the change at the end of the conveying line occurs. This almost eliminates the time delay in the estimation of the mass flow of solids by the DSR method. This time delay increases the RMSEP for the K-method and is a reason why the RMSEP is larger for the K-method compared to the DSR model. The K-method has successfully been implemented in industry by using a scaling up technique. This means that experiments can be run at a research facility test rig and then scaled up to industrial size scales.

5.3 System identification model of the mass flow rate with emphasis on the whole rig as a unit (hybrid model for plant B)

For modelling plant B with the energy density approach, it is needed to have measurement of the total air flow rate and pressure measurements describing the energy density change at key points in the conveying system. The air flow measurements was the main air and bypass air, together these measurements gave the total air added to the system at the start of the conveying system. The key points that was measured in the plant B data for transporting dextrose, was the pressure in the blowtank, the pressure at the main air inlet, the pressure at the bypass air inlet, the pressure at the lowest elevation of the pipeline and the pressure at the point in the pipeline that describes the total elevation best. Together these measurements describes the energy density changes at these key points during transport of particulate solids. By comparing the changes in energy density at the key points with the measured mass flow rate at the end of the conveying line, a model describing the mass flow rate can be found by using system identification.

5.3.1 Selecting the proper inputs and outputs for use in the mass flow rate model for plant B (hybrid model)

System identification was used to find the relationship between the change in energy density (i.e., Energy per unit volume) of air and the mass flow of solids as for plant A, but here the whole plant B including pipeline and blowtank was included in the model. This model was further on used for the MPC since it has controllable inputs, which the model for plant A do not have.

Input measurement, air flow rate

For plant B the main air (air_m) was measured at the start before the blowtank. This measurement gives information about the kinetic energy density sent into the blowtank and controls the fluidization of the particulate solids and the blowtank pressure. The bypass air (air_{by}) was measured at the start before the pipeline. This measurement gives information about the dynamic back pressure to the blowtank and the addition of extra energy density for transporting solids. Together the main air and bypass air gives the total mass flow rate of air used for transporting the particulate solids. These measurements carries information about the kinetic energy density at the start of the conveying line.

Input measurements, blow tank pressure (P_0), main pressure (P_m) and bypass pressure (P_{by})

The blowtank pressure (P_0) was measured and this pressure gives the energy density stored in the blowtank. The main pressure (P_m) carries information about the compression of the main air. The bypass pressure (P_{by}) carries information about the compression of the bypass air and the back pressure to the blowtank.

Input measurement, bypass air intersection pressure (P_1)

Pressure transducer (P_1) was situated to far away from the bypass intersection to give any information about the bypass intersection. P_1 was tried out in the model and it decreased the accuracy of the model. P_1 was therefore discarded as a input to the model.

Input measurement of vertical conveying, pressure transducers P_8 and P_{11}

To take into account the vertical conveying, a pressure measurement of the earliest lowest elevated point in the pipeline and the point describing the total elevation is needed. The pressure transducer measuring the earliest lowest elevated point in the pipeline was pressure transducer P_8. The pressure transducer measuring the total elevation of the pipeline was pressure transducer P_{11}.

Output measurement, measurement of mass flow rate of solids

The mass of solids was measured by a load cell in the receiving tank. By calculating the change in measured load cell data (dm/dt), a measured mass flow was obtained. This measured mass flow was chosen as output variable for the calibration set, using DSR.

Model errors related to measurements

The reasons for model errors is related to the same phenomena as for plant A. The reasons for model errors will be discussed under "MPC results & discussion" where the effect of turbulent air flow gives control problems.

5.3.2 Results and discussion for the model for plant B

The model was made from a calibration set (16110704) and the rest of the data sets were used as test sets. Test sets are data sets used for validation of the calibration model. The model gotten from system identification was a state space model (5.3).

$$\begin{aligned} x_{k+1} &= ax_k + Bu_k, x_0 - given \\ y_k &= x_k \end{aligned} \tag{5.3}$$

where

x_0 = -0.1291 The initial state at discrete time step $k = 0$

x_k = The present state, which is the mass flow of solids at present discrete time step k

x_{k+1} = The next state, which is the mass flow of solids at the next discrete time step $k + 1$

a = 0.0341 The transition matrix, which is a scalar here since there is only one state

u_k = $\begin{bmatrix} P_m - \text{Main pressure} \\ P_{by} - \text{Bypass pressure} \\ P_0 - \text{Blowtank pressure} \\ P_8 - \text{Lowest elevation pressure} \\ P_{11} - \text{Total elevation pressure} \\ air_m - \text{Main air} \\ air_{by} - \text{Bypass air} \end{bmatrix}$ $\left(\begin{array}{l} \text{The control vector, which consists of} \\ \text{all the inputs to the process} \\ \text{at present time step } k \end{array} \right)$

B = $\begin{bmatrix} 0.0033 & 0.1245 & -0.0295 & 0.3358 & -0.3999 & -0.0951 & -0.2011 \end{bmatrix} \cdot 10^{-3}$

The input control matrix, which is a row vector since there is only one state

The input control row vector consists of a weighting of the inputs to the process

y_k = The predicted output state at present time step k,

which is the mass flow of solids at present time step k

In figure (5.4), figure (5.5) and figure (5.6) the measured cumulative mass flows are plotted against the predicted cumulative mass flows, using the DSR-model for 3 different experiments on transport of dextrose with a mean particle size of $138\mu m$. For comparison, the estimation of the cumulative mass flow by the K-method for the same experiments are also plotted in the figures (5.4), (5.5) and (5.6). The whole line in the figures (5.4), (5.5) and (5.6) shows the measured mass in the receiving tank. The dotted line shows the predicted cumulative mass for the K-method and the thick dotted line shows the prediction for the DSR-method.

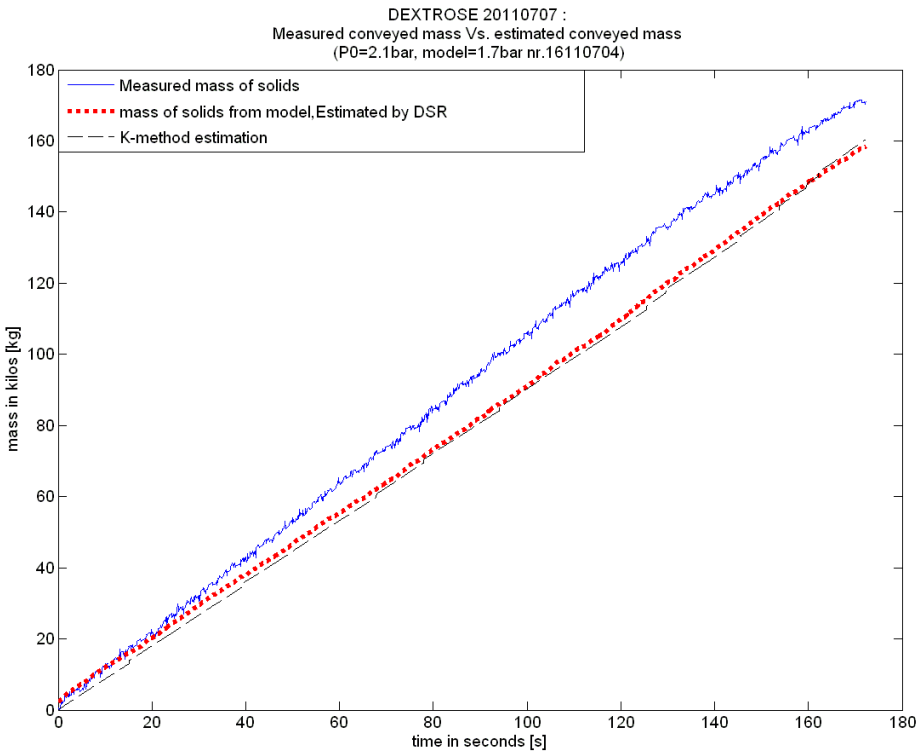

Figure 5.4: Comparison of the mass flow estimations for the DSR- and K-method models for dextrose.

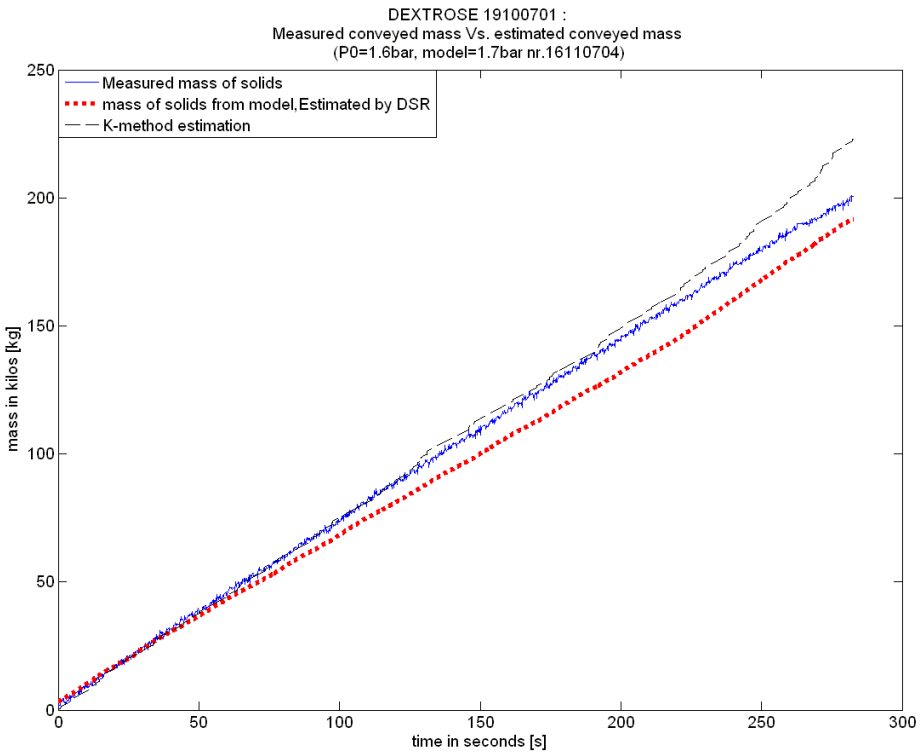

Figure 5.5: Comparison of the mass flow estimations for the DSR- and K-method models for dextrose.

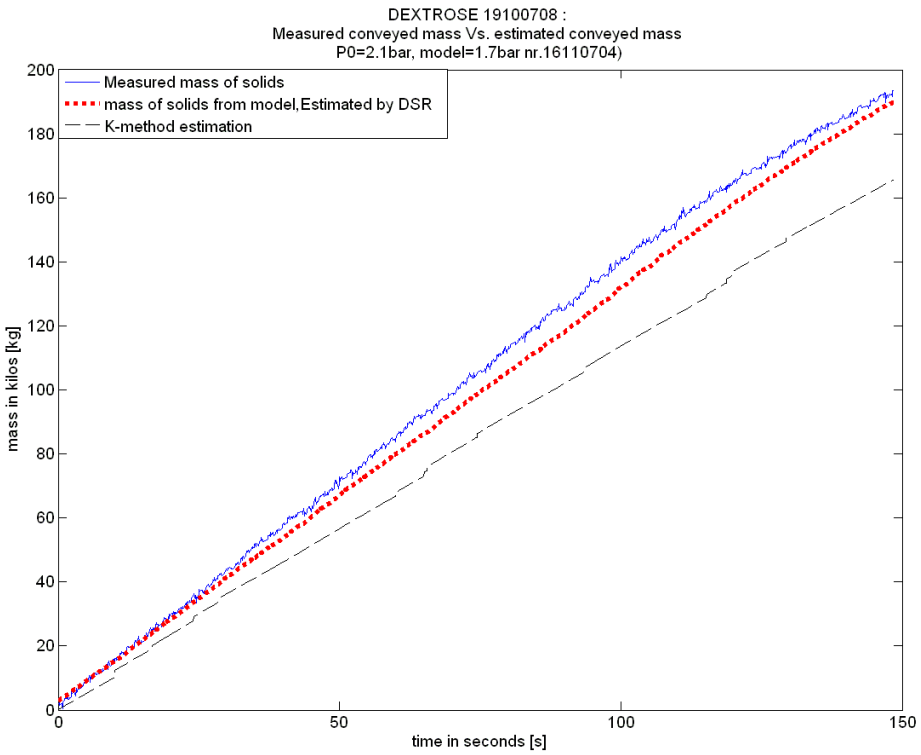

Figure 5.6: Comparison of the mass flow estimations for the DSR- and K-method models for dextrose.

Figure (5.3a) shows the root mean square error of prediction (RMSEP) for the predicted cumulative mass of solids conveyed for the K-method and the DSR-model in percentage of the total measured cumulative mass conveyed. The RMSEP of the predicted cumulative mass in percentage of total mass of solids conveyed was calculated by equation (5.2). The cumulative prediction error is shown in figure (5.7b). Table (5) shows the root mean square error of prediction (RMSEP) for the K-method and the DSR-model against the measured mass flow. Table (6) shows the cumulative error in conveyed mass of solids in percentage for the K-method and DSR model predictions.

Table 5 : RMSEP			*Table 6 :* Cumulative error [%]		
Experiment nr.	K-method	DSR model	Experiment nr.	K-method	DSR model
20.11.07.07	7.6826	6.8853	20.11.07.07	−6.2202	−7.3653
19.10.07.01	3.1788	4.5096	19.10.07.01	11.1763	−4.4845
19.10.07.08	10.6897	2.8718	19.10.07.08	−14.4488	−1.9432

Figure (5.3) shows a graphical presentation of the RMSEP and cumulative error in conveyed mass of solids in percentage.

The cumulative RMSEP in percentage for DSR model is ranging from $2.9 - 6.9\%$, while the K-method gave a range of $3.2\% - 10.7\%$. For these experiments the DSR model has a smaller range of cumulative RMSEP than the K-method. This gives that the DSR model follows the measured mass flow rate, as an average of these experiments, better than the K-method. The cumulative error for the DSR model is ranging from $\pm 1.9 - 7.4\%$, while the K-method has a range from $6.2 - 14.4\%$. This gives that the DSR model ends up with a better estimation of the total mass conveyed than the K-method, for these experiments.

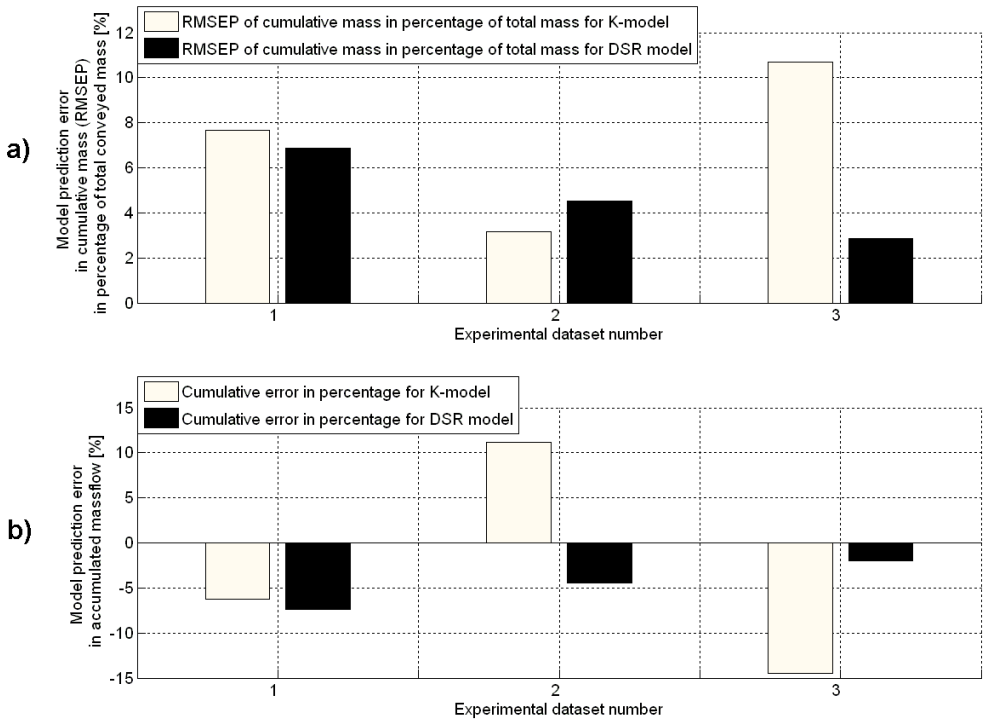

Figure 5.7: a) RMSEP of predicted cumulative mass in percentage of measured total mass conveyed. b) Total cumulative error in transport in percentage.

5.4 System identification model results discussion

As depicted in figures (5.1), (5.2), (5.4), (5.5), (5.6), it is clear that the solids mass flow rate can be predicted using DSR method. With the minor statistical analysis shown in figure (5.3) and (5.7), it is also clear over the range of conditions tested under this investigation that this method gives better accuracy than 'K' method, which has been used as an on-line solids mass flow rate measurement technique. Under this investigation, the DSR model has not been tried out for scaling up purpose and the model is at the moment rig dependent and has been tried out for two rigs. The tests carried out in plant A conveyed baryte in dense phase. The tests for plant A had a solid loading ratio ranging from $28.1 - 79.3$. The tests for plant B had a solid loading ratio ranging from $3.22 - 9.15$, this is dilute phase conveying. This gives that the DSR model based on the energy density approach also works for dilute phase as well as dense phase. It also gives an indication that this approach for a model of the mass flow rate of particulate solids works for different powders and different rigs. A DSR model has to be attained for each rig. A measurement of the mass flow rate is needed for a calibration set to get a DSR model, while the K-method uses a scaling up technique from pressure drop factors (K) gotten from pilot plant test runs. This gives that the K-method is the only choice for estimating the mass flow rate of particulate solids where it is not possible to measure the mass flow rate. Where it is possible to run a test with a measurement of the mass flow rate of particulate solids, the DSR model is better than the K-method. Both the K-method and the DSR model are at the moment powder dependent, consequently each powder needs a model. The K-method is more like a procedure for estimating the mass flow, while the DSR model is on state space form. This gives an advantage to the DSR model for control purposes of the process, since a model on state space form makes it possible to implement control strategies like model predictive control (MPC), which must have a model to be implemented. The DSR model is based on the energy density approach and indicates that it is possible to attain a mechanistic model from the energy density relationships in the pipe line and the blowtank.

Chapter 6

MPC results & discussion

The model used for the MPC was the one attained from plant B, since controllable inputs were available. The controllable inputs were the volumetric flow of main air and bypass air. The measurement data of the airflows were measured in Normal cubic meter per hour $[Nm^3/h]$. That means that the volumetric air flow is normalized with regards to atmospheric pressure. Controlling the air flows gives control of the energy density into the pneumatic system. The pressure measurements are considered as disturbances, since they are indirectly controllable through the air flows. Since the MPC was not tried out on the real process, simulations on measured data was performed. This gives that the set point of mass flow of particulate solids had to be set to the measured mass flows of the test sets, using the model attained from the calibration set.

The measured pressure measurements in the test sets were then used as the disturbances to the process model. If the model is good, the optimal control given by the MPC should follow the original measured air flows in the test sets data. In this thesis, the cost function is the reduction of the rate of change in the control. The weighting matrix for the rate of change cost function is R. The weighting matrices Q and R are important parameters in the MPC controller algorithm. Q is the weighting matrix for the control deviation term and R is the weighting matrix for the cost term. The control deviation term is the term giving the difference between the output value and the set point. The cost term is the term that is reducing the cost of the control signal, conserving energy relating to control of the process. The ratio between the Q matrix and the R matrix is an important factor for the MPC. A high ratio between Q and R $\left(\frac{Q}{R}\right)$ gives high weighting of the deviation term and low weighting of the cost term. The optimal control signal will then focus more on bringing the process to the set point, than reducing the energy cost. A high ratio gives fast control of the process, but for unconstrained MPC control this brings the optimal control to often unrealistic values. A low ratio gives slow control and a high weighting to the cost function. The prediction horizon L is an important parameter. Lowering the prediction horizon gives that the Q weighting has to be adjusted higher to achieve the same result for the optimal controls. A longer prediction horizon gives a smaller Q weighting. The prediction horizon during the simulations here were set to $L = 10$. If the process time delay is known, the prediction horizon should be longer than the time delay. To implement a time delay the delays can be augmented into the model as states. The effect of the prediction horizon has been studied. Time delays has not been considered in this thesis, but should be considered for further studies since the prediction horizon and time delays are often linked. For more about time delays and prediction horizon, see other work on MPC performed at the Telemark University-College, like Bartziokas [21].

6.1 Discussion of the weighting matrices Q and R

The process model has one state which is the mass flow rate of solids and two inputs which are the main air and bypass air. This gives that the weighting matrix Q is a scalar q and the R matrix is a 2×2 matrix. The main air and bypass air can be weighted differently, but in the experiments performed in this thesis they were weighted equal and set to be one(6.1).

$$R = \begin{bmatrix} 1 & 0 \\ 0 & 1 \end{bmatrix} \tag{6.1}$$

The q scalar was tried for different values intuitively. For values tried out, see table (7).

Table 7 : Weighting table for q	
figure numbers	weighting value for q
figures : (6.1), (6.2)	5×10^{60}
figures : (6.5), (6.6), (6.7), (6.8)	4×10^{5}
figures : (6.4), (6.3)	1

The maximum air flow the air compressor at POSTEC/Tel-Tek can give is $1000Nm^3/h$ and the minimum is $0Nm^3/h$. Figure (6.1) shows unconstrained MPC with an enormous q weighting of 5×10^{60}, it is possible to see that the unconstrained optimal control suggested is unrealistic. The same weighting tried out with MatLab QP solver 'quadprog' is shown in figure (6.2). The constraints are input amplitude constraints and are set according to (6.2).

$$\left.\begin{array}{l} 0 \leq u_{main} \leq 300 \\ 300 \leq u_{by} \leq 1000 \end{array}\right\} \tag{6.2}$$

The inequality constraint (6.3) was also implemented, since the compressor cannot give more than $1000Nm^3/h$.

$$u_{main} + u_{by} \leq 1000 \tag{6.3}$$

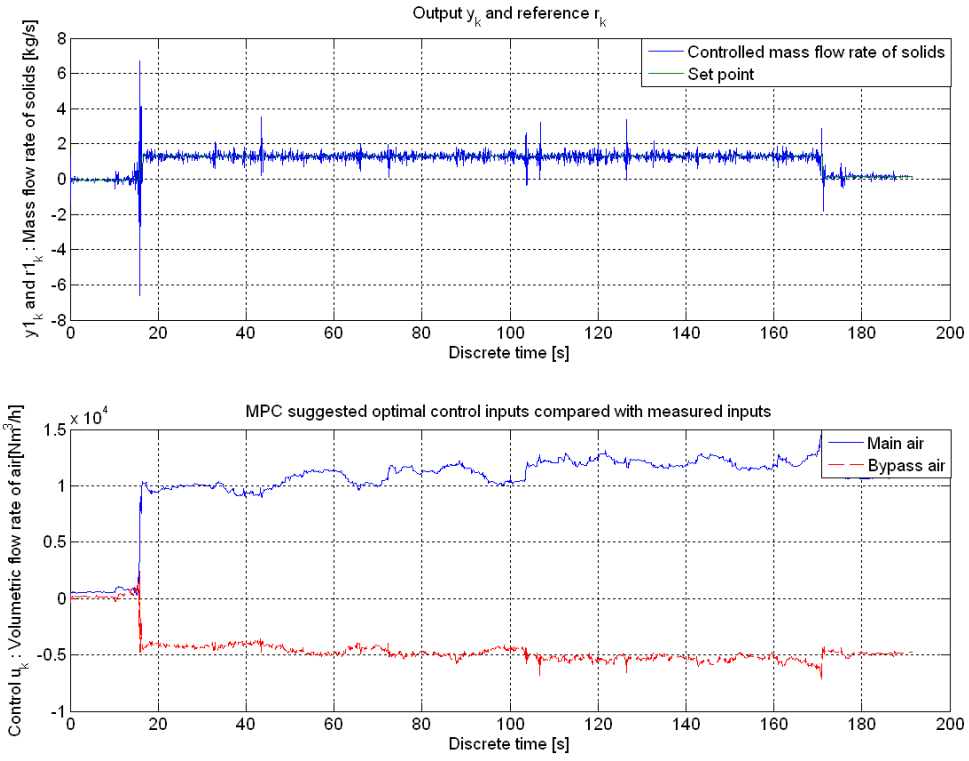

Figure 6.1: Unconstrained MPC control simulating the test 19100708 with q weighting of $5 \times 10^{\hat{}60}$

It is possible to see that the optimal control given by 'quadprog' is better than the optimal unconstrained control given by the MPC algorithm given in the literature review of the MPC. Because of the hard weighting of the q scalar, the 'quadprog' algorithm uses a long time computing the optimal control. This is because of constraints being active almost constantly and the time for computing was timed to be 912.0520 seconds (approximately $15min$ and $12sec$). Further the optimal control, given by 'quadprog' with the given constraints, gives an optimal control that has an unrealistic rate of change of the control. It is obvious that the q weight has to be tuned down.

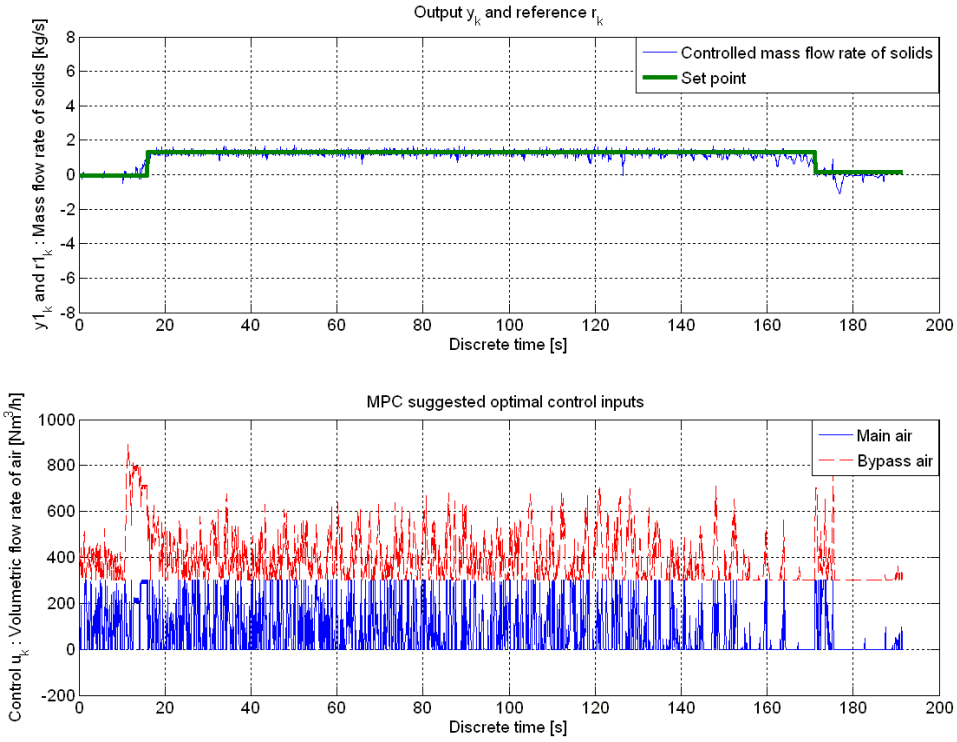

Figure 6.2: Constrained MPC control using 'quadprog', simulating the test 19100708 with q weighting of $5 \times 10\hat{}60$

The q weight was then tuned down to 1, giving a ratio between q and R of 1. This is the same as weighting the deviation term and the cost term equally. By using the custom made algorithm in the literature review of MPC, the results are constant optimal controls during the simulation. The computation time was timed to 1.5420 seconds. See figure (6.3) for plot of the simulation of test set 19100708. The same test was performed using 'quadprog' and gave the same result, except that the main air was computed to be $3.719Nm^3/h$ and bypass air to $504.8Nm^3/h$ compared to $3.712Nm^3/h$ and $504.7Nm^3/h$ respectively by the custom made algorithm. The computation time used by quadprog was 29.1020 seconds.

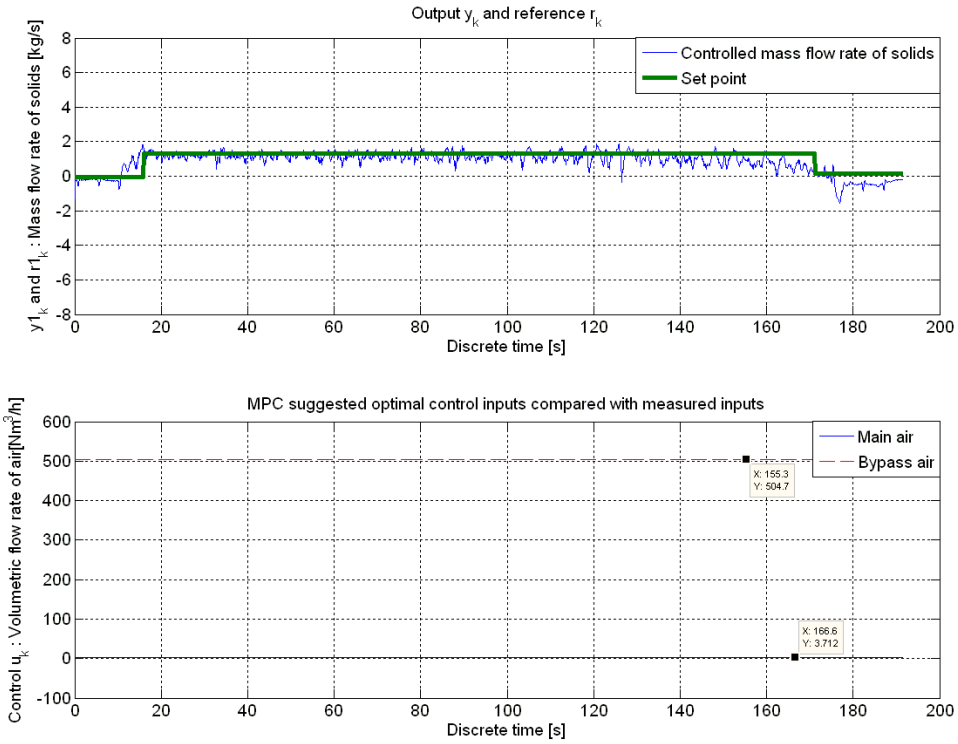

Figure 6.3: Unconstrained MPC control simulating the test 19100708 with q weighting of 1

A closer look at the control of the mass flow of solids show that this control is too slow to follow the dynamics of the process. This results in a deviation in mass flow of solids from the desired set point. Figure (6.4) shows this deviation in accumulated mass during transport. This is because the q scalar is set to be too low giving the deviation term too low priority. The q weighting has to be tuned up.

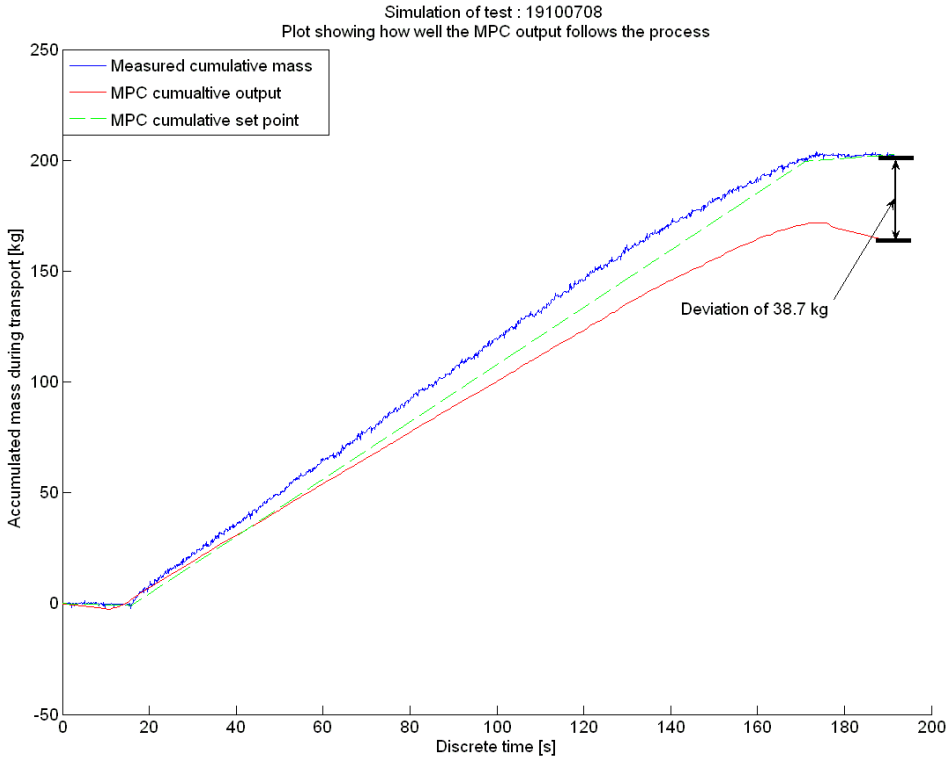

Figure 6.4: Plot showing the deviation in accumulated mass using MPC controls with a q weighting of 1

The q weighting was found intuitively by adjusting a q that gave a reasonable result for the unconstrained optimal controls. A reasonable q was found to be $q = 4 \cdot 10^5$. See figure (6.5) for the unconstrained MPC simulation of test 19100708. Computation time was 1.3720 seconds.

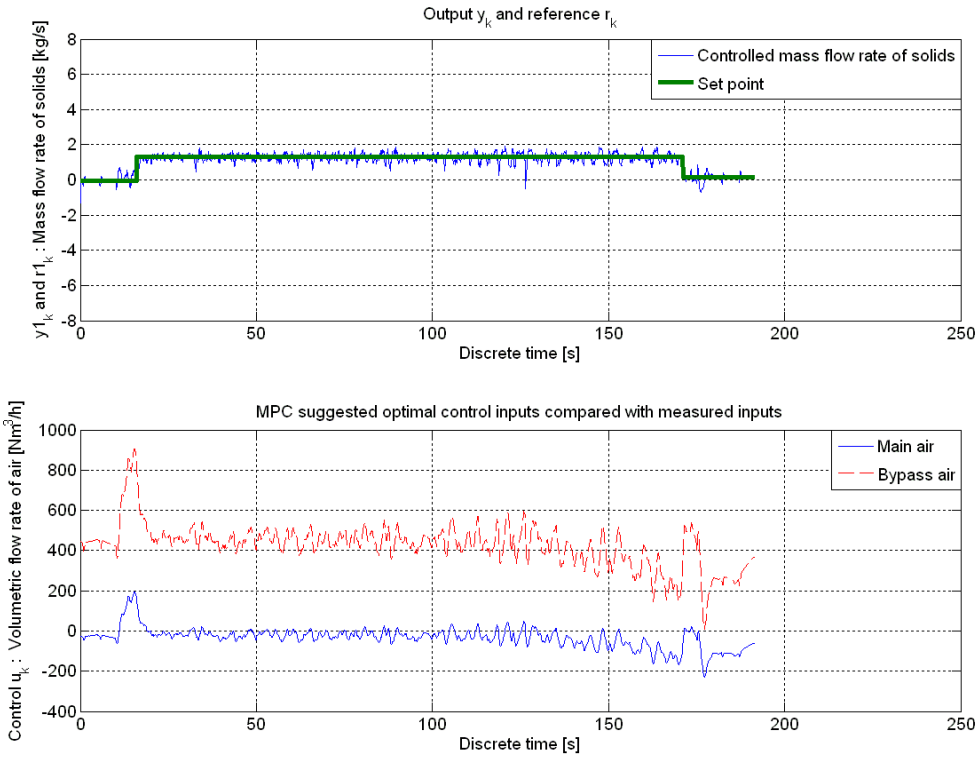

Figure 6.5: Unconstrained MPC simulation of test 19100708 with a q weighting of $4 \cdot 10^5$

From figure (6.5), it is possible to see that the unconstrained optimal control gives a slightly unrealistic main air flow rate that is negative. Comparing the computed unconstrained optimal control inputs with the measured volumetric flows for the test set 19100708, gives that the computed unconstrained optimal control inputs follows the trend in the measured air flows, except for the start and end of the simulation. The reason for this will be explained later. See figure (6.6) for the comparison between measured air flows and suggested unconstrained optimal control inputs.

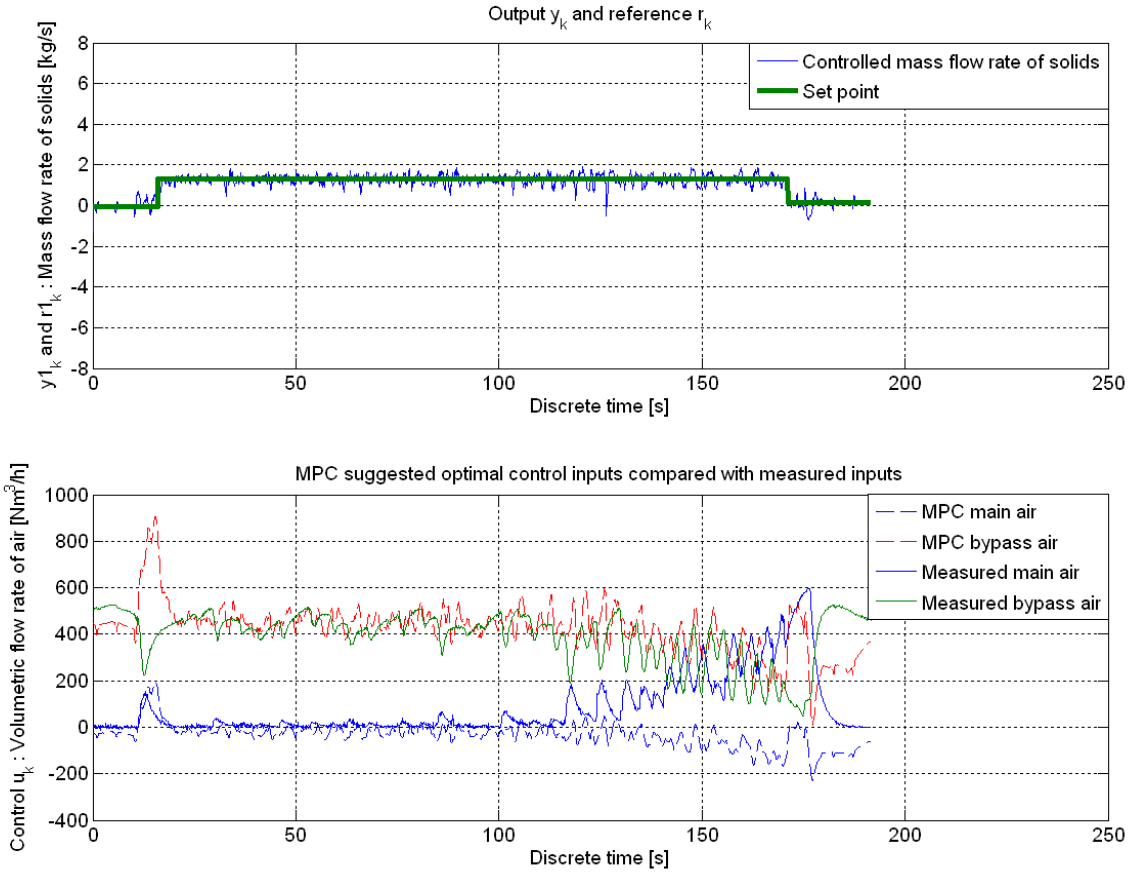

Figure 6.6: Comparison of Suggested MPC unconstrained optimal control inputs and the measured inputs to the process for test 19100708.

Figure (6.7) shows this deviation in accumulated mass during transport.

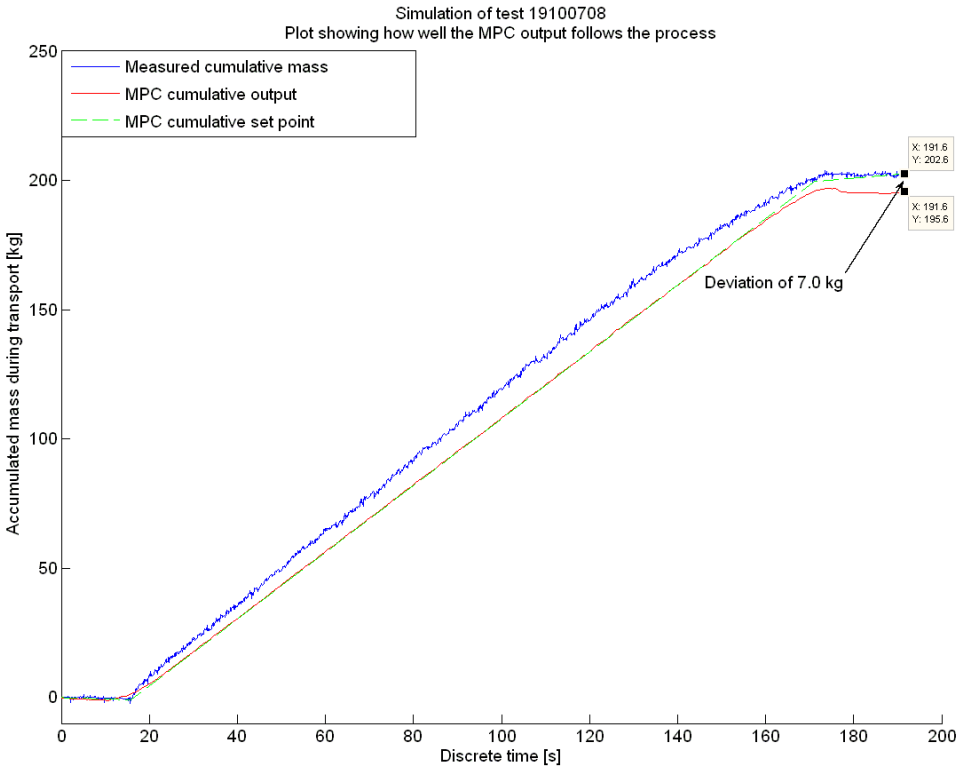

Figure 6.7: Plot showing the deviation in accumulated mass using unconstrained MPC controls with a q weighting of $4 \cdot 10^5$ for test 19100708.

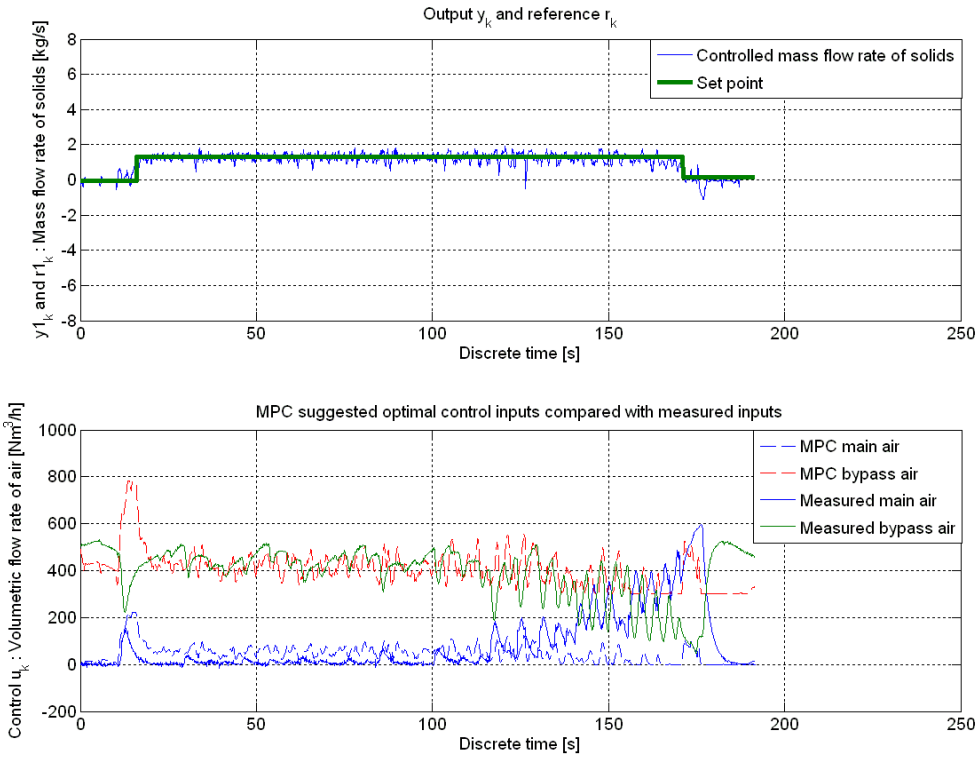

Figure 6.8: Comparison of Suggested MPC constrained optimal control inputs and the measured inputs to the process for test 19100708.

The same weighting of $q = 4 \cdot 10^5$ was then applied to a constrained MPC using MatLab 'quadprog'. The constraints applied is the same as above. The plot of the suggested optimal controls is shown in figure (6.8). The computation time was 54.798 seconds. From now on all the MPC controls will have constraints and use 'quadprog' and computation time will not be mentioned for every plot. Computation time has been mentioned earlier for comparison and to give an indication of proper weighting. The q weighting was tuned down a bit to $q = 10^5$ for the rest of the simulations.

6.2 Constraints for the process of pneumatic conveying

the q weighting was set to (6.4) and the R weighting set to (6.5) for the simulations.

$$q = 10^5 \tag{6.4}$$

$$R = \begin{bmatrix} 1 & 0 \\ 0 & 1 \end{bmatrix} \tag{6.5}$$

Prediction horizon for the simulations was set to (6.6).

$$L = 10 \tag{6.6}$$

The inequality constraints for the simulations was set according to table (8).

Table 8 : Inequality constraints for the simulations

Test set number	Constraints
20110707	$0 \leq u_{main} \leq 100$ $400 \leq u_{by} \leq 805$ $u_{main} + u_{by} \leq 875$
19100701	$0 \leq u_{main} \leq 100$ $400 \leq u_{by} \leq 742$ $u_{main} + u_{by} \leq 822$
19100708	$0 \leq u_{main} \leq 200$ $300 \leq u_{by} \leq 530$ $u_{main} + u_{by} \leq 715$

The rate of change constraints (6.7) relating to valve characteristics was not included, since no such data was available at the time. How fast a valve close and opens is an important parameter for calculating an optimal control, if not the valves sluggishness will work as a filter for the original computed optimal control.

$$\left.\begin{array}{c} \min \# \leq \Delta u_{main} \leq \max \# \\ \min \# \leq \Delta u_{by} \leq \max \# \end{array}\right\} \tag{6.7}$$

The MPC algorithm was set up on deviation form (6.8) and augmented (6.9). The 'quadprog' QP solver needs constraints on the form (6.10), while the deviation form gives constraints on the form $\Delta u_{k|L}$.

$$\left.\begin{array}{c} \Delta x_{k+1} = a\Delta x_k + B\Delta u_k \\ y_k = y_{k-1} + d\Delta x_k \end{array}\right\} \tag{6.8}$$

$$\left.\begin{array}{c} \tilde{x}_{k+1} = \tilde{A}\tilde{x}_k + \tilde{B}\Delta u_k \\ y_k = \tilde{D}\tilde{x}_k \end{array}\right\} \tag{6.9}$$

$$u_{k|L} = S\Delta u_{k|L} + cu_{k-1} \tag{6.10}$$

Conversion of $\Delta u_{k|L}$ to $u_{k|L}$ for use of 'quadprog' can be done according to (6.11) and (6.12) giving (6.13) for input amplitude constraints.

$$\begin{aligned} u_{k|L} &= S\Delta u_{k|L} + cu_{k-1} \\ u_{k|L} &\leq u_{\max} \\ S\Delta u_{k|L} &\leq u_{\max} - cu_{k-1} \\ u_{k|L} &\geq u_{\min} \\ -u_{k|L} &\leq -u_{\min} \\ -S\Delta u_{k|L} &\leq -u_{\min} + cu_{k-1} \end{aligned} \tag{6.11, 6.12}$$

$$\begin{bmatrix} S \\ -S \end{bmatrix} \Delta u_{k|L} \leq \begin{bmatrix} u_{\max} - cu_{k-1} \\ -u_{\min} + cu_{k-1} \end{bmatrix} \tag{6.13}$$

6.3 Using MPC for model validation

As mentioned earlier, if the model is good, the optimal control given by the MPC should follow the original measured air flows in the test sets data. So far, the plots that have been shown has used simulation of the whole data set. In other words, this means the data before transport of solids, during transport of solids and at the end of transport of solids. The data can be given a time axis like shown in figure (6.9). During transport the constrained optimal control inputs follow the original measured air flow rates. At the end of transport, turbulent flow of air occurs and the model only follows the trend of the original measured flows. This gives that the model attained from system identification does not model turbulent flow well. One reason for the turbulent flow is the on-off controller for the blowtank. At the end of transport more air is escaping the blowtank at higher velocity than during transport. The on-off controller tries to compensate for this by pumping in more main air, this results in oscillations in the air flow, giving turbulent flow. Even with the use of a PI-controller for the blowtank pressure, the flow of air will be turbulent at the end of transport. This is because the velocity of air escaping the blowtank at the end of transport will have a velocities reaching up to the velocity of sound. The use of a PI-controller will still be an improvement, especially during transport. By modelling the blowtank, MPC can be applied to control blowtank pressure. Modelling the blowtank pressure gives a non-linear model and leads to non-linear MPC (NMPC) or a non-linear model linearized around an operating point. For more about non-linear model linearized around an operating point, see other work on MPC performed at the Telemark University -College, like Bedelbayev [22].

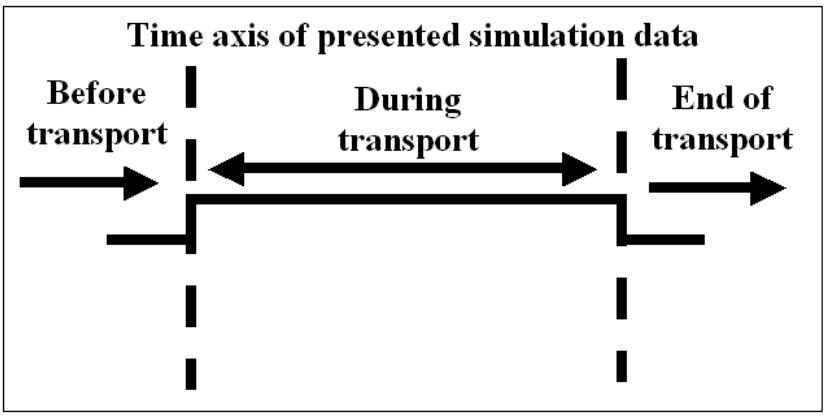

Figure 6.9: Time axis of simulation of test sets.

Figure (6.10), (6.13) and (6.16) shows the constrained optimal control inputs given by 'quadprog' compared with the test set data sets for transporting dextrose in plant B during transport. One reason for deviation between MPC suggested optimal control inputs and the measured control inputs, is related to model error. Another reason for the deviation can be due to that the MPC set point is constant and slightly off the measured mass flow rate. Another issue is the effect of too short prediction horizon. This will be explained more later.

Three subchapters are dedicated to plots of the simulations. The accumulative plots (6.11), (6.14) and (6.17) shows how close the MPC set point is set to the real process. Given optimal control inputs, the controlled mass flow should follow the MPC set point. If the model is good, the MPC optimal controls should follow the original measured controls. Normalized cross correlation, giving a correlation coefficient in percentage, was used for validation of how well the measured and MPC suggested controls follows eachother. MatLab 'xcorr' function was used (6.14).

$$>>[\text{C,lags}]=\text{xcorr(air\_main,u\_opt,'coeff')} \tag{6.14}$$

Cross validation does not give any information about the deviation or magnitude of error, but gives how equal the compared signals are. From figure (6.12), (6.15) and (6.18) it is possible to see that the MPC optimal control for bypass air correlates from $98.5 - 99.3\%$ with the measured bypass air. This gives that the model is able to mimic the effect of changing the bypass air well. The MPC suggested main air, correlates poorly and is between $46.2 - 66.7\%$ with the measured main air. The indication of a lag in the correlation for main air is large and ranging from 359 samples to 555 samples and indicates that the prediction horizon needs to be adjusted. The lag in the correlation plot for bypass air is zero, which gives that a prediction horizon of $L = 10$ is enough for bypass air. This gives that the bypass air can be used for MPC control with good accuracy, while the prediction horizon has to be larger with regards to the main air for MPC control. See figure (6.20) for a plot of the unconstrained MPC optimal control inputs with a prediction horizon of $L = 600$. RMSEP was calculated to take into account the magnitude of the deviation of the MPC optimal control inputs from the measured inputs. See figure (6.19) in subchapter "RMSEP of the optimal control inputs with regards to measured inputs".

6.4 MPC validation of simulation test 20110707

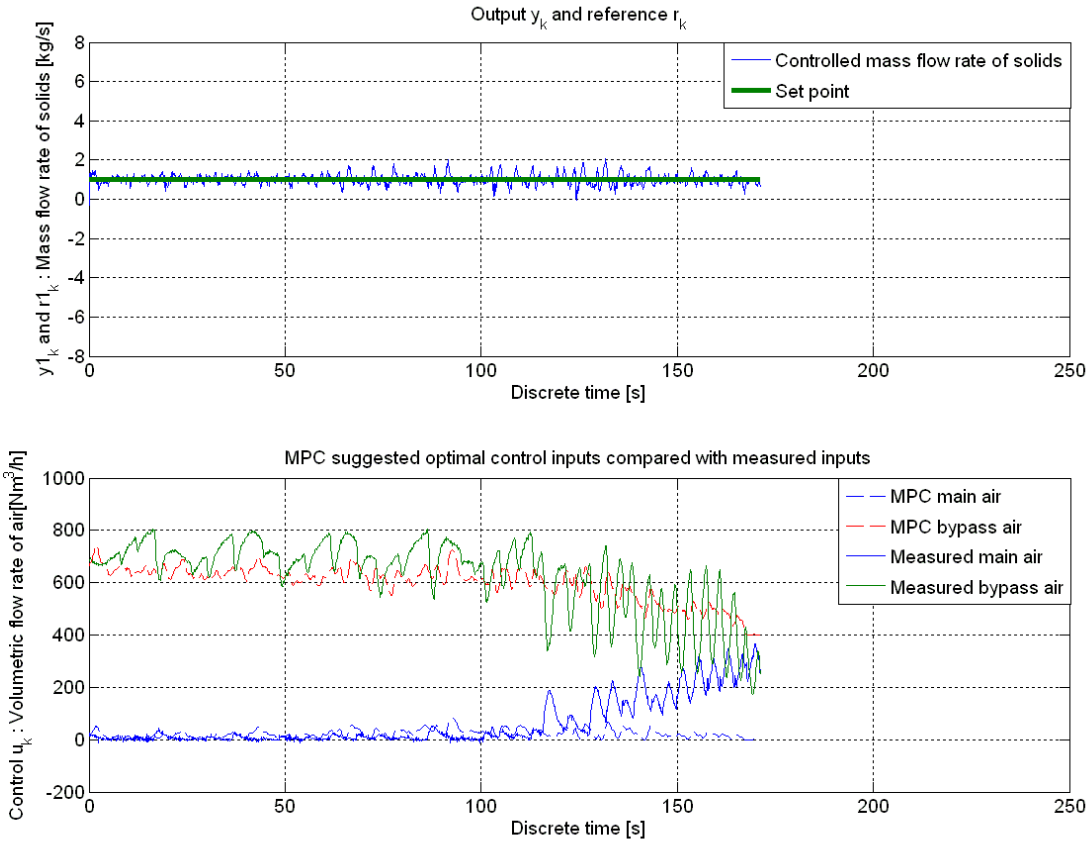

Figure 6.10: Comparison between MPC suggested optimal control inputs and measured inputs for test 20110707.

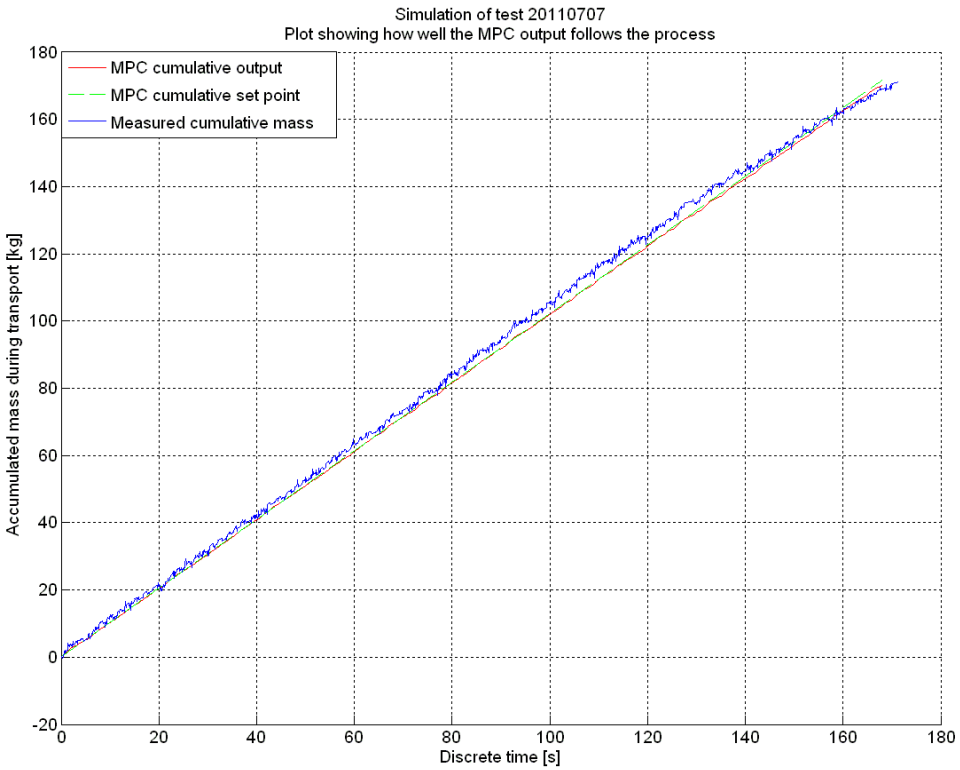

Figure 6.11: Plot showing how close the MPC setpoint is set to the real process for test 20110707.

6.5 MPC validation of simulation test 19100701

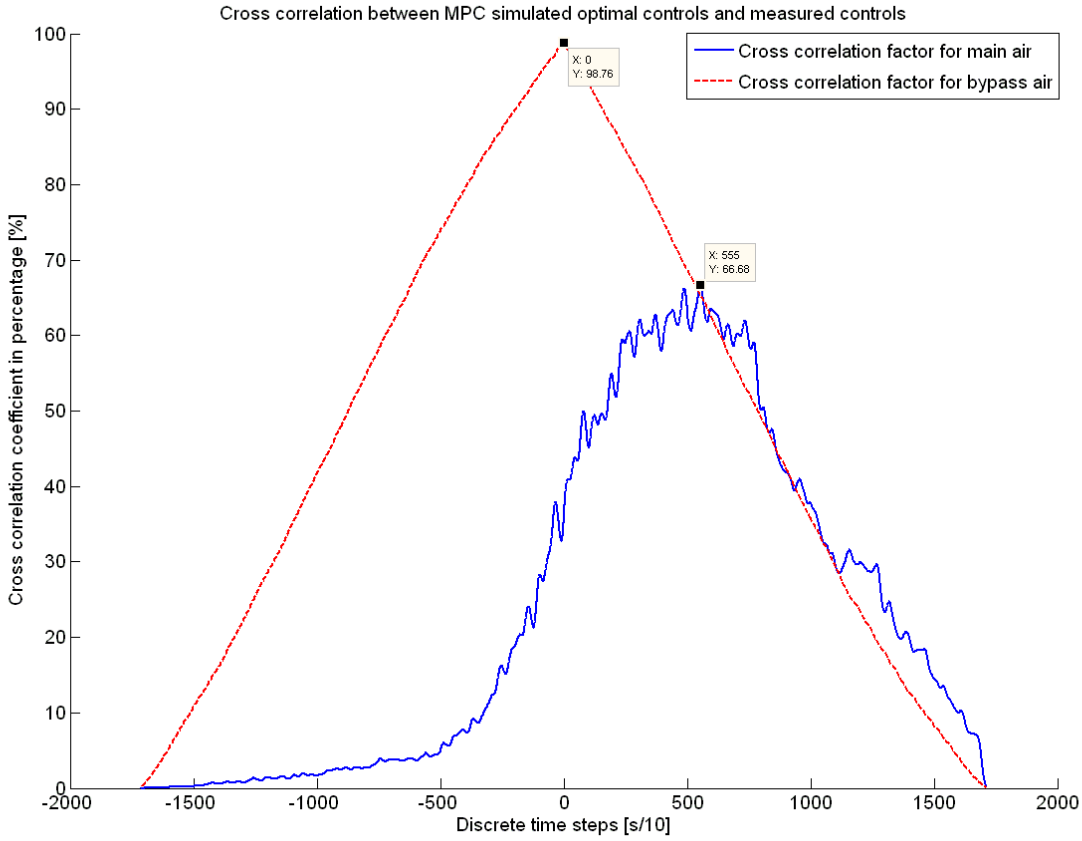

Figure 6.12: Cross correlation between MPC suggested optimal controls and measured controls. Plot is showing how well the model is able to mimic the effect of changing the control inputs with regards to the real process for test 20110707.

6.6 MPC validation of simulation test 19100708

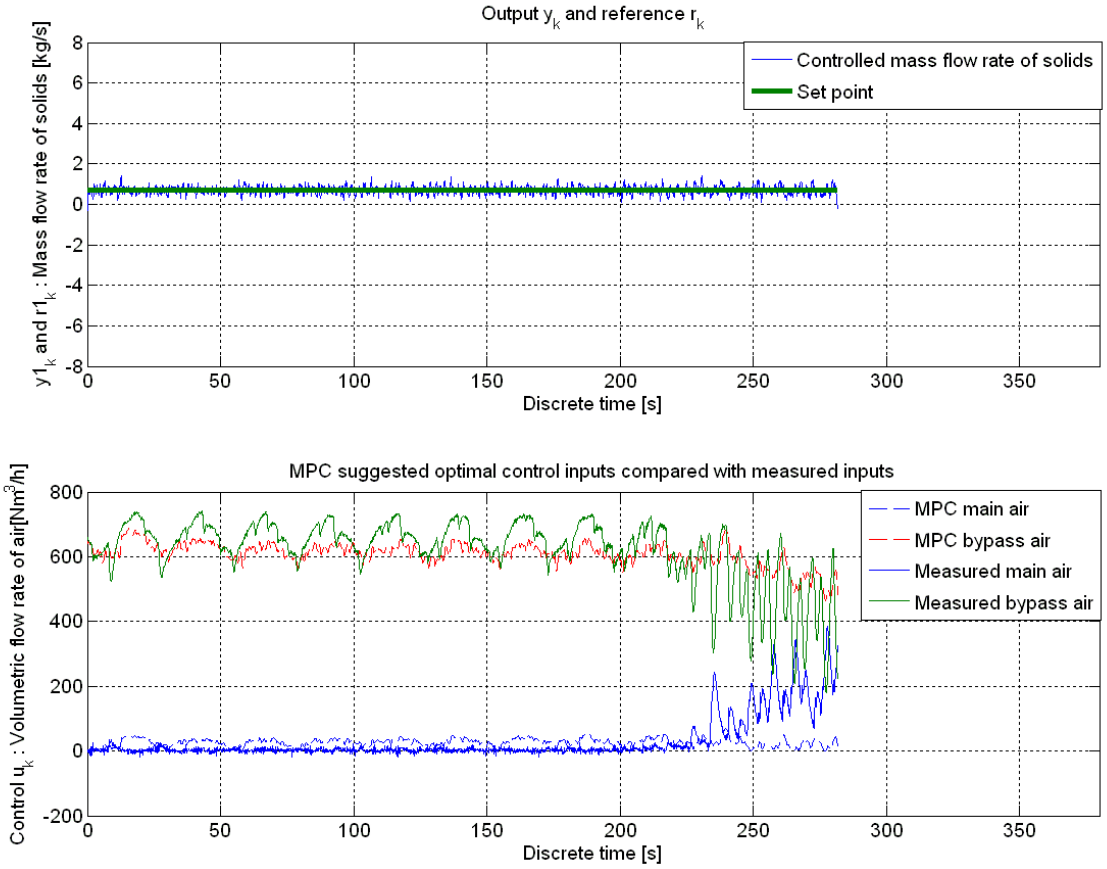

Figure 6.13: Comparison between MPC suggested optimal control inputs and measured inputs for test 19100701.

6.7 RMSEP of the optimal control inputs with regards to measured inputs

Figure (6.19) shows the deviation of the computed optimal MPC control inputs and the measured control inputs in terms of RMSEP. The RMSEP for the bypass air had a range from $71 - 106 Nm^3/h$ and main air $73 - 115 Nm^3/h$. From figure (6.19) it is possible to see that the RMSEP for the main air and bypass air is close to equal in magnitude. One reason for the deviation is that the model has an error. Another is that the bypass and main air does not follow the last part of the simulation well. The model does not describe turbulent flow well. The applied constraints can also be a reason for deviation. The main air is not modelled good enough, and the constraints is reducing bypass air and increasing main air. This can also be seen from the unconstrained plot, where the optimal main air is calculated to be slightly negative. The cross correlation for the main air has a large lag in the correlation plot, the prediction horizon needs to be set larger before a good cross correlation of the main air can be attained.

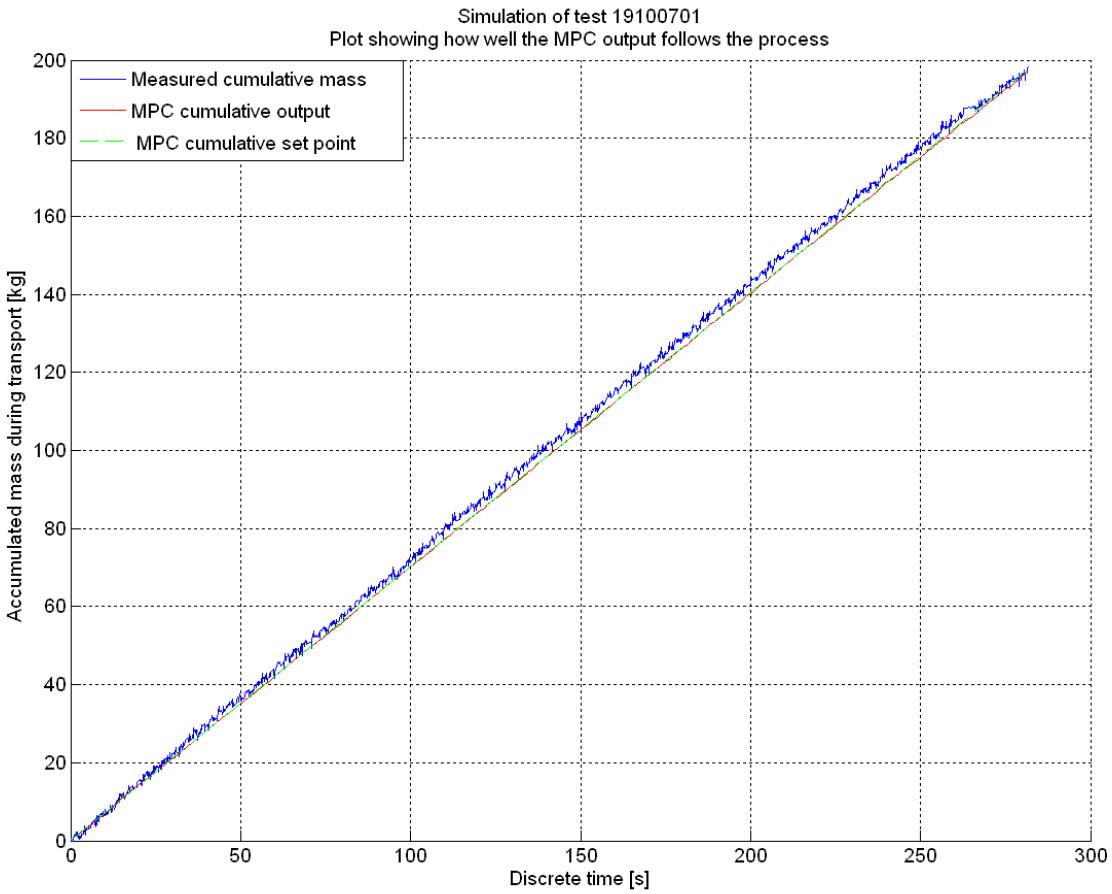

Figure 6.14: Plot showing how close the MPC setpoint is set to the real process for test 19100701.

6.8 Effect of the prediction horizon

In the cross correlation plots, the main air is poorly correlated and mildly suggest a correlation lag of around 390 samples for test 19100708. Figure (6.20) show the unconstrained MPC suggested optimal control inputs with a prediction horizon of $L = 600$. The q weighting was kept to be $q = 10^5$. It could probably have been tuned down a bit. Figure (6.21) shows how close the simulation was to the real process and figure (6.22) shows the new cross correlation plot.

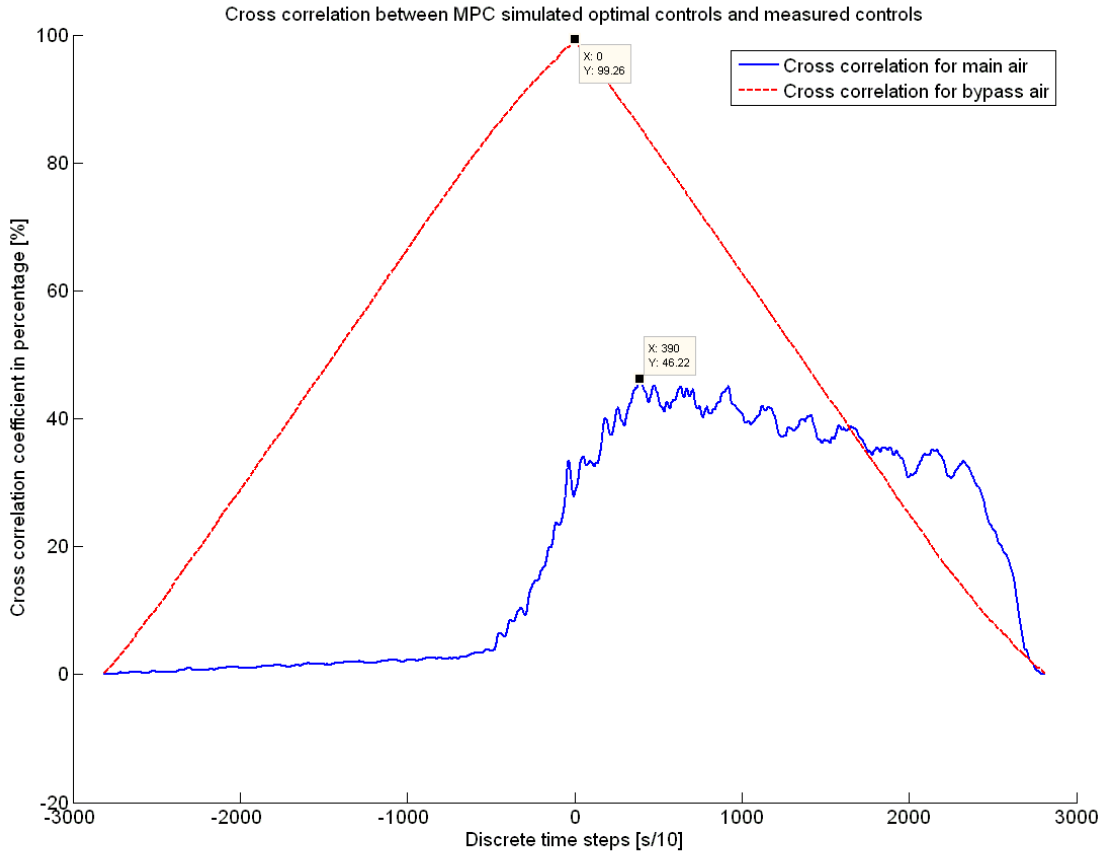

Figure 6.15: Cross correlation between MPC suggested optimal controls and measured controls. Plot is showing how well the model is able to mimic the effect of changing the control inputs with regards to the real process for test 19100701.

Figure (6.22) shows that the main air is negatively correlated and still has what occurs to be a lag. This indicates a slightly larger prediction horizon and that constraints has to be applied. The time of computation for the unconstrained MPC simulation with a prediction horizon of $L = 600$ was approximately $1hour$ using the custom made algorithm. Doing a constrained MPC simulation gives large computation time due to large data matrices to handle. No computer was available at the time, that was powerful enough to handle the MPC with constraints with such a large prediction horizon. Using a more powerful PC would probably solve the problem, but still use a long time computing the simulation. So no simulation was available to give a good cross correlation of the main air. Further studies are needed before any conclusion of how good the main air is as a control input. Still, the indication is that the model should be rearranged with regards to control using the main air as an input.

6.9 Discussion of MPC results

The ratio between the q and R matrices are important when it comes to MPC. The weighting matrices was tuned intuitively and found to be (6.15) for q and (6.16) for R for the simulations.

$$q = 10^5 \tag{6.15}$$

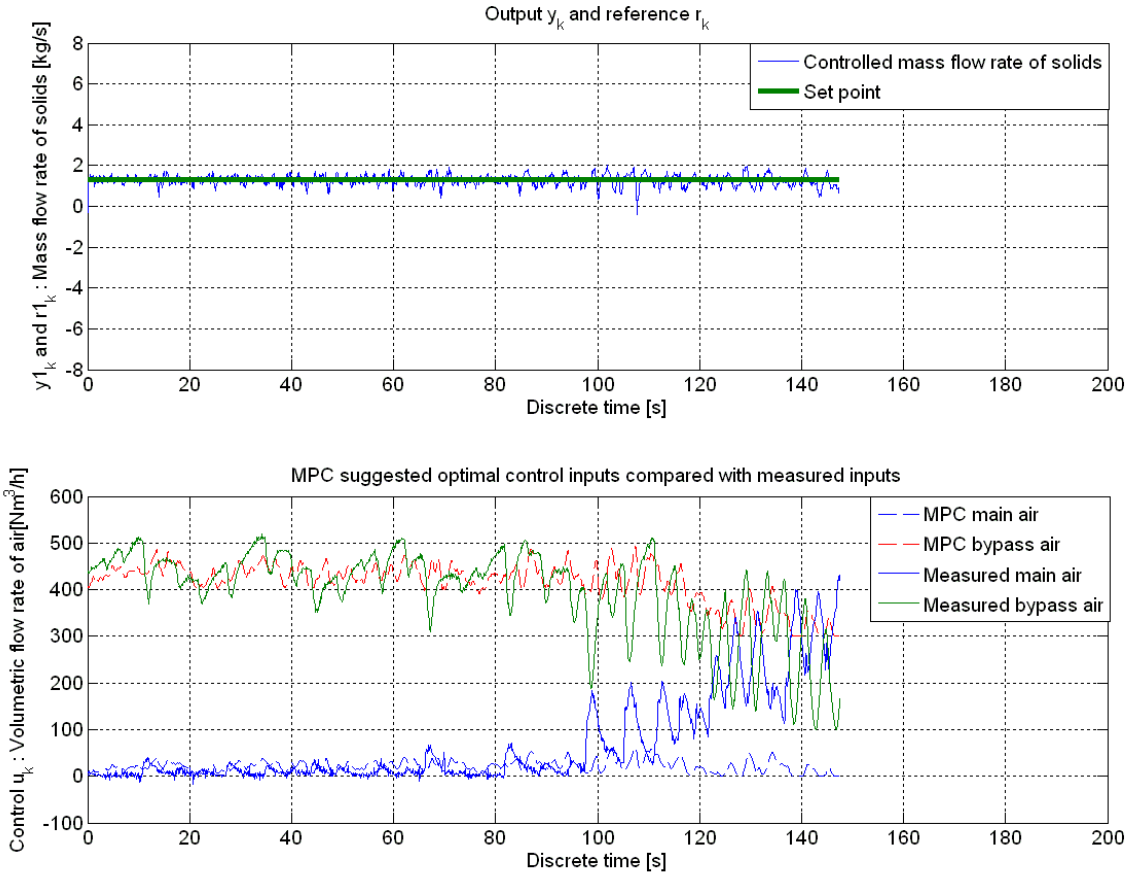

Figure 6.16: Comparison between MPC suggested optimal control inputs and measured inputs for test 19100708.

$$R = \begin{bmatrix} 1 & 0 \\ 0 & 1 \end{bmatrix} \tag{6.16}$$

The prediction horizon was initially set to $L = 10$. The MPC was used as validation for the model attained by system identification. This was done by simulating test sets of real process data. The pressures was seen as disturbances and the volumetric air flows was the considered inputs. Accumulative plots were shown to visualize how close the MPC set point was to the real process and that the MPC output corresponded according to the set point. All the simulations was close to the real process. The MPC suggested optimal inputs was plotted against the measured control inputs. If the model is describing the process well, the optimal control inputs should follow the measured inputs. Cross correlation was performed and showed in plots to show how well the MPC suggested optimal inputs can mimic the effect of changing the air flow rates on the real process. It was found that the MPC suggested optimal bypass air had a cross correlation between $98.5 - 99.3\%$ with the measured bypass air. The RMSEP for the MPC suggested optimal bypass air was between $71 - 106 Nm^3/h$. The cross correlation was good and the deviation was high for the MPC suggested optimal bypass air. Reasons for the high deviation is model error, that the MPC set point is constant and slightly of the real process and that the applied constraints incorporates the poorly model estimated main air. The main air has poor cross correlation between $46.2 - 66.7\%$ and a deviation of $73 - 115 Nm^3/h$. The cross correlation of the main air indicated that the prediction horizon should be larger, with cross correlation

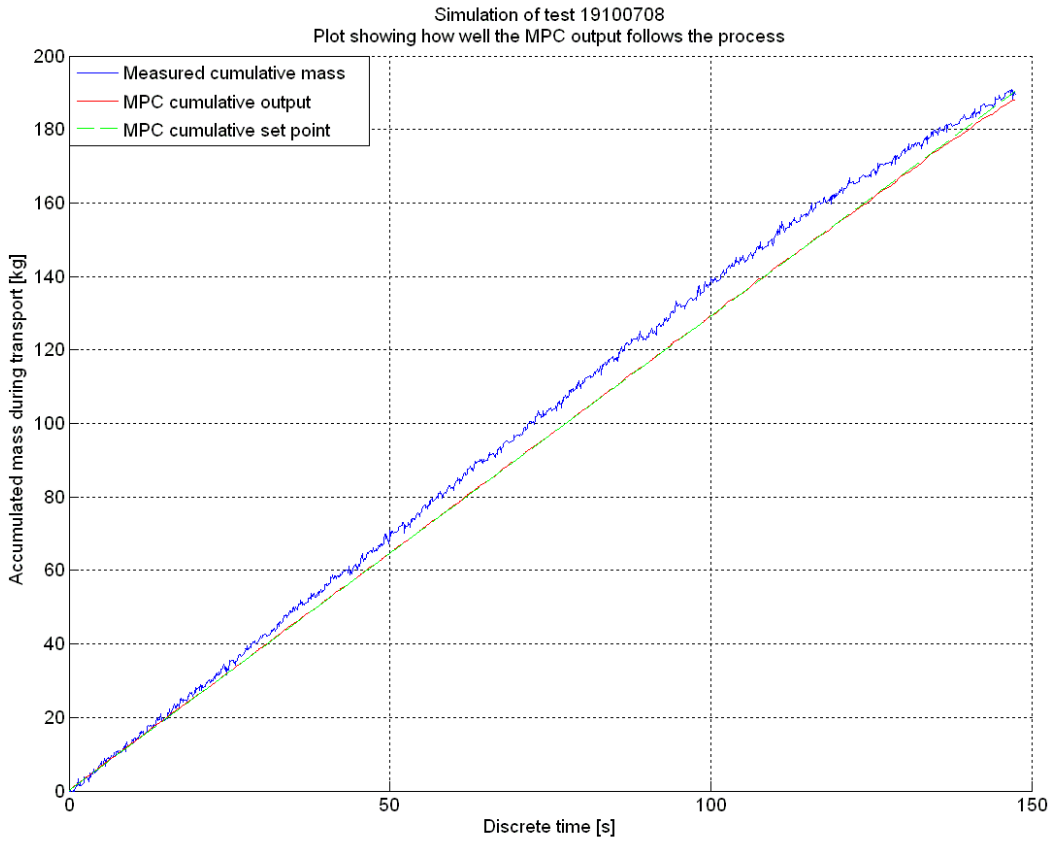

Figure 6.17: Plot showing how close the MPC setpoint is set to the real process for test 19100708.

lags ranging from $359 - 555 samples$. It is still a bit early to say something about the cross correlation of the main air, since constrained MPC with large prediction horizon was not done. Still, it is an indication that the main air is not accurate enough as control input using the DSR model. A way to use the main air as a control input, can be to change the model. The main air has direct effect on blowtank pressure and fluidization of the particulate solids. By introducing the blowtank pressure as a state with the main air as an input, while using the bypass air as a flow adjustor, a model for full model predictive control of the process can be achieved. At the moment the MPC is usable as a mass flow rate of solids adjustor, controlling the bypass air. Meanwhile a PI-controller can be used as a controller for the blowtank pressure and MPC as a mass flow rate of solids adjustor. The model itself can also be used for prediction of mass transported during conveying. For those interested, other works on MPC performed at Telemark University-College is on MPC for oil water separators with slugging inflow by Bartziokas [21] and linearized non-linear process of absorption tower for CO_2 capture by Bedelbayev [22].

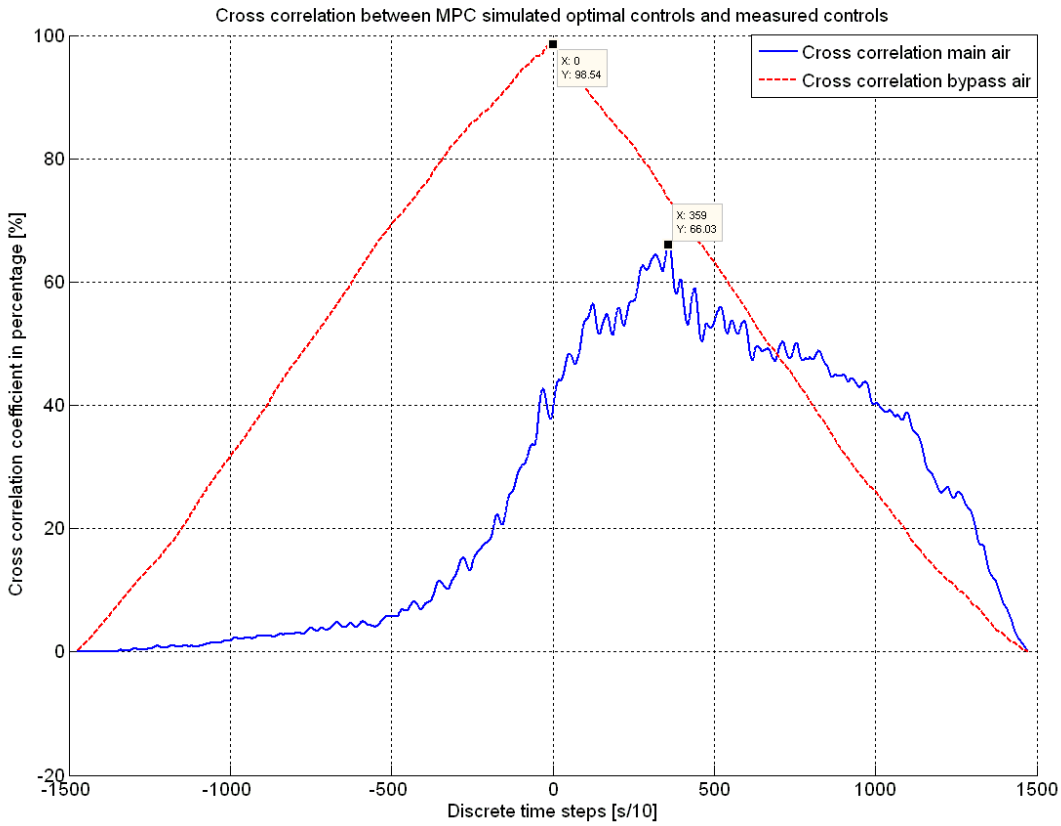

Figure 6.18: Cross correlation between MPC suggested optimal controls and measured controls. Plot is showing how well the model is able to mimic the effect of changing the control inputs with regards to the real process for test 19100708.

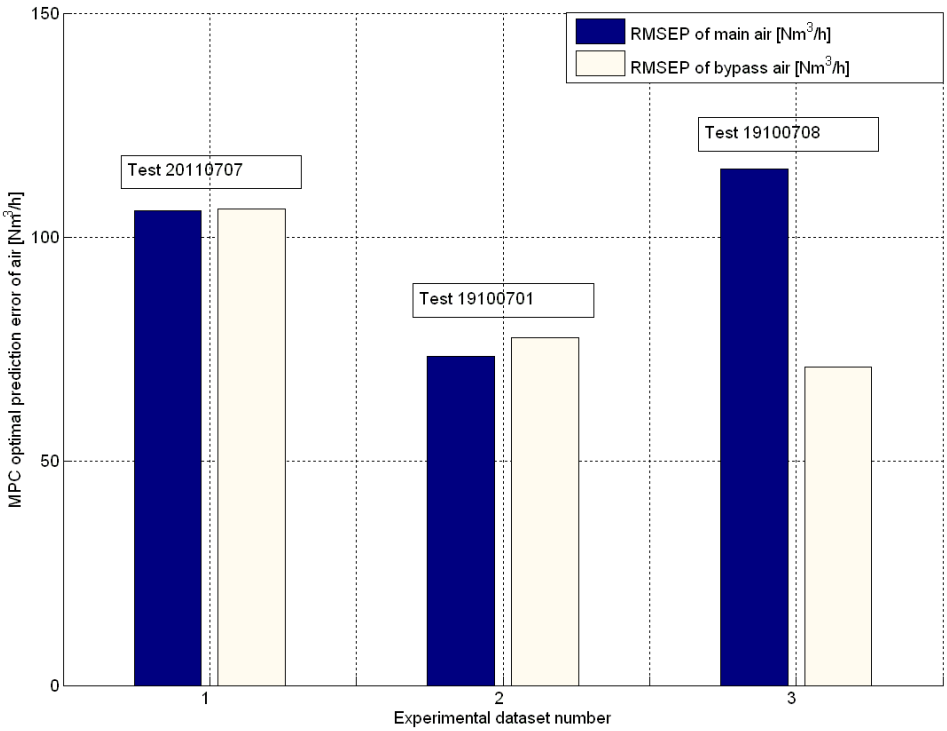

Figure 6.19: Plot showing the RMSEP between the suggested optimal MPC controls and the measured controls for the 3 simulations on transporting dextrose in dilute phase.

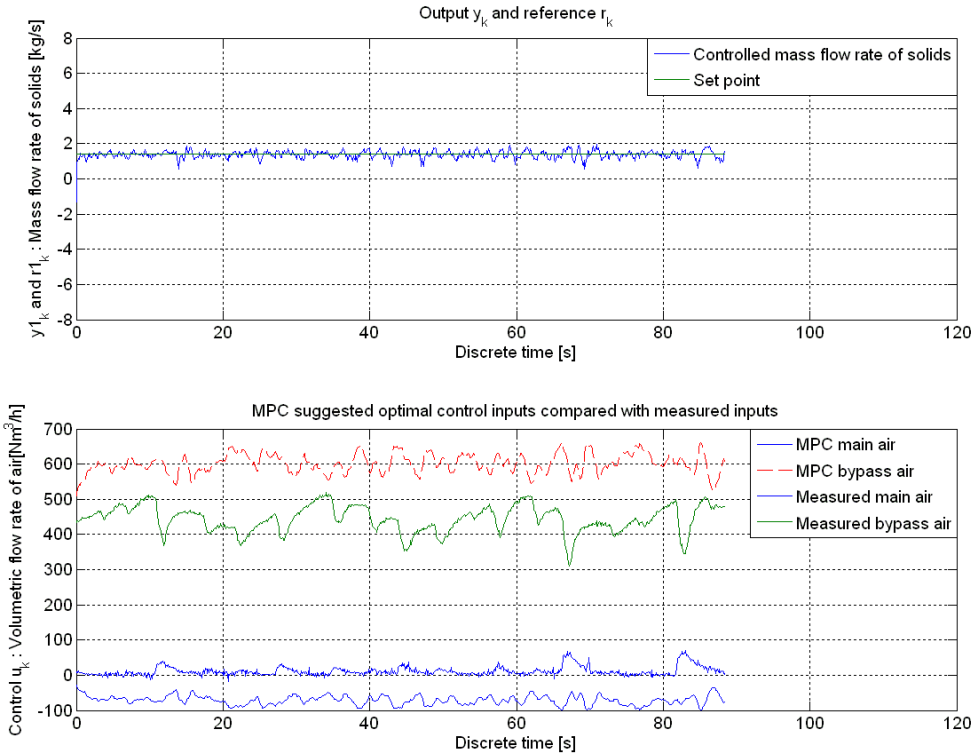

Figure 6.20: Comparison between unconstrained MPC suggested optimal control inputs and measured inputs for test 19100708 using a prediction horizon $L = 600$.

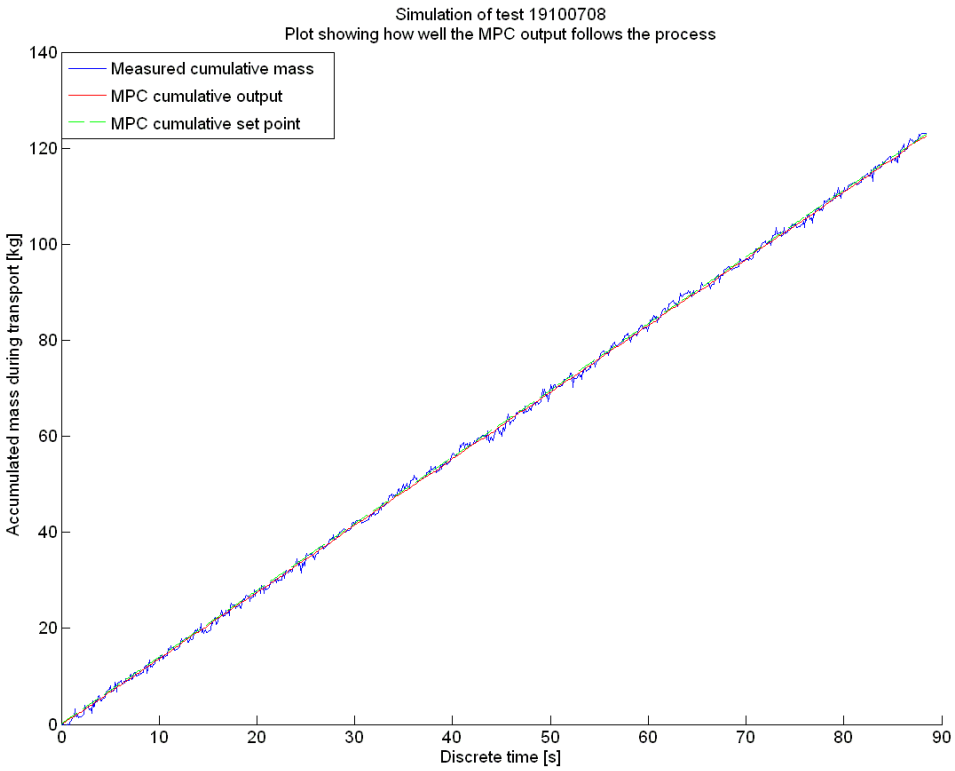

Figure 6.21: Cumulative mass plot for test 19100708 using unconstrained MPC with prediction horizon of $L = 600$.

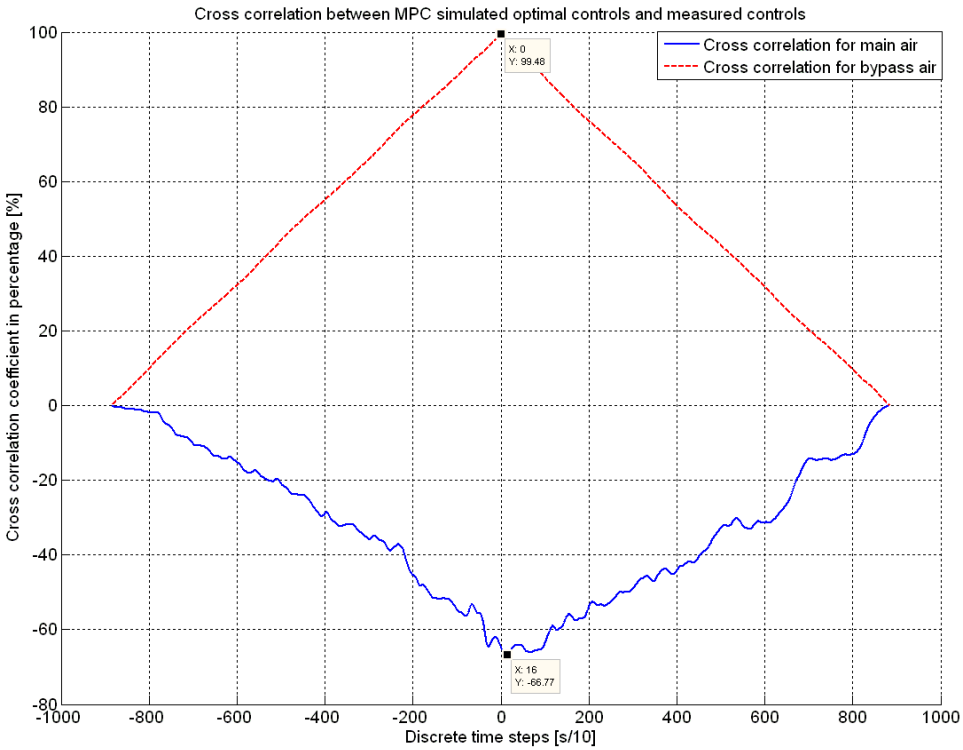

Figure 6.22: Cross correlation between MPC suggested optimal controls and measured controls for test 19100708 using a prediction horizon of $L = 600$.

Chapter 7

Conclusion

The K-method uses a pressure drop coefficient for calculating the mass flow rate of solids. The K-method does not give a model suitable for model predictive control. An expansion of the K-method was done, relating pressure to energy instead of force. Under the pneumatic test runs performed at POSTEC/Tel-Tek in plant A and B, the blowtank pressure was kept close to constant and the air flow rate was kept within a range. This gives close to constant energy into the system, which results in a close to constant linear average flow, justifying the use of system identification for such a non-linear process. This approach has been explained roughly in the thesis and was called the energy density approach to modelling. The system identification method was applied to the energy density approach. The system identification method used was the subspace method "combined Deterministic and Stochastic Realization method" (DSR). The DSR method was compared with the K-method and found to give a slightly better prediction of mass flow rate of solids for the test runs. The cumulative RMSEP expressed in percentage of total conveyed mass for the DSR model was ranging from $1.3 - 5.8\%$ error in cumulative mass estimation for 5 tests on baryte conveyed in dense phase in plant A, while the cumulative error was ranging from $\pm 1.2 - 7.5\%$ of total conveyed mass.

For plant B transporting dextrose in dilute phase, the cumulative RMSEP expressed in percentage of total conveyed mass for the DSR model was ranging from $2.9 - 6.9\%$ error in cumulative mass estimation for 3 tests, while the cumulative error was ranging from $\pm 1.9 - 7.4\%$ of total conveyed mass. This means that the DSR model using the energy density approach could be used for dense phase conveying as well as dilute phase and that it could be applied to the same type of conveying system of different size and dimension.

The DSR method gave a model on state space form, which was later used for Model Predictive Control (MPC). The DSR model based on the energy density approach is easy to implement and only one test run with descriptive data is needed to attain a model. The K-method needs numerous runs and a lot of data processing before it can be used properly. The disadvantage of the DSR model is that it has to have a measurement of the mass flow rate of solids for the calibration set. The parameters necessary for the K-method can be found at a pilot plant and then scaled up. This implies that, where there is no measurement available, the K-method is the only option between the two methods. The use of the DSR model based on the energy density approach, indicated relationships usable for later on making a rough mechanistic model.

The DSR model was used for MPC simulations. The MPC was simulated based on the test set data sets from plant B, transporting dextrose in dilute phase. The MPC was used as a validation method, seeking out how realistic the MPC optimal controls would act on the real process. With an accurate model, simulating the real process, the MPC optimal control inputs should be close to the real measured control inputs. The MPC optimal control for bypass air was cross correlated with the measured bypass and gave cross correlation between 98.5% to 99.3%. The RMSEP for the MPC suggested optimal bypass air was between $71 - 106 Nm^3/h$. The cross correlation was good and the deviation was high for the MPC suggested optimal bypass air. Reasons for the high deviation is model error, that the MPC set point is constant and slightly off the real process and that the applied constraints incorporate the poorly correlated main air. The main air had poor cross correlation between $46.2 - 66.7\%$ and a RMSEP of $73 - 115 Nm^3/h$. The cross correlation of the main air indicated that the prediction horizon should be larger, with cross correlation lags ranging from $359 - 555$ *samples*. At this point, it is not possible to give a definite conclusion about the cross correlation of the main air, since constrained MPC with large prediction horizon was not done. An

indication can be given by the unconstrained MPC simulation, which gave a cross correlation of -66.8%. This is an indication that the main air is not accurate enough as control input using the DSR model. The effect of the prediction horizon has been studied. Time delays have not been considered in this thesis, but should be considered for further studies since the prediction horizon and time delays are often linked. A way to use the main air as a control input, can be to change the model. The main air has a direct effect on blowtank pressure and fluidization of the particulate solids. By introducing the blowtank pressure as a state with the main air as an input, while using the bypass air as a flow adjustor, a model for full model predictive control of the process can be achieved. At the moment, the MPC is usable as a mass flow rate of solids adjustor, controlling the bypass air.

Chapter 8

References

1. Ratnayake, C. , *"A comprehensive Scaling Up Technique for Pneumatic Transport systems"*, PhD thesis in Department of Technology. 2005, Telemark University College : Porsgrunn

2. Klinzing, G. E.; Marcus, R. D.; Rizk, F. and Leung L.S., 1997, "*Pneumatic conveying of solids*", Chapman and Hall, p1-34, p483-499

3. Mills, D., 1990, *"Pneumatic conveying design guide"*, Butterworths, p10-15, p122, p125

4. AIR-TEC System: Official Website, http://www.air-tec.it/index_materialitrasp_uk.html (30.4.2008)

5. Geldart, D., Types of Gas Fluidization. Powder Technology, 1973. 7: p. 285 -292.

6. Yan, Y., 1996, "*Mass flow measurement of bulk solids in pneumatic pipelines*", Measurement Science and Technology, 7, p1687-1706

7. Arakaki C., Ratnayake C., Datta B. K., Lie B., *"Study of Mass Flow of Dextrose in Pneumatic Conveying"*, Biopowders Mini-Conference Budapest 13-14 September, 2007

8. Ljung, L., 2007, *"System Identification"*, Division of Automatic Control, Report no. : LiTH-ISY-R-2809, pp. 1, Department of Electrical Engineering, University of Linkoeping, Sweden

9. Di Ruscio, D., 2003, *"Subspace system identification of the Kalman filter"*, Modeling, Identification and Control, Vol 24, No.3, pp. 125-157

10. Ljung L., 1999, 2nd edition, *"System Identification-theory for the user"*, Prentice Hall, Upper Saddle river, ISBN 0-13-656695-2, 607 pages

11. Esbensen K. H., 2002, 5th edition, *"Multivariate Data analysis - In Practice, An introduction to Multivariate Data Analysis and Experimental Design"*, CAMO Process AS, 1-12, p115-150

12. Di Ruscio D., 2003, 6th edition, "*Subspace system identification, Theory and applications"*, Division of Process Automation, Department of Technology, Telemark University College, Posrgrunn, Norway

13. Lie B.,August 2005, *"Modelling of Dynamic Systems"*, Division of Process Automation, Department of Technology, Telemark University College, Posrgrunn, Norway

14. http://www.merriam-webster.com/dictionary/stochastic (7.5.2008)

15. Di Ruscio D., Lecture notes April 25, 2007, *"Model predictive control and optimization"*, Division of Process Automation, Department of Technology, Telemark University College, Posrgrunn, Norway

16. http://ocw.mit.edu/OcwWeb/web/home/home/index.htm : MIT open courseware (5.6.2008)

17. MatLab version 7.0, System identification toolbox, *"n4sid helpfile"*

18. Nunes G. C., Phd. dissertation, 2001, *"Desigh and analysis of multivariable predictive control applied to an oil-water-gas separator : A polynomial approach",* Univeristy of Florida

19. http://en.wikipedia.org/wiki/Model_predictive_control (13.5.2008)

20. http://www.tateandlyle.com (20.5.2008)

21. Bartziokas A., Master thesis 2008, *"Consider MPC for oil water separators with slugging inflow"*, Division of Process Automation, Department of Technology, Telemark University College, Posrgrunn, Norway

22. Bedelbayev A., Master thesis 2008, *"Model predictive control of absorption tower for CO_2 capture"*, Division of Process Automation, Department of Technology, Telemark University College, Posrgrunn, Norway

Appendix A

Conference paper : " Mass flow rate measurement in a pneumatic conveyor using a system identification modelling approach"

This paper was presented at the conference and published in the proceedings of the international symposium reliable flow of particulate solids IV held in Tromsø, Norway, 10th - 12th June 2008.

MASS FLOW RATE MEASUREMENT IN A PNEUMATIC CONVEYOR USING A SYSTEM IDENTIFICATION MODELLING APPROACH

A. Sæther[1], C. Arakaki[2], C. Ratnayake[2] & D.D. Ruscio[1]
1. Telemark University College
Porsgrunn, NORWAY.
2. Telemark Technological R & D Centre
Porsgrunn, NORWAY

Abstract – Accurate measurements of solids flow rate in pneumatic conveying systems has been a need for the different industries in which these systems are used. In this study, a system identification approach, which is termed as the Deterministic Stochastic Realization (DSR) method is used to obtain a model on state space form. The selection of inputs to the system identification model is based on conservation of energy related to the Bernoulli effect. Under this investigation, attempts were made to predict the mass flow rate of conveying solids in real time, by using pressure data obtained from 3 different pressure sensors located on the conveying line, blow tank pressure and inlet air volume flow rate. To evaluate the performance of the DSR model, the results were compared with one published method based on a scaling up technique of pneumatic conveying [1]. The Root Mean Squared Error of Prediction (RMSEP) of the cumulative mass of transported solids as a percentage of the total conveyed mass using the system identification model was between 1.3-5.8%.

1. INTRODUCTION

Pneumatic conveying systems are suitable for transporting of dry powdered and granular materials in different kind of situations. The quantity of mass of solid particles in gas that flow through the cross sectional area of a pipe per unit time can be defined as mass flow rate of solids**.** With the aim of running reliable pneumatic conveying systems it is of fundamental importance to measure and monitor the mass flow conditions. Industry has looked for alternatives for this purpose in the single phase flow experience and has adapted some of them. Unfortunately, two-phase processes often present additional instrumentation problems, since mass flow rates, solids concentrations and solids composition may vary widely with time at a given position in the plant as mentioned by Williams *et al*., [2]. For this reason, there has been a need to develop new instrumentation and techniques suitable for this purpose. As a result, some of the instrumentation available measure mass flow directly but most of them do it in an indirect way combining two separate parameters measured simultaneously i.e. solids concentration and velocity. The techniques currently available make use of different kinds of sensors, such as ultrasonics, capacitance, microwave, optical, electrical and so on. In addition, there are mechanical devices available to measure mass flow in pneumatic conveying lines. Finally, there are combinations of sensors with different measurement principles. These techniques have been reviewed elsewhere by Green and Thorn [3]; Klinzing [4]; Pugh [5]; Williams *et al.* [2]; Yan *et al.* [6]; Yan [7]. Nevertheless, the techniques available are not completely satisfactory for all the applications and more research needs to be done. In this paper, a model has been developed by using system identification and it is compared with a model that has been patented (Patent application no. 20063698) and is currently used for commercial applications. The patented model is derived from an empirical model based on the flow properties for the calculation of pressure drop developed by Ratnayake [1]. The system identification method is based on a MatLab code developed by David Di Ruscio [8] at Telemark University-College. The requirements for the application of the patented model in terms of instrumentation are pressure sensors and an air flow meter in any position of the pneumatic conveying system. The DSR-model

needs a selected set of pressure measurements in the pipeline, blowtank pressure and inlet air volume flow rate. Pressure waves and fluctuations behavior in a two-phase gas-solid system can give much information about the flow condition within the flow line. The use of transducers to measure these pressure waves is essential since almost instantaneous readings can be obtained as mentioned by Klinzing *et al*. [9].

2. THEORY OF MASS FLOW CALCULATION

2.1 Pressure drop coefficient method 'K-method' [1]

The pressure drop was addressed in a discrete way by considering horizontal and vertical straight pipe sections, bends and other pipe accessories separately. For a straight section the equation has the following form:

$$\Delta p_{st} = \frac{1}{2} K_{st} \rho_{sus} v_{entry}^2 \frac{\Delta L}{D} \tag{2}$$

where v_{entry} is the gas velocity at the entry section of the concerned pipe section or pipe component, K_{st} is the pressure drop coefficient for straight pipe sections whether they are horizontal or vertical and ρ_{sus} can be defined as the density of the mixture when a short pipe element is considered. The equation to calculate ρ_{sus} is shown below:

$$\rho_{sus} = \frac{m_s + m_a}{V_s + V_a} \tag{3}$$

where m_s is the mass flow rate of solids, m_a is the mass flow rate of air, V_s is the volume flow rate of solids and V_a is the volume flow rate of air. Equation 3 could be re-arranged in order to get the mass flow rate of solids, as shown below:

$$m_s = \frac{\rho_a Q - \rho_{sus} V_a}{\frac{\rho_{sus}}{\rho_s} - 1} \tag{4}$$

where Q is the volume flow rate of air obtained by adjusting the experimentally measured air volume flow rate according to the true pressure value at the concerned section of the pipeline. This is done in order to take into account the compressibility effect [10].

2.2 The Deterministic Stochastic Realization ('DSR') method [8]

The DSR is a system identification method. The process of going from observed data to a mathematical model is fundamental in science and engineering. In the control area this process has been termed "System Identification" and the objective is then to find dynamical models (difference or differential equations) from observed input and output signals. Its basic features are however common with general model building processes in statistics and other sciences. [11].

The DSR method is a system identification black box model, where a linear model is found based on measured inputs and outputs. The DSR method gives a model on state space form. A state space model is a set of first order ordinary differential state equations, describing the change in the states in the process. A state space model can be divided into a set of states (x), a set of inputs (u), a set of known constants (θ) and a set of selected states as outputs (y). This can briefly be expressed as shown in 5 :

$$\frac{dx}{dt} = f(x,u;\theta) \tag{5}$$

Models on this form can be non-linear and needs an Ordinary Differential Equation (ODE) solver to compute a solution. The sets of ordinary differential state equations can be set up on matrix form for computational simplicity, when the problem can be considered linear. The process of pneumatic conveying itself is dynamic and non-linear, due to compression and expansion of the air/gas through the pipe. A state space model on matrix form can be made, assuming linear transition between the states.

3. EXPERIMENTAL TEST SET-UP

For this investigation, the pipeline configuration shown in Figure 1, was used to perform the pneumatic conveying tests.

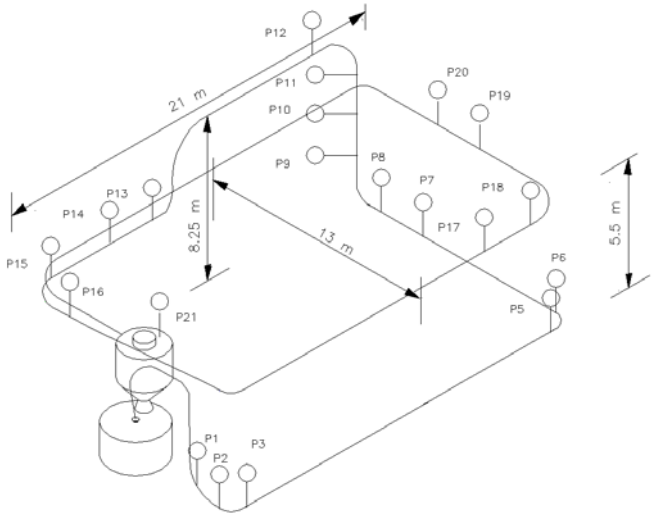

Figure 1: Schematic view of the pneumatic conveying test rig including pressure transmitter locations.

The conveying line was a constant diameter pipeline which was approximately 140 m long and of 75 mm diameter. The pipeline made a close loop conveying system by mounting the receiving tank just on top of the blow tank, so that the conveying material could be re-circulated after each test run. Few pressure transducers, as shown in Figure 1, were placed on the conveying line in discrete positions, so that the pressure drop values could be determined across different features, like straight pipe sections, bends, etc. All bends used in the conveying line were 90° standard bends, while there was a fully open butterfly valve between pressure transducers P19 and P20. A load cell in the receiving tank was used for measuring the transported mass of solids.

3.1 Test Material

The material used for the tests was baryte, which is used in oil industry as a weighting material. The tested quality of baryte has a mean particle size of 12 μm and a particle density of 4200 kg/m^3. For each test, approximately 0.5 - 1.0 m^3 of bulk material was used.

3.2 Test Procedure

Table 1: Corresponding blow tank pressures for different test runs

Test No. T=test set C=Calibration set	Blow Tank Pressure (bar)	Avarage inlet suspension density [kg/m^3]	Solids loading orati	Avarage inlet air velocity (m/s)
01120501 T	4.0	275	50.3	6.3
01120502 T	3.5	312	60.8	6.1
01120504 T	3.0	216	28.1	8.4
30110502 T	4.5	218	48.9	8.3
30110505 C	3.5	289	79.3	5.5
30110507 T	3.0	256	68.2	5.9

The tests were conducted at different start pressures at the blow tank and the corresponding pressure for each test run is as shown in table 1. During the test runs, all the data including the pressure values have been recorded using a data logging system. The signals from all the pressure transmitters were recorded every 0.5 second. After the test runs, the variation of air mass flow rate and the different pressure readings were studied , using the data logging and retrieving software program. During test runs, samples were collected on line and tested for particle size distribution in order to check any size degradation. As soon as size degradation could be noticed, the bulk powder was always replaced with a fresh powder. For those interested, the details of the test procedure is reported elsewhere [1]. The inlet air velocity was calculated at transducer P1. The solids loading ratio was ranging from 24 to 43, this gives that these test runs was conveying in dense phase. The suspension density was calculated at transducer P1 using the K-model [1].

4. DSR METHOD RESULTS AND COMPARISON WITH THE K-METHOD RESULTS

The selection of measurement input variables for the DSR method is based on conservation of energy related to the air and the Bernoulli effect. System identification was used to find the relationship between the change in energy density (i.e, Energy per unit volume) of air and the mass flow of solids. The blow tank pressure is seen as the driving force in the system. The energy density in the blow tank is transferred into kinetic energy density of air for transporting solids. The transference from energy density in air into kinetic energy of solids generates a loss in energy density in the air. Due to forces like drag, pipe wall friction and particle collisions there is an additional loss in kinetic energy of the transported solids. This loss of kinetic energy for the solids also causes a loss in the energy density of the air. These losses are hard to distinguish from eachother and approximate correctly and leads to an error in the model. After the blow tank there is a juncture where the bypass air is pumped into the pipeline. This juncture is the point in the pipeline where the total energy density of air in the pipeline describes the flow of solids best. Pressure transducer "*P1"* describes this juncture best, since it is closest to the juncture. The pressure transducer "*P2"* is mounted at the first horizontal section of the pipeline. Pressure transducer "*P2"* is at a point in the pipeline that has the lowest elevation in the pipeline. The pressure difference between "*P1"* and "*P2"* is descriptive for the horizontal conveying in the test-rig. A pressure measurement describing the total elevation of the pipeline gives an indication of the total change in potential energy density for the air due to vertical conveying, consequently pressure transducer "*P13"*, was selected to represent the change in potential energy density. By calculating the change in measured load cell data (dm/dt), a measured mass flow was obtained. This measured mass flow was chosen as output variable for the calibration set, using DSR. A system identification model on state space form was then obtained by finding the relationship between the pressure at selected points in the pipe line and air flow against the measured mass flow. The measurement points chosen give information about the change in energy density at given points. The model was made from a calibration set (30110505) and the rest of the data sets were used as test sets. Test sets are data sets used for validation of the calibration model.

The DSR model presented on discrete state space form is stated in 6:

$$x_{k+1} = ax_k + Bu_k, x_0 - given$$
$$y_k = x_k \tag{6}$$

$x_0 = 19.9815$ The initial state at discrete timestep $k = 0$

x_k = The present state, which is the mass flow of solids at present discrete timestep k

x_{k+1} = The next state, which is the mass flow of solids at the next discrete timestep $k+1$

$a = 0.2548$ The transition matrix, which is a scalar here since there is only one state.

This scalar is describing the change in the state for a discrete timestep k

$$u_k = \begin{bmatrix} p_0 - \text{Blow tank pressure} \\ p_1 - \text{Juncture pressure} \\ p_2 - \text{Lowest elevation pressure} \\ p_{13} - \text{Highest elevation pressure} \\ air_{in} - \text{Conveying air (volumetric flow)} \end{bmatrix} \begin{pmatrix} \text{The control vector,} \\ \text{which consists of all the inputs to the process} \\ \text{at the present timestep } k \end{pmatrix}$$

$B = \begin{bmatrix} 0.0013 & 0.0031 & -0.0049 & 0.0033 & -0.0041 \end{bmatrix}$

The input control matrix, which is a row vector since there is only one state

The input control row vector consists of a weighting of the inputs to the process

y_k = The predicted output state at present timestep k, which is the mass flow of the solids at present timestep k

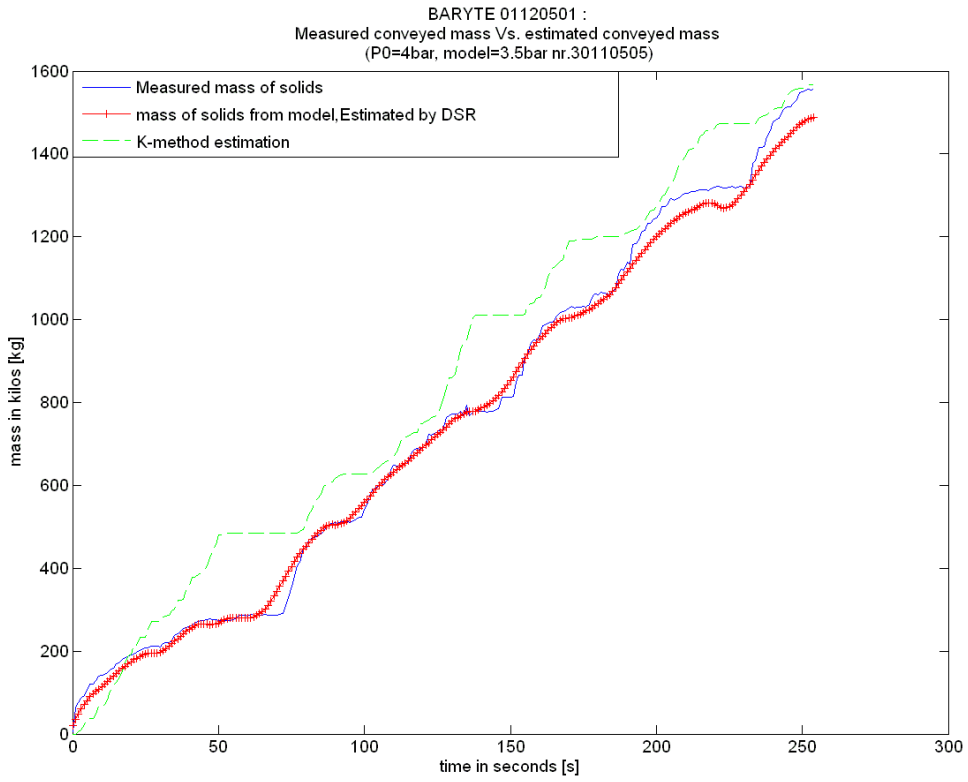

Figure 2 Comparison of mass flow predictions for the DSR- and K-method models.

In figure 2 and figure 3 the measured cumulative mass flows are plotted against the predicted cumulative mass flows, using the DSR-model for 5 different experiments on transport of baryte with a mean particle size of 12µm. For comparison, the estimation of the cumulative mass flow by the K-method for the same experiments are also plotted in figure 2 and figure 3.The whole line in figure 2 and 3 shows the measured mass in the receiving tank. The dotted line shows the predicted cumulative mass for the K-method and the thick line shows the prediction for the DSR-method.

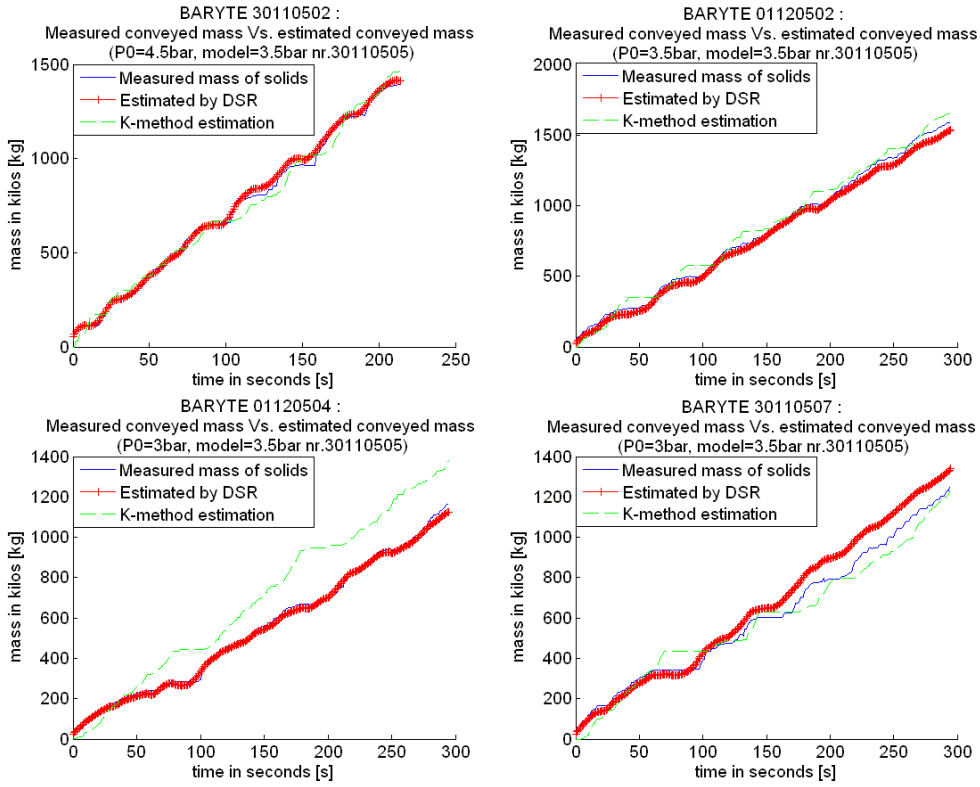

Figure 3 Comparison of mass flow predictions for the DSR- and K-method models

Figure 4a shows the root mean square error of prediction (RMSEP) for the predicted cumulative mass of solids conveyed for the K-method and the DSR-model in percentage of the total measured cumulative mass conveyed. This plot shows how good the prediction of the cumulative mass follows the measured mass, i.e how good the model follows the real process. The RMSEP of the predicted cumulative mass in percentage of total mass of solids conveyed was calculated by equation 7. The cumulative prediction error is shown in figure 4b , this plot shows how well the prediction ends up compared to the measured cumulative mass.

$$RMSEP\ of\ \ cum\ in\ \% = \left(\frac{\sqrt{\frac{1}{N}\sum_{i=1}^{N}\left(\hat{y}_i - y_i\right)}}{mass\ \ conveyed} \right) \bullet 100\% \qquad (7)$$

where

$RMSEP\ of\ \ cum\ in\ \%$ = RMSEP of predicted cumulative mass in percentage of total conveyed mass

$\hat{y}$ = Predicted cumulative mass of solids

y = Measured cumulative mass of solids

N = Number of samples

mass conveyed = Total mass of solids conveyed during test run

Figure 4a gives that the cumulative RMSEP expressed in percentage of total conveyed mass for the DSR model ranges from 1.3-5.8% error in mass estimation, while the error for the K-method ranges from 3.2-14.5% error in mass estimation. It is evident from the experimental data that the DSR model follows the measured cumulative mass better than the K-method for these experiments. From figure 4b the cumulative error for the DSR model is ranging from ±1.2-7.5%, while the K-method ranges from ±1.3-18.3%. It is evident from the experimental data that the DSR model has a smaller range of cumulative error than the K-method for these experiments.

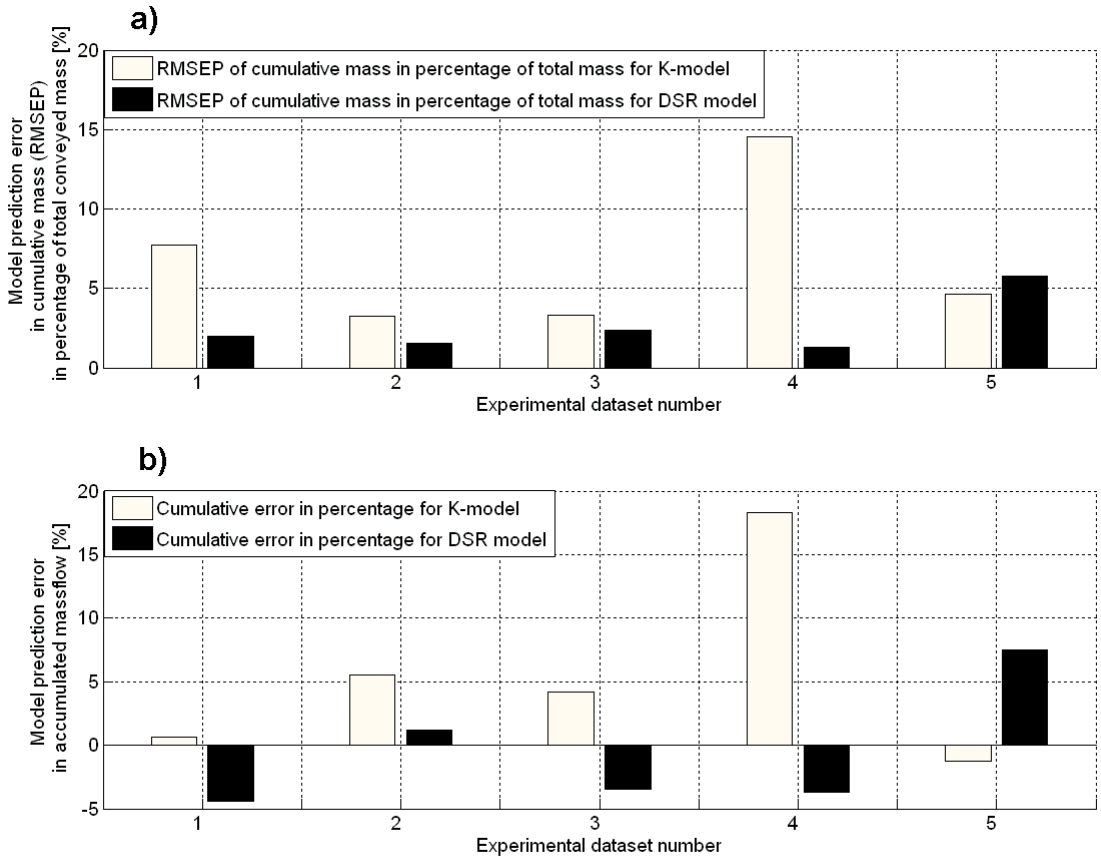

Figure 4 a) RMSEP of predicted cumulative mass in percentage of measured total mass conveyed. 4 b) Total Cumulative error in transport in percentage.

The model based on system identification by DSR is robust considering different blowtank pressures compared to the K-method which has a different model for different blowtank pressures. The reason for this is that the DSR model takes into account the blowtank pressure fluctuations in the model. This makes the DSR model more robust regarding variations in the blowtank pressure than the K-method. The DSR model data is unfiltered while the K-method needs filtering of the raw

data to give a good estimation. This is due to the sensitivity of the pressure gradient Δp_{st}, using the K-method. This sensitivity to noise in the pressure measurements is a weakness in the K-method, since a small deviation in pressure gradient affects the calculation of the suspension density. The DSR model is more robust to such noise variations in the pressure measurements. This can explain the reason why the DSR method has a smaller range of cumulative error than the K-method. The DSR model is based purely on the relationships within the measurement data and is sensitive to boundary conditions for the process, like saturation of inlet airflow and large variations in blowtank pressure, unless a model is made from a data set that takes this into account. Such a model may suffer from less accuracy under normal conditions.The K-method uses an estimation of the mass flow at an earlier stage in the pneumatic conveying process rather than at the end, this results in a time delay in the estimation of the mass flow. This time delay can be seen in figure 2 and figure 3. The DSR model makes a model that takes this into account by making an estimation based on when the change at the end of the conveying line occurs. This almost eliminates the time delay in the estimation of the massflow of solids by the DSR method. This time delay increases the RMSEP for the K-method and is a reason why the RMSEP is larger for the K-method compared to the DSR model.The K-method has succesfully been implemented in industry by using a scaling up technique. This means that experiments can be run at a research facility test rig and then scaled up to industrial size scales.

5. CONCLUSIONS

As depicted in figures 2 and 3, it is clear that the solids mass flow rate can be predicted using DSR method with high accuracy. With the statistical analysis shown in figure 4, it is also clear over the range of conditions tested under this investigation that this method gives better accuracy than 'K' method, which has been used as an on-line solids mass flow rate measurement technique. Under this investigation, the DSR model has not been tried out for scaling up purpose and the model is at the moment rig dependent. Both the K-method and the DSR model are at the moment powder dependent, consequently each powder needs a model. The K-method is more like a procedure for estimating the mass flow, while the DSR model is on state space form. This gives an advantage to the DSR model for control purposes of the process, since a model on state space form makes it possible to implement control strategies like model predictive control (MPC), which must have a model to be implemented.

6. REFERENCES

1. Ratnayake, C. , *A comprehensive Scaling Up Technique for Pneumatic Transport systems*, PhD thesis in *Department of Technology*. 2005, Telemark University College : Porsgrunn
2. Williams, R. A.; Xie, C. G.;Dickin, F. J.;Simons, S. J. R. and Beck M. S., 1991, Multi-phase flow measurements in powder processing, *Powder Technology*, 66(3), 203-224
3. Green, R. G. and Thorn, R., 1998, Sensor systems for lightly loaded pneumatic conveyors, *Powder Technology*, 79-92
4. Klinzing, G. E., 2001, Pneumatic conveying: transport solutions, pitfalls, and measurements, *Handbook of Conveying and Handling of Particulate Solids*, 291-301
5. Pugh, J., R., 2001, The crucial role of on-line measurement of bulk solids handling, *Handbook of Conveying and Handling of Particulate Solids*, 793-806
6. Yan, Y., Byrne B. and Coulthard, J., 1995, Sensing field homogeneity in mass flow rate measurement of pneumatically conveyed solids, *Flow Measurement and Instrumentation*, 6(2), 115-119
7. Yan, Y., 1996, Mass flow measurement of bulk solids in pneumatic pipelines, *Measurement Science and Technology*, 7, 1687-1706

8. Di Ruscio, D, 2003, Subspace system identification of the Kalman filter, *Modeling, Identification and Control*, Vol 24, No.3, pp. 125-157
9. Klinzing, G. E.; Marcus, R. D.; Rizk, F. and Leung L.S., 1997, *Pneumatic conveying of solids*, Chapman and Hall
10. Arakaki C., Ratnayake C., Datta B. K., Lie B., *Study of Mass Flow of Dextrose in Pneumatic Conveying*, Biopowders Mini-Conference Budapest 13-14 September, 2007
11. Ljung, L., 2007, *System Identification*, Division of Automatic Control, Report no. : LiTH-ISY-R-2809, pp. 1, Department of Electrical Engineering, University of Linkoeping, Sweden